Faculty of Science and Engineering

Department of Civil Engineering

Stress Concentration Factors for fatigue analysis of circumferential welds in very thick tubular members in fixed offshore structures

Ehsan Heshmati

This thesis is presented for the Degree of
Doctor of Philosophy
of
Curtin University

March 2016

Declaration

To the best of my knowledge and belief this thesis contains no material previously published by any other person except where due acknowledgment has been made.

This thesis contains no material which has been accepted for the award of any other degree or diploma in any university.

Signature:

Ehsan Heshmati

Date: 21st March 2016

Contents

Index of Figures

Index of Tables

Dedication

This thesis is dedicated to the memory of my late best friend and colleague for over 30 years, *Dr Nahid Javadi,* her passing away at a young age and her absence will truly be felt by her young family and close friends for many years to come.

Acknowledgement

I would like to acknowledge my sincere gratitude to my supervisor Professor Hamid Nikraz, for his continuous support, encouragement and constructive criticism during the years I have been engaged on this project. Without his encouragement I would have not been able to complete this work and abandoned the project.

I would like to sincerely thank my colleagues, Dr Martand Rao, Mr Mathew Thomson, Mr Ankur Negi, Mr Anand Vishwakarama and Mr Daniel Heminsley, at SNC-Lavalin in UK, who during the design of two platforms for the North Sea with dedication persevered against all continuous challenges encountered by the limitations imposed by the codes and standards and to overcome them successfully.

It was their concerted encouragement for me to embark on this PhD research project.

Much appreciation goes to Mr Patrick Joyce, my colleague and friend for over 30 years who provided some of the data to be used in this thesis.

Abstract

In this thesis, the numerical analysis work performed, using Finite Element Method, assesses cases beyond the limits imposed by industry standards on end configurations for tubular circumferential joints in offshore structures. It concludes by proposing that current limitations on thickness ratio and thickness transition slope require relaxation/revision to allow alternative possibilities be used in design of joints with high thicknesses. Hence, allowing potential cost savings without altering the risk of failure in such welded joints.

Summary

Offshore jacket structures have been designed and constructed since early 1900's in shallow waters to a depth of around 500m in 1980's. Design and construction complexity has increased to provide a cost effective platform structure from which oil/gas exploration and production can be performed. Analysis and design of these types of structures rely upon advancement in methodologies for a more economical design.

Jacket structures are made up of welded tubular sections either tube to tube end-to-end fabrication to form a longer member (a brace) or tube to tube surface to form an intersection (a node).

The focus of this research project is on practical issues encountered frequently, during normal design of a jacket platform structure, with stress concentration for tube to tube end-to-end fabrication.

The project concentrates on assessing the limitation of codes, standards and fabrication practices imposed on the configuration at the member intersections to be circumferentially welded on steel jacket tubular connections and evaluation of SCF variation trends for different configurations inside and outside these limits.

The practices and limitations have been in place since early 70's and 80's and are found to be impractical in some cases, adherence to which will bear substantial implications in real practical designs and cost increase implication in use of materials and fabrication. The limitations considered are on thickness transition tapering slopes which are limited to 1:4 and thickness ratios (thicker to thinner) of the connecting tubular member which are limited to a maximum of 2.

Research publications, international codes and standards have been reviewed to summarize historic and current developments covering the issue and performing analytical work to advance a way forward.

In this research project analyses and assessments have been performed on joints outside these limits and have shown that many practical configurations encountered in actual design of offshore platforms which fall outside these limits can have acceptable SCF values. Therefore, revisions to these limits are called for.

Design cases, indicate that configurations outside these limits are possible, practical, and necessary and in many cases more cost efficient. Therefore limitations imposed restrain designers from taking advantage of practical possibilities.

Recommendations for further work have been proposed.

Outline of the Thesis

The chapters of this thesis are structured in the following manner:

Chapter 1 Introduction: Provides a brief summary of offshore platform fabrication processes pertinent to the current research and identifies the issues involved that will be expanded in the thesis. The chapter describes the process from initial to final stages of fabrication and highlights the issues involved in the process.

Chapter 2 Literature Review: Summarizes the historic research since early days and developments carried out during the last 30-40 years on this subject and highlight their strength and shortcomings. Research by many investigators are outlined and strength and shortcomings highlighted.

Chapter 3 Present Research: This chapter elaborates on the efforts and intentions of this research and summarises the objective and aims of this work and how the project is planned. Scope of the project and major undertakings are outlined and exclusions of some scope which do not affect the work has been explained.

Chapter 4 Methodology: Alternative assessment methodologies are summarized in this section. The chapter outlines the assumptions and methodology used in performing this work and explain them further. In addition, the basis for structural modelling and selection criteria for parameters, based on practical design case, used for this study are fully explained.

Chapter 5 Finite Elements Models: This chapter describes the basis for the models and assumptions used in this study. Parameters and sensitivity assessment carried out for standardization of the work and adjustment to models are described.

Chapter 6 Analysis Results: The section provides full details of the analyses and numerical results obtained. The results are presented in tabular and graph forms and discussed in detail. New findings deduced from the results are explained and practical implications outlined.

Chapter 7 Transition Zone Stress Distribution: The stress variation along the model from the point of application of stress and through the model has been assessed and discussed in this chapter.

Chapter 8 Effect of Fabrication Misalignment: The fabrication misalignment is a related issue that its full treatment is outside the scope of this work, however, some of the effects have been analysed and discussed in this part.

Chapter 9 Conclusions and Recommendations: This final chapter summarises the main findings of the work, and implication for future designs of offshore structures are explained. Some suggestions for the future potential research work to be performed in this area have been highlighted.

Chapter 10 References: Include all relevant previous published literature, code and standards and industry guidelines that have been used in this research work.

Appendix A: Provides a short summary of definitions and terminology used in the industry to facilitate the readers who may not be fully familiar with the terminology related to this work.

Appendix B: Provides some typical model plots and typical results. It was deemed unnecessary and not useful to include all and numerous plots or output from the analyses.

Chapter 1

Introduction

1. INTRODUCTION

1.1. BACKGROUND

Oil industry started in early 1800's in Baku Azerbaijan according to Aliyev (2016). Offshore designs developed using wooden pier platforms extending into the oceans in 1896 in Summerland California, in USA. (Figures 1-1, 1-2) and then took off in Gulf of Mexico.

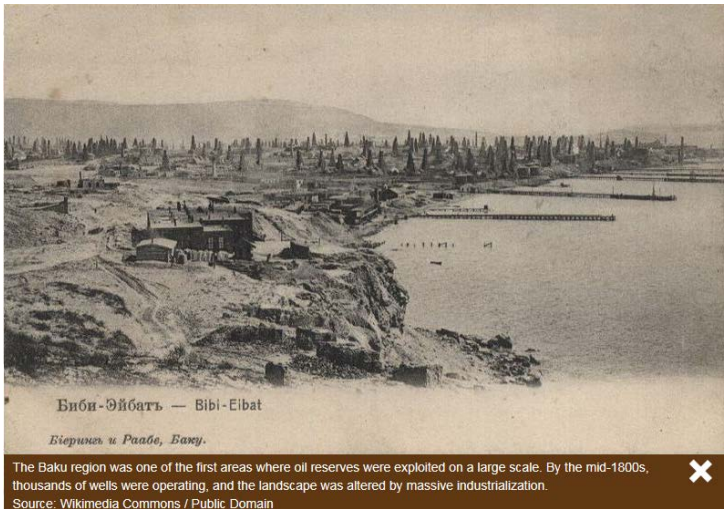

Figure 1-1 Azarbaijan Oil Fields

http://history.alberta.ca/energyheritage/oil/pre-modern-global-history/early-human-pre-industrial-history/baku-azerbaijan.aspx

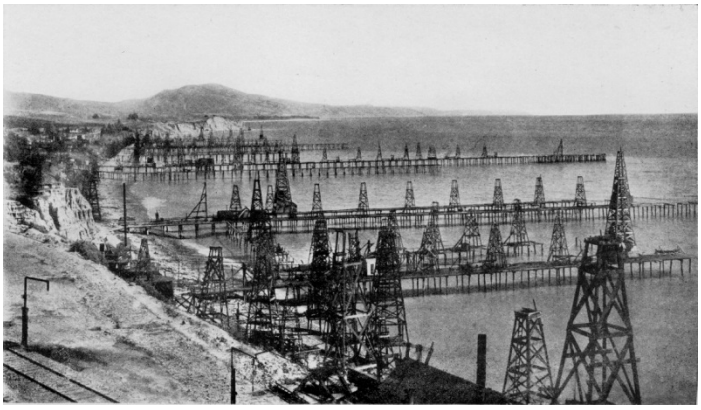

Figure 1-2 Wooden Piers Summerland Field

https://upload.wikimedia.org/wikipedia/commons/5/5d/Oil_wells_just_offshore_at_Summerland,_California,_c.1915.jpg

Development and design of offshore platforms started in 1947 in the Gulf of Mexico (GoM) with Kerr-McGee Oil Industries drilling the first offshore well and an out of sight platform Kermac 16 and has continuously progressed to date (Schempf, 2007).

Fixed offshore platforms provide suitable offshore bases to house equipment for drilling into reservoirs and production of oil and gas fluids from the reservoirs.

The structural design of this type of platform underwent substantial developments from its early beginning in fairly benign shallow waters of the GoM (Figure 1-3) to the more hostile and much deeper Central and Northern North Sea (Figure 1-4) This type of platforms are now used extensively worldwide, currently more than 14,000 offshore jacket structures have been installed worldwide.

Figure 1-3 Early Offshore Platform in GoM

Photo courtesy New Orleans Times-Picayune
American Oil and Gas Historical Society, http://aoghs.org/

Figure 1-4 BP Magnus Platform – Northen North Sea

https://c1.staticflickr.com/3/2770/4123138036_4672b683cc_b.jpg

Figure 1-5 Nexen Petroleum Golden Eagle – North Sea

http://subseaworldnews.com/wp-content/uploads/2013/01/Nexens-Golden-Eagle-Development.jpg

Offshore structures are designed to provide a stable platform for different operational facilities and functions either individually, such as drilling, production, process and utilities, accommodation, or a combination of these functions and facilities on one platform. They are designed to operate safely for their design lifetime up to 20-30 years or more, in different water depths and environments, some in very harsh environment such as the North Sea. This type of steel platform is generally divided into two parts; a substructure and topside.

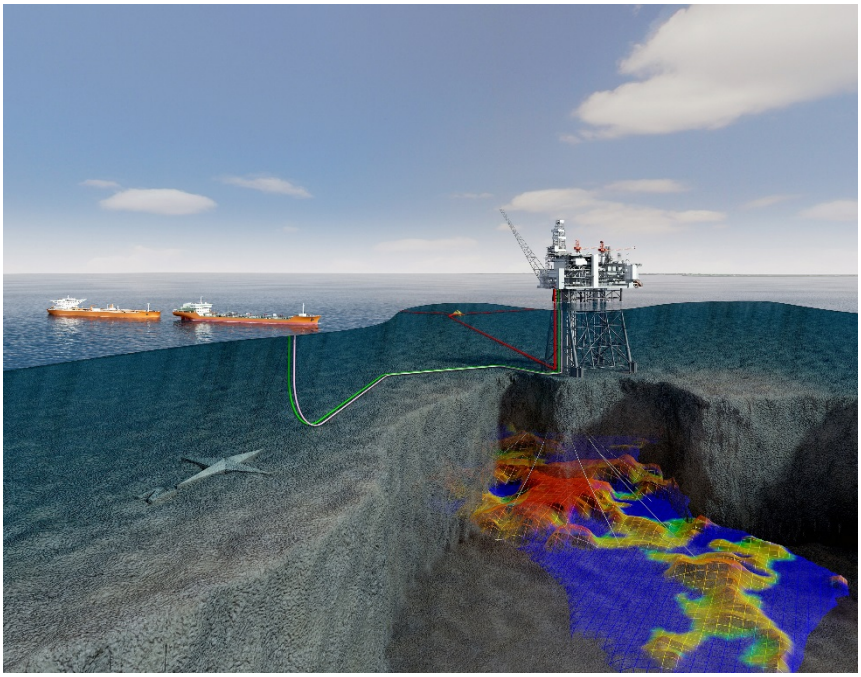

Figure 1-6 Modern Offshore Platform

http://www04.abb.com/global/seitp/seitp202.nsf/0/8c20417eecc7dff0c1257c970031679c/$file/0086353+-+Mariner+with+reservoir+-+Photo++-+Statoil.jpg

The ***substructure*** is fabricated by welding varying lengths and sizes of circular tubular members together to form a strong three dimensional space frame structure, secured by piles to the ground using a number of piles to take the weight of equipment and structure on top as well as resist environmental loads. In the case of a drilling or a production platform the space frame is to house and protect drilling conductors or production risers (hence called a jacket structure). The substructure supports conventional multi-storey ***topside*** steel structure consisting of beams, columns and plated structures which accommodate and support the oil and gas drilling, production equipment and various other facilities. (Figures 1-5 & 1-6).

Offshore platform design must satisfy three conditions:

- Must be suitable for intended purpose and perform its required function.
- Must provide adequate structural safety and integrity during its intended operating life.
- Must be capable of being fabricated easily and economically and be installable.

These structures are generally subject to two critical loading conditions during their life time:

1) High magnitude loading due to severe storms (including wind, wave and current) potentially causing over loading and structural collapse.

2) Low magnitude cyclic wave loading potentially causing fatigue failure in the long term.

Other major loading conditions may also exist depending on location and environment such as icebergs, earthquake and hurricane loading amongst others.

General analyses and design of offshore platforms is outside the scope of this thesis. The emphasis of this research is on the local stress concentrations on tubular member's circumferential weld locations affecting fatigue performance.

1.2. PROBLEM DESCRIPTION

Fixed offshore platform jacket substructures, as explained, are three dimensional space frames fabricated from tubular members and tubular joints welded together. Tubular members are produced from plates, initially plates of 3 or 4 m width with varying nominal thickness are rolled into tubes and seam welded along their lengths.

Then a number of these tubular sections 3 or 4m long (or part thereof) are welded together circumferentially to obtain the desired length required forming what is called a brace member. These processes are shown in Figures 1-7 to 1-9.

Figure 1-7 Plate Rolling

http://www.steelplate.co.uk/uploads/images/products_53_0_main.jpg

Figure 1-8 Plate Rolling into Tube

http://www.bladt.dk/UserFiles/image/Newsletter_Photo/NewsNo19/19_Ny%20valse(1).jpg

Figure 1-9 Brace Member

http://bwshells.com/src/uploads/2012/03/OFFSJORE-2.jpg

The brace members are connected at joints forming a space frame. The space frame is supported by 2, 4, 6 or 8 integrated large tubular members, called legs, which support the topside above the water and extend down to the seabed and connected to the seabed using single piles or pile groups, (Figure 1-10).

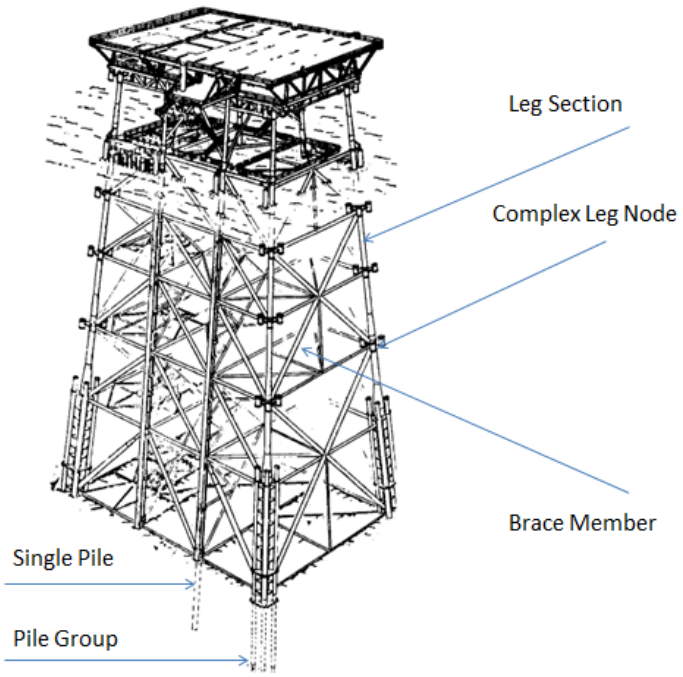

Figure 1-10 An 8 Legged Offshore Platform 1970's – North Sea

Furnes & L¢set 1981

A number of issues arise during fabrication process of tubular members;

1) During initial plate making process there may be thickness variation from the nominal thickness (within a specified range).

2) During plate rolling process the cross section of the formed tube may not be a perfect circle and suffer from a degree of ovality.

3) Ovality of two adjoining tubular sections may not be to the same degree around the circumference.

4) The out of roundness and non-perfect circular shape of the formed adjoining tubular members can cause alignment mismatch of the

thicknesses. This type of mismatch, hence, results in a point with a stress concentration.

5) During production a certain variation in thickness from nominal constant design value, within a specified limit, around the circumference of the tubular may be present which when brought close together to be joined may create additional source of mismatch.

6) For tubular members with different thicknesses the situation is exacerbated as the two members cannot be welded together unless a transition with an appropriate slope is provided to nominally match the thicknesses of the two tubular members at the welding point.

7) The difference in the thicknesses causes eccentricity of the centreline of the two members as well as potential for a mismatch.

8) The total misalignment due to mismatch and centreline eccentricity is combined to cause secondary bending and stress concentration at the welded joint. Stress concentrations are detrimental to the fatigue performance of the joints.

9) The higher the difference in the thickness of the two joining members the higher is the Stress Concentration Factor (SCF) due to centreline eccentricity.

Hence design codes, ISO 19902 (2003), DNVGL-RP-C0005 (2014), API RP 2A (2001) and fabrication procedures, EEMUA 158 (1998, 2014) provide guidance and limitation on the ***"thickness ratio",*** that is, the ratio of the thicker to thinner thickness to be limited to a maximum of 2 and the

"transition slope" of 1 in 4 for tapering the thicker members down to the thinner member. Although DNVGL fabrication standard DNV-OS-C401 (2010), DNVGL-OS-C401 (2015) states that maximum slope should not be steeper than 1 in 4.

These guidance and limitations have been in place since early days of jacket design and fabrication in the North Sea in late 1970's and early 1980's.

During these early times, in order to strengthen the joints, ring stiffeners were used either internally or externally as shown in Figures 1-11 and 1-12. External use of ring stiffeners was eliminated early on as they were not very effective, cumbersome to fabricate, and had adverse effects, details of which are outside the scope of this work. However, the use of internal ring stiffeners to strengthen nodes continued for some time and may still be used in certain design conditions.

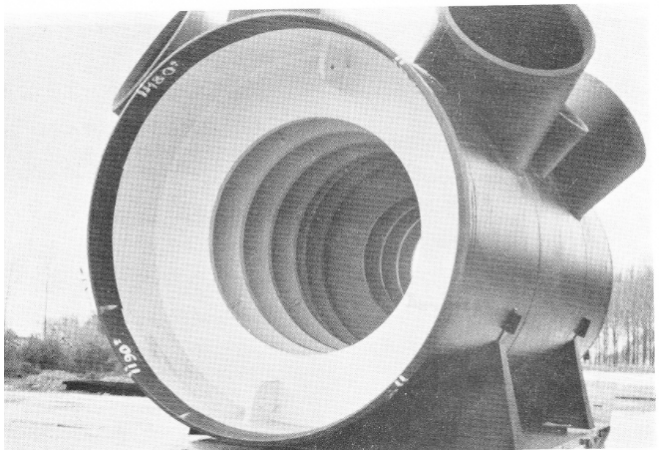

Figure 1-11 Node with Internal Ring Stiffener

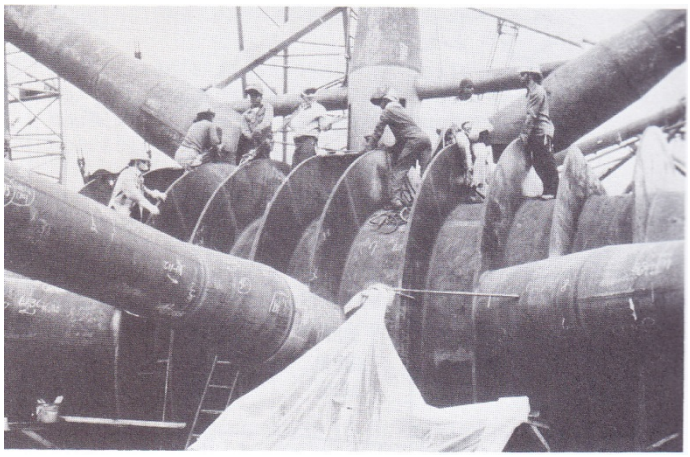

Figure 1-12 Node with External Ring Stiffeners

OTC 3878 (1980)

The use of ring stiffeners was aimed at strengthening the joints with thin walls to prevent brace members punching through or pulling out the thin wall of the nodal chord plate under compression or tension respectively. Additionally, the use of ring stiffeners had the effect of strengthening the joint for fatigue performance. (Callen et al., 1981; Sawada et al., (1979).

However, a number of developments in late 80's and 90's provided solutions that allow some better and more efficient designs to be used, such as cast nodes (Webster et al., 1981) and use of thicker nodes instead of ring stiffeners, (Heshmati, 1990).

Figure 1-13 Cast Node

Xu et al (2015)

However, despite being the most popular option and more common use of much thicker nodes with their design and performance effectiveness, the limitations on thickness ratios and transition slopes set for end preparation for circumferential welding still remain the same in the design codes, and prevent more efficient design solutions with large thicknesses to be used more effectively. Compliance with the codes, limits the use of alternative designs, hence substantial cost penalties in extra design effort, material and fabrication are incurred by the owners of the platform assets in many occasions.

1.3. RESEARCH PURPOSE, OBJECTIVES AND SCOPE

1.3.1 The Purpose

This research project aims to evaluate the effect of breaching the limits imposed by the codes on the configuration of joints and assess possibility of reduction in material use and fabrication costs, by going outside these norms, without increasing or altering the failure risk associated with circumferential girth welds.

The purpose of this research is to assess and "fill the gap" in the current available information related to Stress Concentration Factors (SCF) for joints within the upper ranges of the thickness (50 to 125mm) often used in offshore structures, especially on leg node sections, which so far have not been addressed, and assess the effect of code limitations in this thickness ranges.

1.3.2 The Objective

The objectives for the research are as follows:

- To perform a series of finite element analyses, using ABAQUS commercial Finite Element package version 6.10, on tubular joints with varying thickness transitions and different configurations used in typical offshore platforms.

- To assess and evaluate possibility of eliminating the need for current limitations imposed by the design codes on thickness ratio and transition slopes especially on joints with high thicknesses.

1.3.3 The Scope

The scope of this research is to perform the following:

- Study the effect of large tubular thickness ratios
- Study the effect of transition slopes
- To assess if the current limitations can justifiably be removed
- To derive, from the results of the studies, conclusions and possibly construct more practical design alternatives to be used by the designers.

Chapter 2

Literature Review

2. LITERATURE REVIEW

2.1. SUMMARY OF DEVELOPMENTS

During late 1960's, into 70's research on welding issues on steel plate welded sections for the ship building and pressure vessels, identified potentially damaging stress raisers or stress concentration due to misalignments at the welded joints, (Nishimaki, 1969 ; Wylde & Maddox, 1979).

In 1970's and 80's with the expansion of the oil and gas industry in the North Sea considerable development of technology took place in terms of structural strength and fatigue assessment methodologies of complex tubular members and joints and fabrication methods using welding technology, (UK Department of Energy, 1974) .

During these years substantial information from the ship building, aerospace, nuclear and process plant industries were used as background and experience for developments in the offshore industry in the field of fatigue assessment methodologies and influence of factors affecting fatigue performance in harsh environment of the North Sea, such as the effect of stress concentration on fatigue life.

For tubular joints in offshore structures research and experimental work (Kuang 1975; Wordsworth & Smedley 1978) and later using Finite Element modelling and analysis (Efthymiou & Durkin 1985) culminated in development of a series of equations, to estimate Stress Concentration Factors (SCFs) to be used for assessment of fatigue of the complex tubular joints due to cyclic environmental loading and variability during the life of the platform.

Concurrently, further research on stress concentration on butt welded plates was performed, (Burdekin, 1979; Maddox, 1985; Wylde, 1979). Knowledge gained and applied to developments for determination of SCFs on circumferential girth welds for joining tube to tube were under investigation which resulted in a number of alternative estimations methods using curves or equations, based either on Finite Elements Analyses (FEA) or experimental investigations, (Heshmati, 1986; Connelly & Zettlemoyer, (1993).

Use of fixed jacket platforms with complex tubular joints continued until the depth of the oceans, where reservoirs were found, limited the viability and cost effectiveness of this type of platform in comparison with more advanced types of structures, such as Spar and Tension Leg Platforms (TLP) or Floating Production and/or Storage and offloading Platforms (FPSO), which are more suitable for deeper oceans.

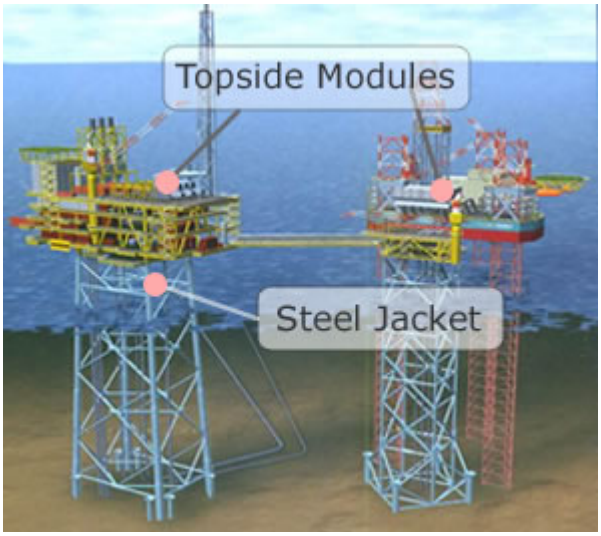

Figure 2-1 Shell Shearwater Platform Structure
http://www.subctest.com/images/background_2.jpg

Viability and suitability of the use of fixed platforms is limited to shallow waters depths to less than 400-500m. Due to maturity of technologies

involved, research and development for this type of structures slowed down to some extent and attention was diverted to the new floating technologies requiring further research and development. Hence available and common practices and norms for jacket design and fabrication continued to date with limited major new developments (UK Department of Energy 1974, 1993, 1995).

The methodologies and practices for analysis, design, and assessment of circumferential butt welds for joining tubes remained the same for nearly two decades.

More recently, a summary paper (Lotsberg, 2009) has been published with further FE analyses to re-iterate the past expressions and formulize the old equations with slight modifications without any major developments.

In a recent design project consisting of two platforms in Central North Sea completed in 2012, where the author was heavily involved in design, it became apparent that further assessment and expansion of existing norms specially with respect to the use of SCF equations and their limitations in design and fabrication of girth welds, could be beneficial as there has been almost no further developments since 1990's on girth welds assessment methodology used in design and construction of fixed offshore structures. The current norms stipulated in the codes limited design alternatives at substantial cost penalties in materials and fabrication.

2.2. OFFSHORE PLATFORMS AND FATIGUE

Offshore platforms have been designed and developed all around the world for extraction of oil and gas. More recently similar designs are being used in the renewable energy industry as support structures for wind turbines and rotating blades. These offshore platforms continue to support heavy topside loads in sever dynamic ocean environment, where cyclic loading due to waves causes fatigue loading which is a critical design loading condition for the integrity of these structures.

Under static load a ductile metal when loaded from zero to a value which causes the metal to fail and rupture, large strains appear before fracture, therefore it is possible to design the structures to sustain loaded below the yield stress with limited strains of metal to prevent such catastrophic ruptures.

However, under cyclic fatigue load the failure would occur under a much lower value than yield stress of the metal without plastic deformation. Fatigue loading after some time causes initiation of cracks in a welded structure which is hard to detect. Therefore, since no significant dimensional changes occur before a crack is formed, failure may not be detected until the crack has propagated through the member, (Gurney, 1968).

All steel offshore platforms are fabricated from welded tubular members. Hence, fatigue performance of these welded tubular joints under cyclic wave loading is of paramount importance as a long term design condition for platforms with 25 to 30 year design life.

In assessing the fatigue behaviour of welded engineering structures the focus is generally on structural details. This is due to the fact that fatigue

cracking is highly localized. Therefore, for design each detail must be considered locally.

Fatigue cracks due to fluctuating loads are developed due to microstructural changes as a result of

- Stiffness changes in local structural details
- Geometry of the weld
- Weld toe condition

Fatigue Failure can be defined in a number of ways (Romejin, 1994);

- Appearance of first visible crack
- Development of crack length of a certain length
- Crack through the thickness of the material

In offshore tubular joints fatigue assessment, the last criterion is defined as the failure in fatigue. (Gurney, 1968)

2.3. TYPES OF JOINTS

Design of jacket platform components such as structural leg and brace members and other components such as caissons, risers require tubular members with varying thicknesses to be welded together.

Diameters of members can vary between 500mm for the brace member to 10m or more on jacket legs (BP Magnus Platform, Blake, 1989).

Thicknesses of these tubular members typically vary between 25mm for brace members to in excess of 125mm at jacket nodes.

There are basically two types of tubular joints:

a) Circumferential Joints - End to end connection of two tubular members using circumferential girth welds forming a longer tubular member.

   For large diameter members, at a girth weld joint, butt welding can be performed either from both sides of the joint. However for small diameter members welding can only be performed from external side due to limited access from the internal side of the joint. A typical long brace member formed of a number of short 3 or 4m length tubes is shown in Figure 2-2.

Figure 2-2 Brace Member

b) Complex Multiplanar Joints - Long brace members are connected to the body of another tube member called a chord forming “multi brace complex tubular joint” at a jacket node, Figure 2-3, to form a three dimensional frame structure, as shown in Figure 2-1.
Planar chord-brace members are a subset of this complex joint type.

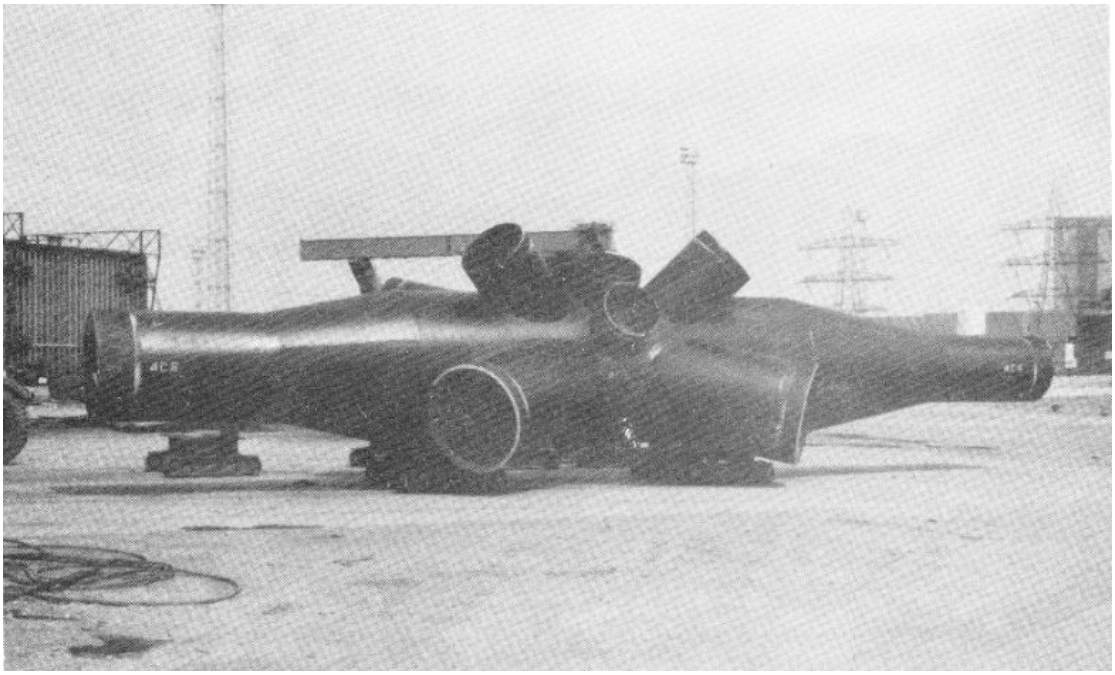

Figure 2-3 Multi Brace Fabricated Jacket Node

This research project focus is on the first type of connection using circumferential girth welds. Issues related to complex multi brace nodal joints is outside the scope and focus of this thesis.

2.4. TYPES OF BUTT WELDS

There are many types of butt weld depending on applications; these are pictorially shown in Figure 2-4. The most common for offshore structures is a V-butt weld, welded from one or both sides.

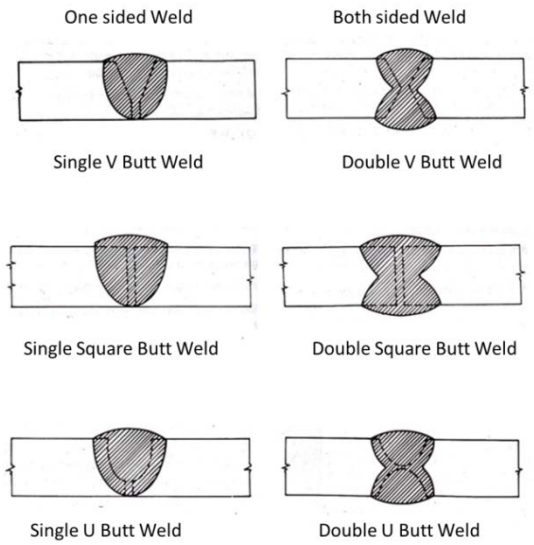

Figure 2-4 Types of Butt Weld

2.5. FATIGUE ASSESSMENT AND SIGNIFICANCE OF SCFS

For design of offshore structures, there are generally two types of fatigue analyses methods, deterministic and spectral methods. Fracture Mechanics methodology of fatigue assessment, however, is often used for inspection or conducting integrity assessment. Complete details of these methods are outside the scope of this project, one can refer to other sources for details such as Almar Naess (1999) and Anderson (1991),

In general the simplest and most common approach is based on the work of Wöhler (1860), Palmgren (1924) and Miner (1945), where nominal stress ranges on the member under consideration and their number of cycles of occurrences is determined, then the stress ranges are amplified by

stress concentration factors and from appropriate S-N curves, number of cycles to failure is obtained and damage is estimated for the stress range, summation of total damage for all stress ranges would give an indication of fatigue life of the member. Further details of the procedure are given in chapter 4.

Very briefly, a typical deterministic fatigue analysis of offshore structure requires the following steps to be performed:

- Determination of cyclic loadings due to environmental loading at a joint for each wave

- Determination of applied stresses and stress ranges at the joint for each wave, Δs

- Amplification of stress ranges by the appropriate geometric Stress Concentration Factors (SCF) for the type and shape of the joint,

$$\Delta S = SCF.\Delta s \qquad \text{Eqn 2.1}$$

- Use of an appropriate design S-N curve (stress range vs. number of cycles to failure) for the type of joint under consideration,

  S-N curves relate the stress range to the number of cycles to failure and are mathematically represented by the equation:

$$N(\Delta S)^m = K \qquad \text{Eqn 2.2}$$

or

$$Log_{10}(N) = Log_{10}(K) - mLog_{10}(\Delta S) \qquad \text{Eqn 2.3}$$

Where:

N= No of cycles to failure at a specific stress range

K= constant

m = slope of the curve

ΔS = Amplified stress range

Different standards have slightly different S-N curves, such as API RP 2A (various editions), DNVGL-RP- 0005 (2014), BS 7608 (2014), and ABS (2014) Guides.

A full study and comparison of S-N Curves can be found in UK HSE Report OTO No 83 (2001).

- Estimation of the actual number of cycles of occurrence (n) of stress range ΔS from wave data for the life of the structure

- Estimation of the number of cycles to failure (N) for each stress range ΔS from S-N curve

- Estimation of fatigue damage (n/N), for each stress range ΔS which is the ratio of actual number of occurrences of stress range (n) to the number of cycles to failure (N)

$$\text{Damage} = n/N \qquad \text{Eqn 2.4}$$

- Palmgren (1924) and Miner (1945) suggested an approach to combine individual damage contributions, known as Palmgren-Miner's linear damage hypothesis or Miner's rule

- Estimation of total damage using Palmgren-Miner (1945) summation rule is given as

$$\text{Total Damage} = \Sigma n_i/N_i \qquad \text{Eqn 2.5}$$

Where i = the number of all stress ranges considered

- Determination of indicative fatigue life,

$$\text{Life} = 1 / \text{Total Damage} \qquad \text{Eqn 2.6}$$

2.6. FACTORS AFFECTING FATIGUE PERFORMANCE

There are a number of local parameters that affect fatigue performance of welded joints and susceptibility of joints to fatigue failure:

a) Stress concentration caused by detail at a structural discontinuity and change in stiffness and the stress raising effect of the weld shape itself.

b) Axial and angular misalignment, and imperfect weld profile.

c) Potential weld defects during welding process which can include: cracks, solid inclusions, porosity, slag, under/over penetration, lack of fusions.

   A comprehensive classification of the various types of potential weld flaws is given in ISO 6520 (2007), or AWS D3.5 (1993, R2000).

d) Residual stresses in the vicinity of the weld due to shrinkage during solidification and cooling of the weld metal.

Other general parameters that affect fatigue performance include loading, geometry and material properties of the component and the operating environment.

However, the primary factors that affect the fatigue performance are the fluctuation in the local stress or strain and stress concentrations.

Consequently, the most efficient way of reducing the effect is reducing the severity of applied nominal stress in magnitude and reducing the stress concentration by design.

Therefore, reduction in local stress concentration factor (SCF) is a priority in design.

2.7. S-N CURVES

For determination of the fatigue strength of a typical joint it is necessary to obtain an S-N curve. S-N curves are generally developed from testing programs for a specific type of weld. They relate the stress range to the number of cycles to failure.

S-N Curve is also known as Wöhler curve, as August Wöhler (1860) was the first person to investigate fatigue behaviour of material and produce such results from tests. His Pioneer work was performed during 1858 to 1870. Initially he had produced his results in tabular form.

Spangenberg (1874) later on represented the data in linear curves and Basquin (1910) represented that data in log-log form. (Walter Schultz 1996).

According to Gurney (1979) there are four possible parameters that can be used for defining stress range to be used for fatigue testing. These parameters are as follows:

- Minimum stress in a cycle S min
- Maximum stress in a cycle S max
- Mean Stress S mean = ½ (S min + S max)
- Stress range S range = S max – S min

The fatigue test “Stress Cycle” can be fully defined by any two of these parameters.

In certain types of fatigue testing equipment mean stress and stress range are only required for setting up the test. As the equipment is loaded to the mean stress and then fluctuates and cycles around the mean stress with the stress range.

There are three possibilities for setting up the stress ranges cycles, these are showman Figure 2.5

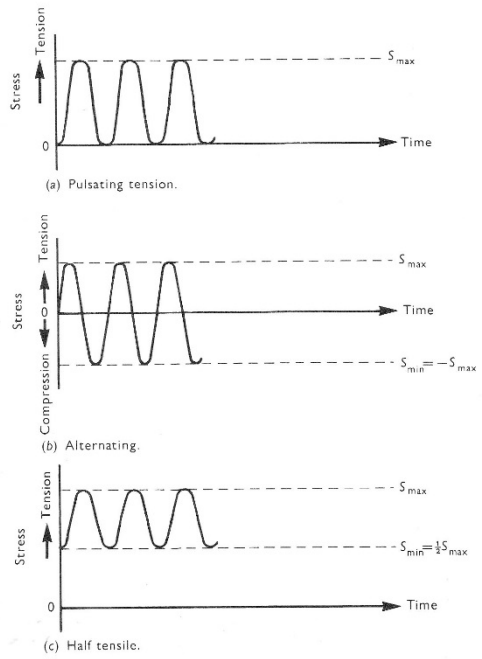

Figure 2-5 Fatigue Test Stress Cycles

Gurney (1979) states that the pulsating tension test has been found to be the most common in fatigue testing. In order to obtain the S-N curve for a particular detail, in general a large number of tests between 8-12 specimens are used. Each specimen is subjected to a certain stress ranges and cycled to failure. In general machines used for testing have a cycling speed between 3 and 16 Hertz (cycles per second).

The results of tests in general form a curve shown in Figure 2.6

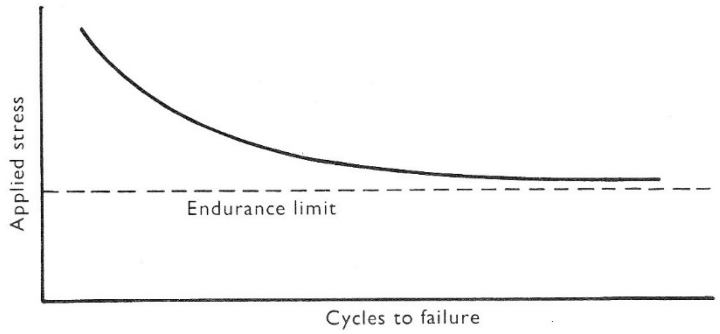

Figure 2-6 Typical S-N Curve on Linear Scale
Gurney (1979)

However, it is now, normal to draw the curve in a log-log scale and obtain straight line curves, as was developed by Basquin (1910).

Typical design curves for steel connections are given in BS 7608 (2014) as shown in Figure 2-7 which are drawn in a Log-Log scale:

Figure 10 **Standard basic design S_r-N curves**

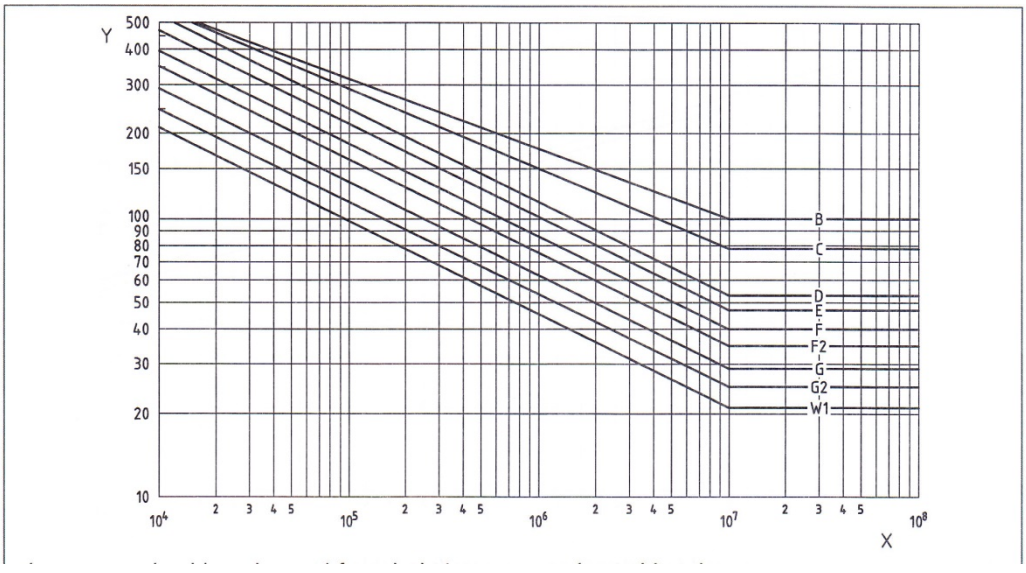

Figure 2-7 Typical S-N Curves on Log-Log Scale
Extracted from BS 7608 (2014)

During testing, it has been found that there is a significant scatter in the test results especially at the lower end of stress ranges. Statistical distribution of scatter is shown in the Figure 2-8, and fully described in Schijve, (1994, 2005)

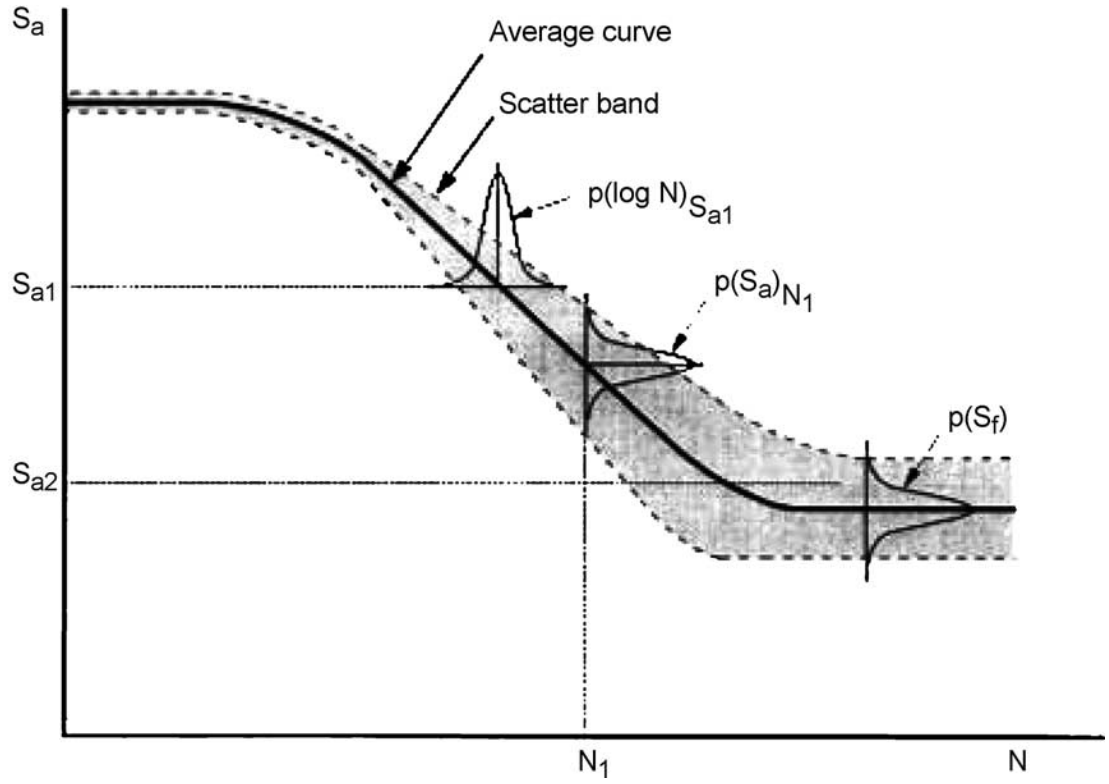

Figure 2-8 Test Results Scatter Band
(Schijve, 2005)

S–N curve with narrow scatter band at high stress Sa (low cycle fatigue) and wide scatter band at low stress Sa (high-cycle fatigue). Three probability density functions are indicated in Figure 2-8 (Schijve, 1994, 2005)

However, for offshore structures the mean curve from test results are obtained and then a curve representing (mean – 2 x standard deviation) is drawn to be used in design, HSE (UK)

There are other less common methods of fatigue testing which have been used in research and are described by Gurney (1979).

2.8. STRESS CONCENTRATION FACTOR

Stress Concentration Factor (SCF) is defined as the ratio of elevated stress due to geometric changes at the location of a "hot spot" under consideration divided by the nominal stress away from the location.

For determination of SCF at "hot spot" locations various modelling techniques are possible and the definition of the location for which SCFs are determined is required. In general the hot spot is defined either at a weld toe or at the point of stiffness/geometry change. Figure 2-9.

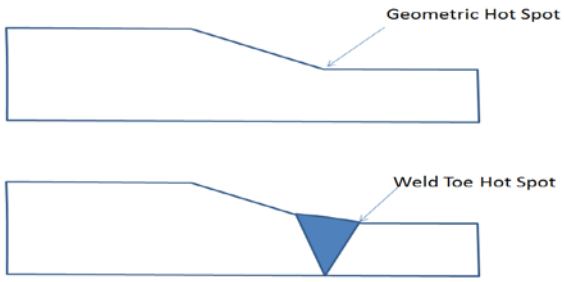

Figure 2-9 Hot Spot Definitions

A number of parameters contribute to the geometric stress concentration at this type of joint:

1- Thickness Ratio (T/t), is the ratio of thicker (T) to thinner (t) member, Figure 2-11

2- Transition slope (S), is the slope of transition from the thicker member to the thinner member, Figure 2-11

3- Eccentricity is the centreline eccentricity of the two members, either due to potential mismatch in alignment of the two sections, or due to variation in thickness or both as shown in Figures 2-10 to 2-13.

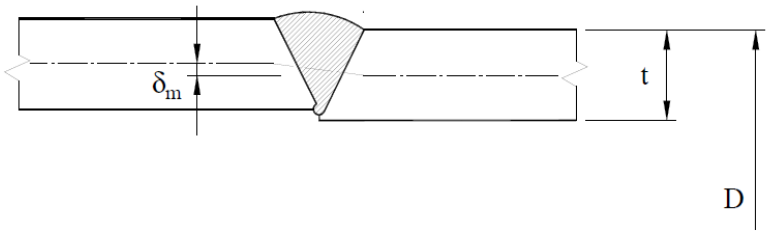

Figure 2-10 Eccentricity due to alignment mismatch
Extracted and simplified from DNVGL-RP-0005 (2014)

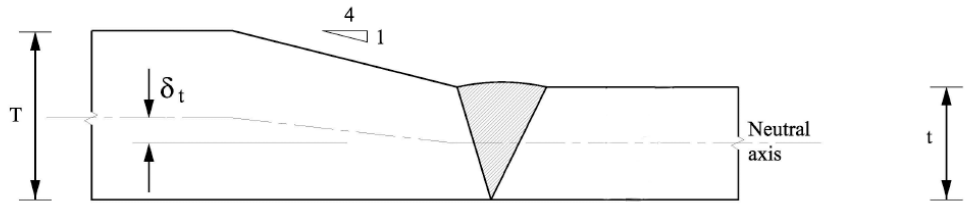

Figure 2-11 Eccentricity due to variation in thickness
Extracted and simplified from DNVGL-RP-0005 (2014)

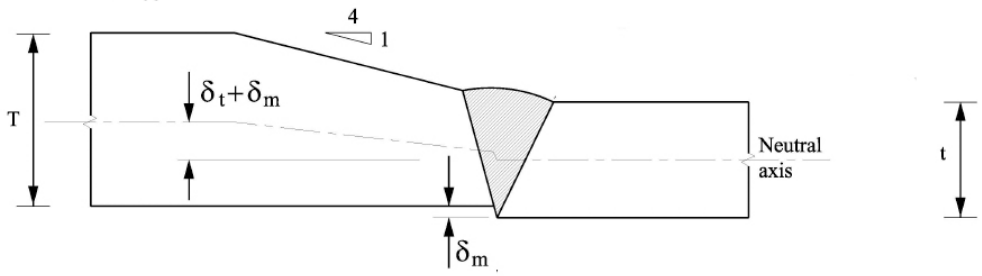

Figure 2-12 Eccentricity due to variation in thickness and positive misalignment
Extracted and simplified from DNVGL-RP-0005 (2014)

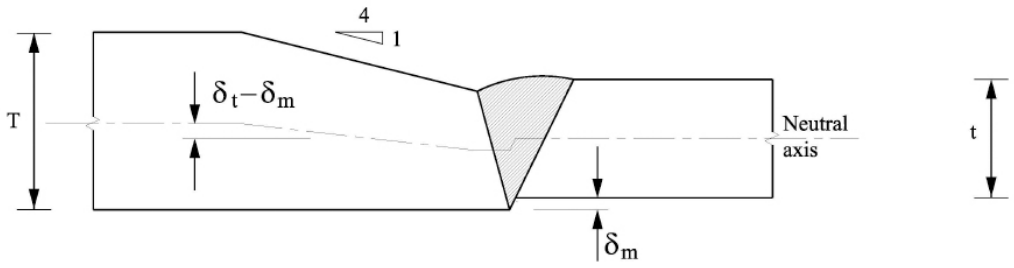

Figure 2-13 Eccentricity due to variation in thickness and negative misalignment extracted and simplified from DNVGL-RP-0005 (2014)

The above three factors are to some extent related, as the T/t ratio increases the eccentricity of the centreline increases hence increase in bending due to axial load, in addition if there is a alignment mismatch then depending on the direction of misalignment the total eccentricity either increases or decreases as shown in Figures 2-11 & 2-12.

In addition, during fabrication, there are other factors which may affect the stress concentration

4- Fit up, prior to welding the two members must be brought close together to have a required small gap and be aligned. The gap can generally be controlled to a high degree, however, uncontrolled gap is a source of increase in SCF.

5- The perfect alignment may be jeopardized by fabrication ovality of the two tubular members.

   During fabrication there is generally a tight tolerance on the ovality of the fabricated tubular members which is specified (EEMUA 158, 2014) and shown in Table 2-1.

Dn Nominal (mm)	Dmax-Dmin Not to exceed
≤ 610	1% Dn
610<Dn≤2000	Max (0.75% Dn or 6mm)
>2000	Max (0.50% Dn or 3mm)

Table 2-1 EEMUA Ovality Limits

Ovality is generally measured at eight diametrically opposite points to determine the maximum and minimum deviation. Figure 2-14

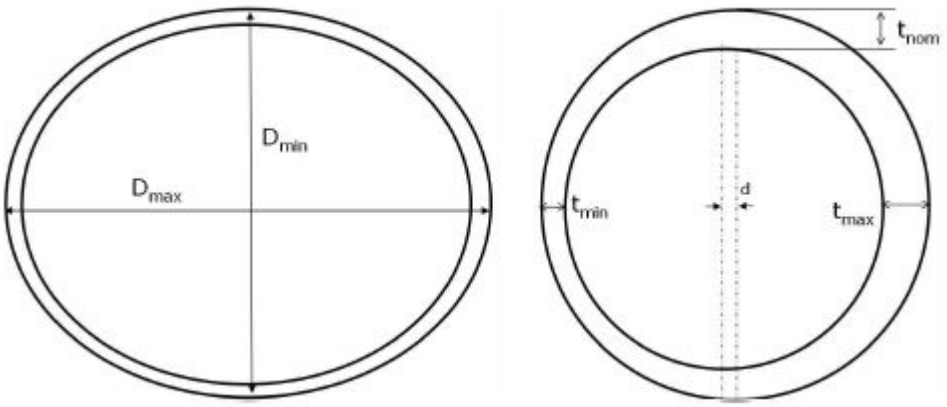

Figure 2-14 Ovality and Thickness Variation

6- The perfect alignment may also not be possible and suffer from possibility of variation in the thickness around the circumference of the tubular member, Figure 2-15, although there are tight tolerances in terms of variation in design nominal thickness.

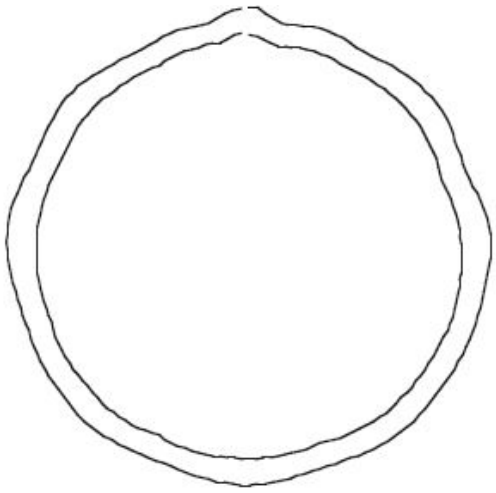

Figure 2-15 Thickness Variation around the Tubular

There is also a further requirement that the longitudinal seam weld along the members should be staggered by at least 45 degrees and preferably by 90 degrees from each other at the circumferential weld position.

These two requirements may necessitate that the effect of ovality be reduced by minimising the mismatch by generally rotating one member relative to another prior to line up and fit up before welding.

7- Welding Workmanship, The welding defects, such as undercut, lack of penetration, excess penetration, missed edge as shown in Figure 1-13 and fit up mismatch can affect SCFs to a large degree.

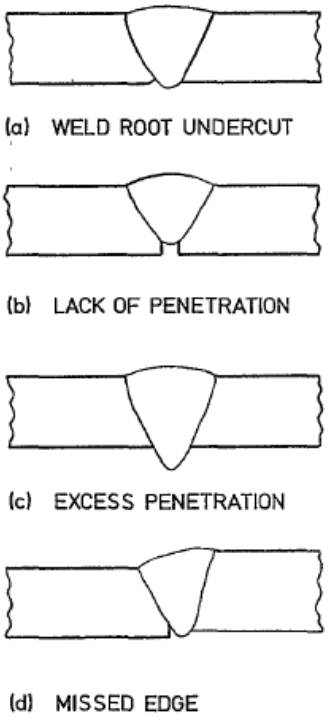

Figure 2-16 Weld Root Imperfection
Extracted from OTC 5351, Heshmati (1986)

Misalignments due to variation in thickness of two connecting members or members with unequal thickness and ovalized cross sections and fabrication tolerances that cause stress concentration at the joint transition and affect fatigue performance are shown in Figure 2-17.

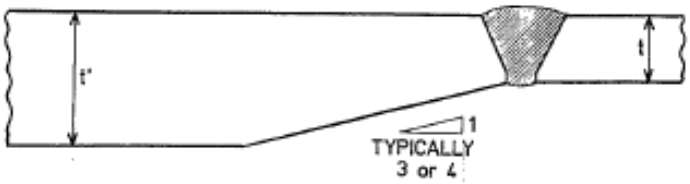

Figure 2 : THICKNESS TRANSITION

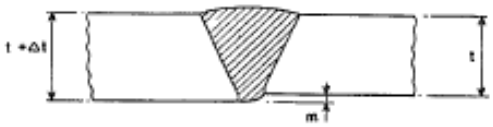

a : MISMATCH DUE TO VARIATION IN NOMINAL THICKNESS

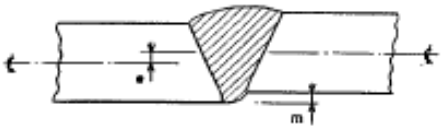

b : MISMATCH DUE TO MISALIGNMENT OR OVALITY

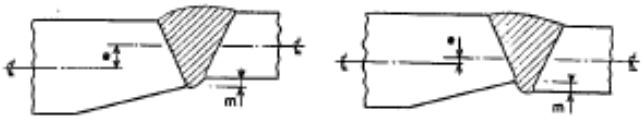

c : MISMATCH IN MEMBERS WITH UNEQUAL THICKNESSES

Figure 2-17 Potential Mismatch

Extracted from OTC 5351 Heshmati (1986)

Angular distortion may also appear at the seam weld position at the crown of the tube. This type of distortion as shown in Figure 2-18, can be dealt with separately which is outside the scope of this work. For further information reader is referred to Gurney (1979).

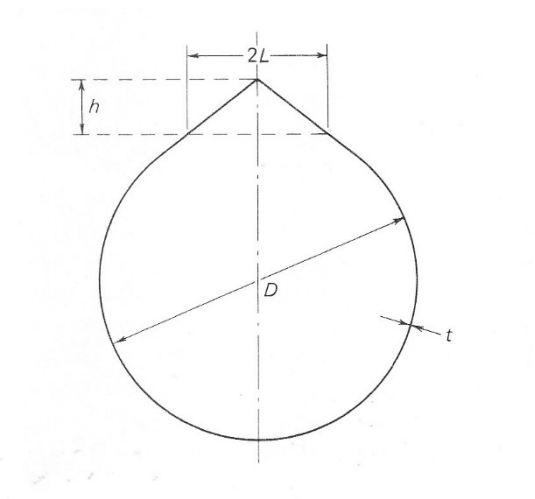

Figure 2-18 Angular Distortion

2.9. HISTORICAL WORK – EARLY DAYS

In the following paragraphs major research works which have contributed substantially to the current state of knowledge are briefly summarized:

Gunn & Webster, in 1960 in order to simulate fatigue loading carried out pulsating axial tension tests on aluminium alloy test specimens of plate sections 3.2mm thick with misalignment of 0.5mm (16%). Their axial load test results indicated a sever reduction in fatigue strength of misaligned specimen compared with correctly aligned specimens. This reduction was proportional to the extent of misalignment. Also, their results showed that in bending the effect of misalignment were relatively unimportant. Their work resulted in an equation to estimate the stress concentration factor for misalignment in joints subjected to axial loads, as follows:

$$SCF = 1 + 3e/t \qquad \text{Eqn 2.7}$$

Where:

e = eccentricity due to misalignment

t = thickness of plate

According to the Welding Institute Research Report (Wylde 1979), this equation was initially incorporated in the UK Code of Practice for the structural use of Aluminium CP 118 in 1969.

Then after, other researcher conducted similar experiments on steel specimens. Nishimaki in 1969, conducted pulsating axial tests on mild and high strength steels of 6 and 16mm thickness with 20, 40 and 50% misalignment. The results indicated progressive reduction in fatigue strength. Priddle in 1973 conducted similar tests on steel with misalignments of up to 60% of plate thickness and found similar indicative results with reduction in fatigue strength.

Berge and Myher in 1977, carried out theoretical investigation into fatigue performance of misaligned cruciform and butt welded joints and reported that the specimen end restraints had considerable effect on the secondary bending responsible for reduction in fatigue life of misaligned weld.

They proposed the following equation for SCF of misaligned joint allowing for the end restraint effect.

$$SCF = 1 + \lambda\, e/t * \psi/L \qquad \text{Eqn 2.8}$$

Where;

t = thickness,

e = misalignment and

λ = a non-dimensional parameter dependent upon the degree of restraint imposed upon the joint. For conventional fatigue specimen supported at mid-point Ψ=L/2, where L is length between restraint points.

Values of λ were provided in a tabular form for cruciform joints; however, no guidance was given for the transverse butt joints.

Early research in 1960s and 1970s were directed toward pressure vessels and nuclear industry, and as a result of a number of failures on welded pressure vessel construction in Japan, attention was focused on the potential defects in the welded joints. The very first acceptance criteria for defect size were developed (in UK) during late 60's (Harrison, Burdekin, and Young 1968)

Based on theory, Burdekin (1979) provided a number of equations for calculations of SCFs for butt welded steel flat plates. Major deviations, from ideal configuration, at a weld location such as misalignment, and angular distortion (Figure 2-19) were considered as well as ovality for tubular members.

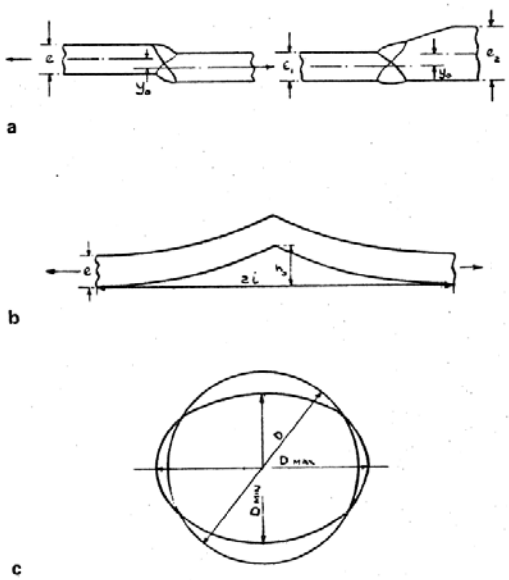

Fig. 1 Types of misalignment and distortion considered

a offset misalignment
b angular distortion
c ovality

Figure 2-19 Types of Misalignment

Burdekin (1979)

In general, the definition of stress concentration factor can be given as:

$$\sigma = \sigma_n + \sigma_b \qquad \text{Eqn 2.9}$$

$$\sigma = \sigma_n(1 + \frac{\sigma_b}{\sigma_n}) = \sigma_n * SCF \qquad \text{Eqn 2.10}$$

Where:

σ = stress due to deviation

σ_b = bending stress

σ_n = nominal stress

For plates of equal thickness (t) welded with a misalignment (e) Burdekin's equation is given below (Please note change in nomenclature from Figure 2-19), this equation is also derived independently by others.

$$\sigma_b = \frac{3e}{t}\sigma_n$$

$$\sigma = \sigma_n(1 + \frac{3e}{t}) \qquad \text{Eqn 2.11 a \& b}$$

$$SCF = 1 + 3e/t \qquad \text{Eqn 2.12}$$

Where:

e = eccentricity due to misalignment

t = thickness of plate

σ_b = bending stress

σ_n = nominal stress

This equation, for steel plates of equal thickness, is identical to the equation derived for aluminium by Gunn & McLester (1960)

The equation provided by Burdekin (1979), for steel plates of unequal thickness, is given below:

$$\frac{\sigma_b}{\sigma_n} = \frac{3\left(\frac{t_2}{t_1} - 1\right)}{\left(1 + (\frac{t_2}{t_1})^3\right)}$$

Where: t_1= thinner member, t_2, thicker member

σ_n = Nominal stress in the thinner member

Eqn 2.13

$$SCF = 1 + \frac{\sigma_b}{\sigma_n} = 1 + \frac{3\left(\frac{t_2}{t_1} - 1\right)}{\left(1 + (\frac{t_2}{t_1})^3\right)}$$

Eqn 2.14

Finally, for tubular specimen with ovality the derived equation is given as:

$$\frac{\sigma_b}{\sigma_n} = 1.5\frac{D_{\max} - D_{\min}}{t}$$

Eqn 2.15

$$SCF = 1 + \frac{\sigma_b}{\sigma_n} = 1 + 1.5\frac{D_{\max} - D_{\min}}{t}$$

Eqn 2.16

In 1979, J G Wylde conducted basic research with the aim of providing basic data upon which the severity of defects can be assessed on a fitness for purpose basis. He reported a number of further test carried on 12.5mm thick specimens with 25,50,75,100% misalignment and found considerable reduction in fatigue strength. He utilized the equation proposed by Berge

and Myher in 1977 and recommended the same equation for SCF with parameter λ equal to 6

$$SCF = 1 + \lambda\ e/t * \psi/L \qquad \text{Eqn 2.17}$$

Obtaining the same equation as others:

$$SCF = 1 + 3e/t \qquad \text{Eqn 2.18}$$

Where:

t = thickness,

e = misalignment and

λ = a non-dimensional parameter dependent upon the degree of restraint imposed upon the joint. For conventional fatigue specimen supported at mid-point Ψ=L/2, where L is length between restraint points.

Wylde, (1979), compares the experimental results with the above equation and his comparison is shown in Figure 2-20.

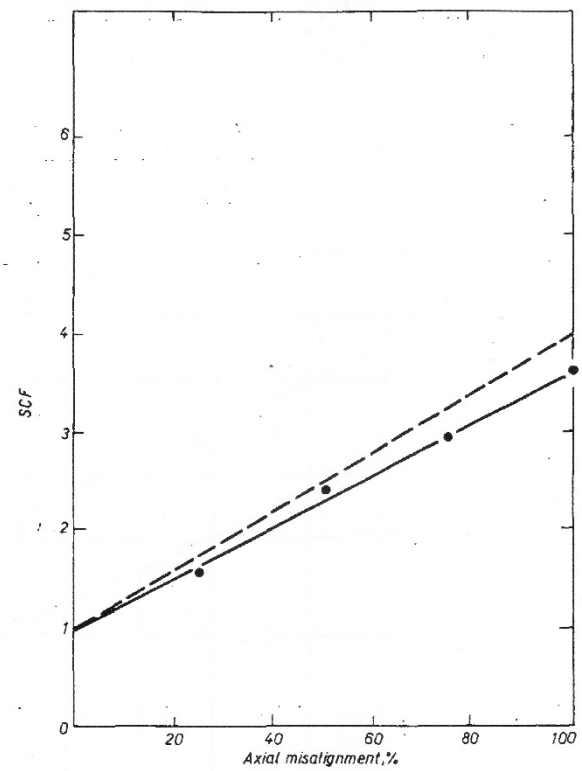

Fig. 13. Comparison between measured values of SCF and those predicted by eq. 2. ● — experimental values; - - - - values predicted from $K_t = 1 + \lambda \frac{el}{tL}$ taking $\lambda = 6$ and $l = \frac{L}{2}$.

Figure 2-20 SCF Comparison: Test vs Equation

Extracted from Wylde, (1979)

It can be seen that the given equation provides a conservative estimate compared with the test results.

In a published paper by Maddox (1985), it is stated that, at that time, many codes included acceptable level of misalignment based on workmanship, however, these acceptance criteria would not be sufficient for fitness for purpose assessment.

Hence he performed a number of studies on butt welded steel plates, Maddox, (1985, 1997), and provided design equations for plates based on tests within a specific range.

Similar to Burdekin (1977), Maddox (1985) provided the following analytical solutions:

Actual stress is nominal stress plus bending stress due to misalignment which can be written as:

$$\sigma_{actual} = \sigma_{nominal} + \sigma_{bending}$$

Hence effect of misalignment could be viewed as geometric SCF given by

$$\sigma_{actual} = SCF * \sigma_{nominal}$$

where:

$$SCF = (\sigma_{nominal} + \sigma_{bending}) / \sigma_{nominal}$$

$$SCF = 1 + (\sigma_{bending} / \sigma_{nominal}) \qquad \text{Eqn 2.19}$$

$\sigma_{nominal}$ = for unequal thicknesses nominal stress is in the thinner member

Misalignment of equal thickness flat plates

$$SCF = 1 + 3e/t \qquad \text{Eqn 2.20}$$

Misalignment of unequal thickness flat plates

$$SCF = 1 + \frac{3}{2} * (\frac{t_2}{t_1} - 1) \qquad \text{Eqn 2.21}$$

However, Burdekin (1977) had noted the effect of stiffness of the two plates. By introducing the condition that the slopes of the two plates as a result of induced bending moment should be equal at the joint, Burdekin provides the following equation:

$$SCF = 1 + \frac{3\,[(\frac{t_2}{t_1}) - 1)]}{[(1 + (\frac{t_2}{t_1})^3)]}$$

Eqn 2.22

Finally, Maddox (1985), proposed the following equation for axial misalignment between plates of unequal thicknesses with a total eccentricity at the centreline (e) including difference in thicknesses and misalignment.

$$SCF = 1 + \frac{6e}{t_1}\left(\frac{t_1^3}{t_1^3 + t_2^3}\right) = 1 + \frac{6e}{t_1}\left(\frac{1}{[1 + (\frac{t_2}{t_1})^3]}\right)$$

Eqn 2.23

Maddox then performed experimental tests and based on the results concluded that the above equation (Eqn 2.23) would be more applicable if the exponents are reduced to 1.5 instead of 3, giving:

$$SCF = 1 + \frac{6e}{t_1}\left(\frac{1}{[1 + (\frac{t_2}{t_1})^{1.5}]}\right)$$

Eqn 2.24

However, no guidance was given for the tubular circumferential welds.

2.10. HISTORICAL WORK – FOCUSED RESEARCH

Heshmati et al (1986) specifically provided a practical design curve for single sided circumferential girth welds on offshore jacket members.

Based on finite element studies and fracture mechanics SCFs were related to the thickness ratio of tubular members for single sided weld with fabrication misalignment of 0.1t and different weld flaw sizes. The usual transition slope of 1:4 as recommended by design and fabrication codes and the UK Department of Energy Guidance Notes 1974, were assumed. This work was a risk based assessment relating design, fabrication, and inspection at these critical joints.

The work again was constrained by the use of the thickness ratios and thickness transition slopes customary at that time. The SCFs obtained for this type of circumferential butt welded tubes with and without root defects are given below.

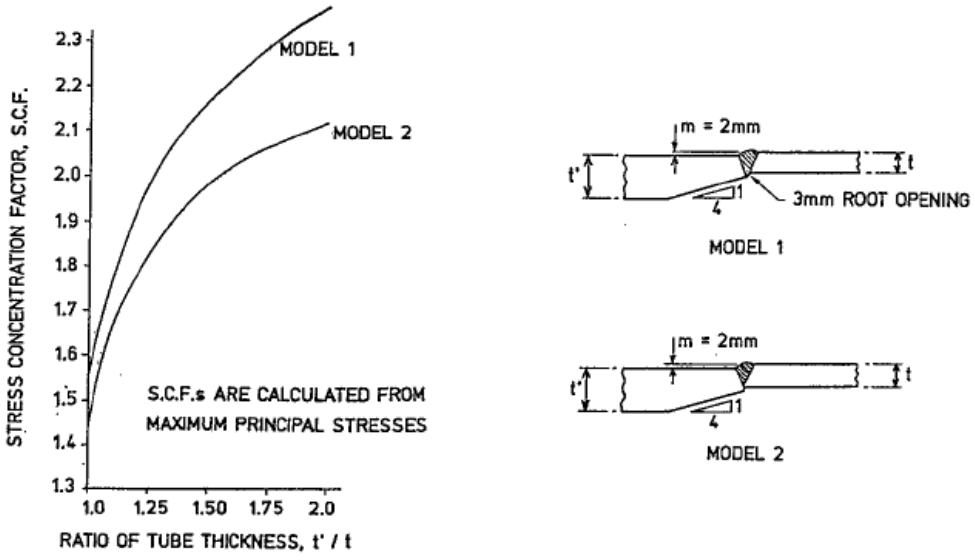

Figure 2-21 SCF Model Comparison

Heshmati et al 1986, Offshore Technology Conference, OTC 5153

Heshmati et al (1986) recommended a curve for determination of SCF for single sided closure welds as given in Figure 2-22. This curve was used to design many assets owned by British Petroleum such as BP South East Forties and BP Miller platform structures in the North Sea.

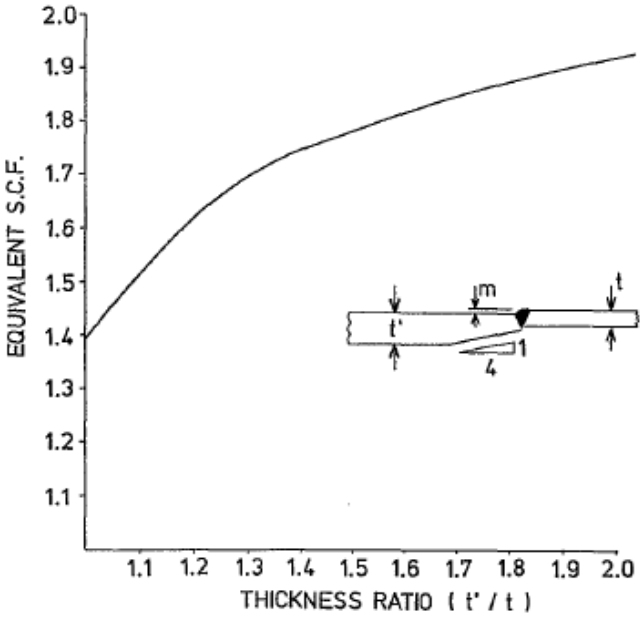

Figure 2-22 SCF vs Thickness Ratio

Heshmati et al 1986, Offshore Technology Conference, OTC 5153

Connolley and Zettlemoyer (1993) later on used finite element analyses and provided design equations and compared the equations to experimental test result. Test results for thicknesses in the ranges up to 25mm for both plates and tubulars with varying axial misalignment were provided.

These studies were based on an assumed equation as follows:

$$SCF = 1 + a\frac{e}{t_1}\left(\frac{1}{[1+b(\frac{t_2}{t_1})^n]}\right) \qquad \text{Eqn 2.25}$$

The equation is very similar to Maddox equation with parameters a, b and n to be determined.

In their work, Connolley and Zettlemoyer (1993), for plate models, t_2/t_1 ratio is up to 2, where t_1 is the thinner member. For tube models t_2/t_1 ratio varies between 1 and 3.57. The maximum plate thickness of the specimen used in the tests was 25mm.

The best fit equation to the experimental data was given as

$$SCF = 1.0 + 2.6\frac{e}{t_1}\left(\frac{1}{[1+0.7(\frac{t_2}{t_1})^{1.4}]}\right)$$

Eqn 2.26

Based on the assumption of a transition slope of 1:4 the equation was further adjusted to provide a conservative value and was given as

$$SCF = 1.2 + 6.2\frac{e}{t_1}\left(\frac{1}{[1+3.1(\frac{t_2}{t_1})^{1.4}]}\right)$$

Eqn 2.27

This again assumed 1:4 transition slope limitation which may not be optimal for thicker sections, but it is used as a norm in the industry.

In their research Connolley and Zettlemoyer (1993) made a number of parametric assessments.

- Effect of sharp notch
- Effect of thickness ratio t_2/t_1
- Effect of eccentricity e/t_1

a) Effect of Sharp Notch

A study was performed to determine the effect of presence of a notch at the weld. SCFs for models (Figure 2-23) with no taper (a straight notch) and with a taper with a transition slope of 1:4 were determined. It was concluded that the notch effect with no taper model was much greater than for the sloped model.

Connolley and Zettlemoyer (1993), state that as the notch effect is included in the determination of S-N curves the 1:4 taper and its effect was considered to be reasonably represented in the S-N curves.

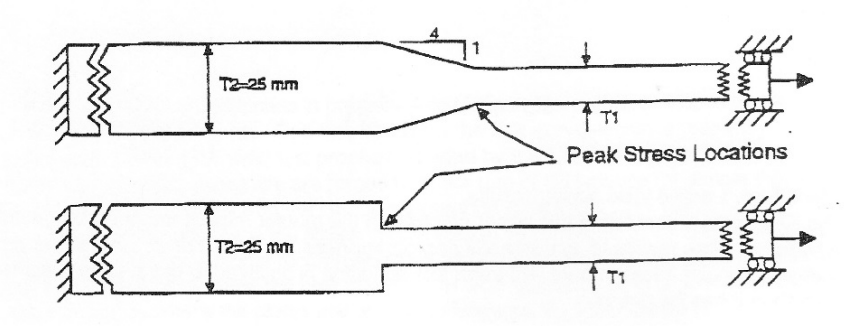

Figure 2-23 Notch and Transition Models

Extracted from Connolley and Zettlemoyer (1993)

b) Effect of Thickness Ratio

Connolly and Zettlemoyer (1993) evaluated the variation of SCFs against t_2/t_1 with variation in e/t_1 and found that for a constant e/t_1 as t_2/t_1 increases the SCF decrease.

c) Effect of Eccentricity

Connolly and Zettlemoyer (1993) also evaluated the variation of SCFs against eccentricity e/t_1 and found that as e/t_1 increases the SCF increase.

2.11. HISTORIC WORK – MORE RECENT

Maddox (2005) states that finite element analysis of misaligned girth welds has shown that Connolly and Zettlemoyer (1993) equation can seriously underestimate SCF for well-aligned joints.

Consequently, based on work presented in Maddox (2004) the BS7910 now recommends that:

- Small misalignment in girth welds be assessed using the simple plate equation as follows:

$$SCF = 1 + 6\frac{e}{t\min}\left[\frac{1}{1+\left(\frac{t\max}{t\min}\right)^{1.5}}\right]$$

Eqn 2.28

- Connolly and Zettlemoyer (1993) equation be used only when SCF is greater than 2.

Lotsberg (2009) carried out a series of FE analyses with the aim to further improve upon previously published equations.

An equation for plate has been developed based on the shell theory as

$$\mathrm{SCF} = 1 + \frac{6(\delta_t + \delta_m)}{t}\frac{1}{1+\left(\frac{T}{t}\right)^{2.5}}e^{-\alpha}$$

where

$$\alpha = \frac{1.82L}{\sqrt{Dt}}\cdot\frac{1}{1+\left(\frac{T}{t}\right)^{2.5}}$$

Eqn 2.29

In the above equation the exponent for (T/t) for flat plates is 1.5 and adjusted for tubular members for D/t of 20 to be 2.5 as given in the equation.

He then further modified the equation to have a variable exponent β as follows :

$$SCF = 1 + \frac{6(\delta_t + \delta_m - \delta_0)}{t} \frac{1}{1 + \left(\frac{T}{t}\right)^{\beta}} e^{-\alpha}$$

where

$$\alpha = \frac{1.82L}{\sqrt{Dt}} \cdot \frac{1}{1 + \left(\frac{T}{t}\right)^{\beta}}$$

$$\beta = 1.5 - \frac{1.0}{Log\left(\frac{D}{t}\right)} + \frac{3.0}{\left[Log\left(\frac{D}{t}\right)\right]^2}$$

Eqn 2.30

However, these models are still limited to a transitions slope of 1:4 and thickness ratio of T/t less than or equal to 2 and based on lower thickness ranges (20-40 mm) but include a variable for D/t.

Lotsberg (2009) considers a D/t range of 10 to infinity which is not practical but analytical.

The practical design range of D/t ratio is between 15 and 120. D/t ratio of 15 is being limited by rolling and fabrication facilities capabilities and D/t of 120 is being limited by buckling requirements. Therefore although the practical range is being covered but Lotsberg's emphasis is on a much larger theoretical range.

Lotsberg's equations have been incorporated into DNVGL Standard DNVGL-RP-0005 (2014) with some modification. This code distinguishes

between transition slopes being outside or inside the tube as shown on extracted figures from the code, Figure 2-24 and 2-25

When the transition is from outside Figure 2-24 the above equations can be used to estimate the SCF for the outside hotspot location shown, provided T/t is less than or equal to 2. Transition from outside is unusual for offshore jackets, as constant outside diameter is a common general requirement for jacket design.

If the transition is from inside Figure 2-25 and welded from outside, the code again requires the above equation be used for the inside hotspot location.

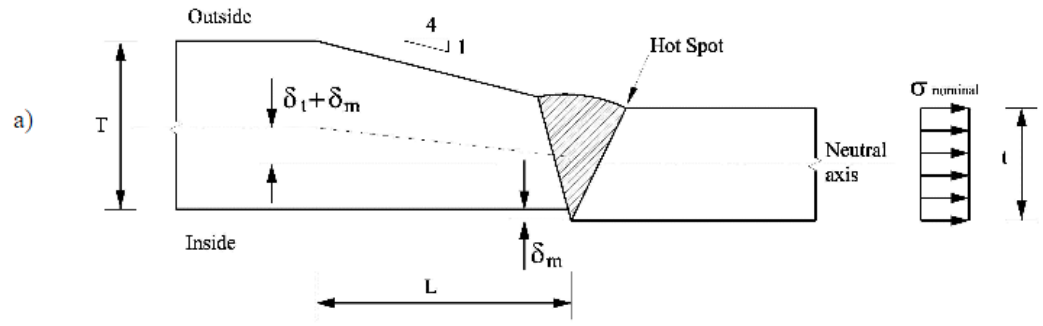

Figure 2-24 External Slope Transition

Extracted from DNVGL-RP-0005 (Figure 3.12a)

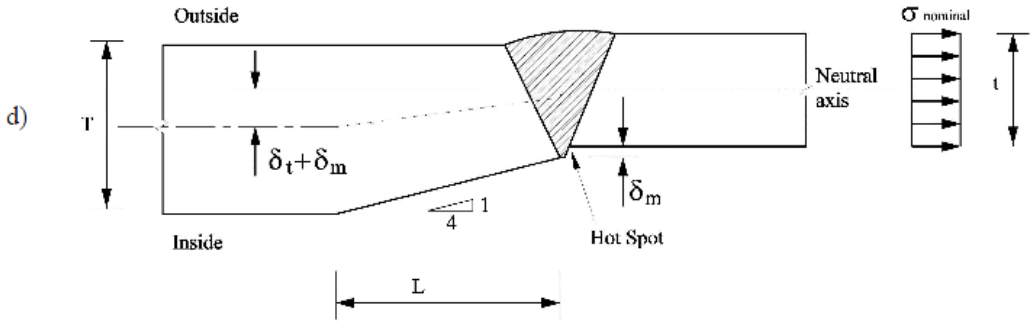

Figure 2-25 Internal Slope Transition

Extracted from DNVGL-RP-0005 (Figure 3.12d)

The above code also states that if the weld is made from both sides and the transition is inside the same equation can be used for the inside hotspot.

The following equation can then be used for the weld toe on the opposite side without the transition:

$$SCF = 1 - \frac{6(\delta_t - \delta_m)}{t} \frac{1}{1 + \left(\frac{T}{t}\right)^{\beta}} e^{-\alpha}$$

Eqn 2.31

2.12. THE LIMITATIONS

Although these historic equations proposed by researchers provide many advancement, however, the equations have a number of limitation as they are based on one or more of the following:

1. Majority are based on welded plate tests
2. Very limited welded tube tests
3. Fairly limited experimental data
4. Limited to plate thicknesses less than 50mm
5. Limited to slope of 1:4
6. Limited to thickness ratios less than 2

During the 1970's and 1980's, at the peak of jacket platform fabrication in the UK, Department of Energy Guidance Notes (1974) stipulated the use of 1:4 thickness transition slope with a limitation of joining plate thickness ratios to 2:1 (ie larger to smaller thickness of tubes connected at a joint), and a maximum misalignment of 0.1 times the thinner thickness at a joint.

Since early 90's Fabrication Guidance EEMUA 158 (1994, 2000, 2014) recommends 0.1t (t being the thinner member thickness) or 3mm as maximum misalignment for one sided weld and 6mm for two sided weld.

Most offshore platforms were being designed and built to these required industry practices and standard since early 80's.

In summary, many theoretical, numerical and experimental testing methods have been employed to develop SCF equations and graphs for practical design purposes. However, these studies have been limited to the lower ranges of thickness with thicknesses from 12mm to 45mm, and often results are extrapolated to other thickness ranges.

Heshmati in 1990, has conducted research to obtain an upper limit of plate thicknesses most suitable for complex nodal construction to minimize SCFs on complex joints. In a published paper, Heshmati (1990), produced a series of graphs addressing the issue with a conclusion that the maximum practical upper thickness limit for nodal construction is about 125mm. His conclusions were based on tubular joint SCF equations, rolling mill and fabrication capabilities and cost of steel plates.

Since then, use of thick walled nodal construction accelerated and replaced the more common ring stiffened nodes customary at the time.

More recent Design Codes such as HSE Report OTO-022 (1999), BS 7910 (2015), Eurocode EN 1993-1-9 (2005), DNV-RP-C203 (2010), and DNVGL-RP-0005 (2014) do contain guidance for design which is based on specific thickness ranges and specific weld geometry and do not cover some other details.

2.13. PRACTICAL CHALLENGES

Majority of offshore pipelines, tendons, caisson and other components of structures fall within the general assumption of a thickness ratio of 2:1 as stipulated by the codes of practice.

However, as shown by Heshmati (1990) in the construction and fabrication of offshore platform structures, nodal joints usually require thicker sections on the chord members to satisfy fatigue requirements by reducing SCFs, and in many cases uses of very thick chord plates up to 125mm in fabricated nodes are required. More recently cast steel nodes with ultra-thick section in excess of 150mm are used.

On the leg sections, in between the thick walled chords on the nodes, however, strength and buckling requirements do not require as thick a section as adjacent nodes and much smaller thicknesses satisfy the requirements. This situation sometimes calls for thickness ratio in excess of 2:1 which falls outside what has been the main assumption of the previous studies and code of practice requirements.

Considering the case where a thick walled chord on a node is required to be connected to members with much smaller thickness where the thickness ratio is more than standard 2, the option that is usually available to the designer is to use what is called a pup-piece as show in Figure 2-26. A pup-piece is a tube of usually 1-1.5m length with an intermediate thickness between the node chord and the member thickness. This is the usual option that is available to a designer to comply with the codes and standards.

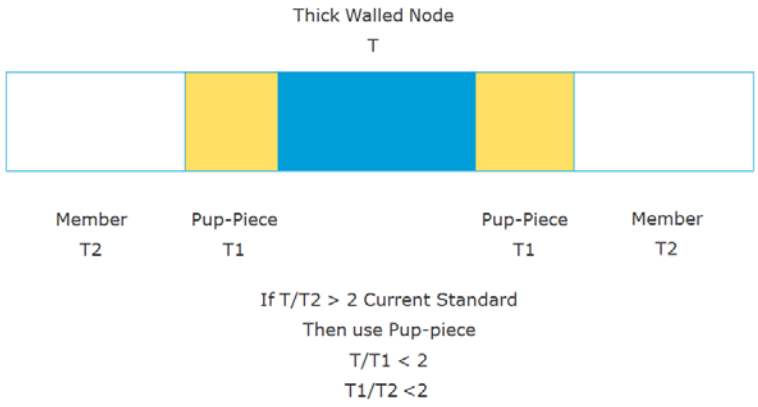

Figure 2-26 Pup Piece

However, this option usually requires extra material and two additional welds hence adding considerable fabrication time and expense as the two extra welds are between thick walled tubes.

As an example of this situation, the actual design from a North Sea platform is shown in Figures 2-27 to 2-29, which indicate a node of 2000mm diameter by 100mm thickness to be joined with two members either side 2000mm diameter by 40mm thickness which falls outside the stipulated requirement in the design and fabrication codes and standards with a thickness ratio of less than or equal to 2. The actual thickness ratio is 100/40 = 2.5.

Considering this case on four jackets legs, requires additional 8 Pup-Pieces and 8 extra welds between 100mm and 70mm plates.

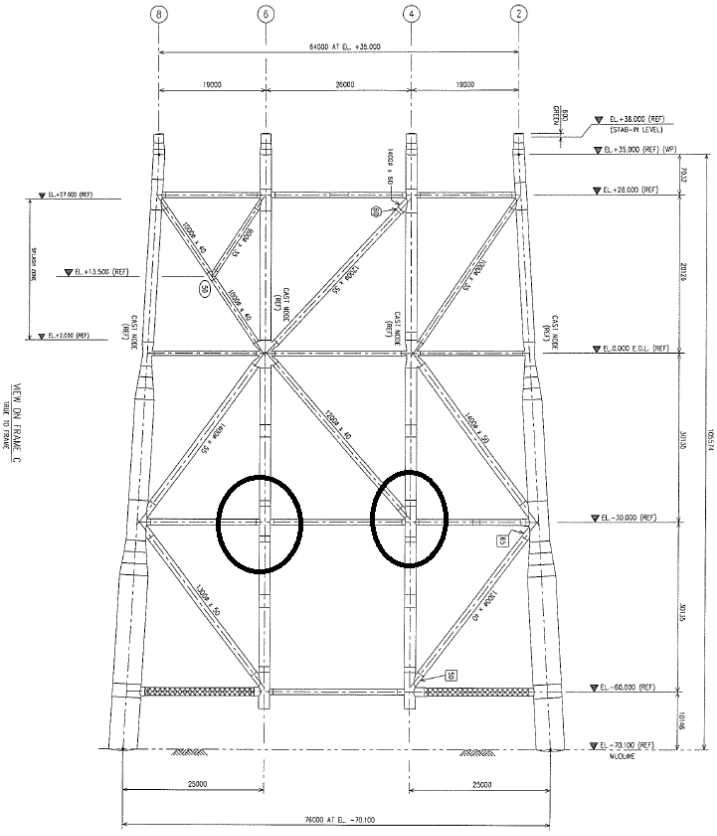

Figure 2-27 Jacket Frame with Thick Walled Node and Pup-pieces

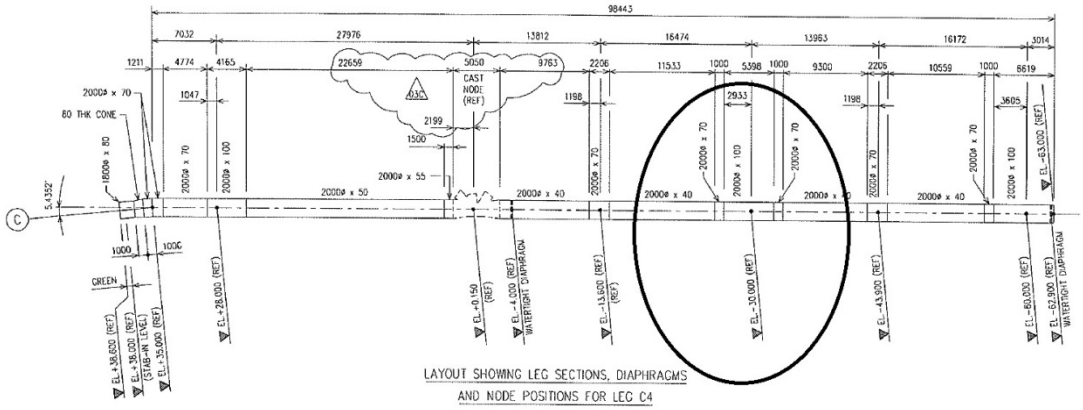

Figure 2-28 Jacket Leg with Thick Walled Node and Pup-pieces

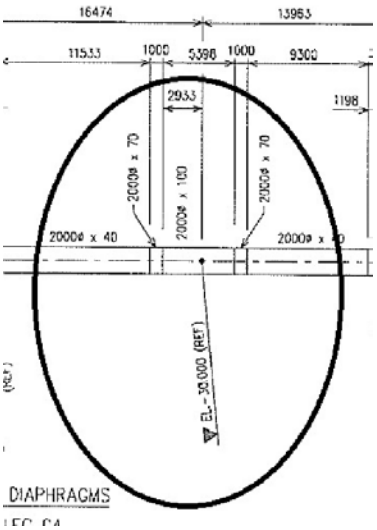

Figure 2-29 Thick Walled Node and Pup-pieces

During past two decades capability of rolling presses and fabrication methods of tubular members have improved which allow common use of these thicker plates to facilitate weight optimisation and more elegant design solutions.

Although FE methods have improved substantially and computer hardware and software advance continually not much effort has been directed to use these technological advances to review these SCF formulations further for the required higher thickness ranges.

Therefore, currently, limitations are imposed by the codes and standards which are based on limited number of test data in 1970's, 80's and 90's on much thinner test specimens. Practical design situation are, hence, constrained due to limitation outlined above with substantial penalties on steel weight, material and fabrication costs.

Chapter 3

Present Research

3. PRESENT RESEARCH

In this research project a number of practical issues, will be investigated by the use of Finite Element Analysis, and are as follows:

3.1. HIGHER THICKNESS RANGE

Majority of previous studies as described in Chapter 2, either numerical or experimental have focused on joints with thinner plate thickness ranges below 50mm.

However, many offshore platform designs in deeper waters and harsh environment incorporate nodes with chord thicknesses up to 125mm or more produced from fabricated plates or cast nodes in excess of 200mm. In order to evaluate joints within the higher thickness ranges, a number of studies will be performed to evaluate and review the findings for these higher thickness ranges up to 125mm.

3.2. THICKNESS RATIOS

In the past the adjoining tubular thickness ratios (ratio of thicker member to thinner member) have been limited to 2 or less. This limitation has been accepted in industry practices during late 70's and early 80's but has not been reviewed or re-evaluated since.

The use of other thickness transitions in excess of 2 although allows for more efficient design, their use is prevented by the industry practice as a result of not been assessed or allowed for in the codes and standards.

Studies will be performed to define and provide guidance for alternative higher acceptable thickness ratios which may prove to be more practical.

3.3. THICKNESS TRANSITION SLOPES

Currently almost all of platform designs are based on a thickness transition slope of 1 in 4 between the two adjoining tubular members. This is due to standard of practice since the early days of offshore fabrication in 1970's.

However, on many occasions it is necessary to use other transition ratios to optimise weight and fabrication costs. No public study or data is available for these potential alternatives as yet. Studies will be performed to investigate efficacy of other transition slopes from 1 in 2 down to 1 in 10.

3.4. THICKNESS TRANSITION CONFIGURATIONS

In practice alternative configurations are available for joining tubulars, namely diameter inside matching, outside matching and centreline matching (Appendix A). The first two types of joints can be welded either from one side or both sides depending on the pipe diameter. However, the last method requires welding from both sides.

The effect of these alternatives on SCFs will not be investigated as they depend on the required design philosophies and do not affect current research.

In this work outside matching configuration which is most common will be assessed.

3.5. USE OF FINITE ELEMENT METHODOLOGY

Previous studies which have concentrated on smaller thicknesses (6mm-50mm) have conventionally employed the use of thin shell finite elements in their models to assess these practical issues.

However, for larger thicknesses, eg 50mm to 125mm, solid elements may be required for modelling purposes. An initial study will be performed to

compare these modelling methods and assess their suitability for application to thick sections.

3.6. FABRICATION IRREGULARITIES / TOLERANCES

A major issue for fatigue life estimation of circumferential weld is fabrication defects which affects the SCFs. These include fit-up mismatch thickness tolerances and mismatch due to ovality of tubular members which is controlled by tolerances within a certain allowable limits as per EEMUA 158. The effect of these mis-matche tolerances on the SCFs will not be fully investigated. These fabrication tolerances do not affect the SCF trend assessment which is the aim of this work. However, some indicative assessments are made.

3.7. EXPERIMENTAL INVESTIGATIONS

Due to very high expense and heavy equipment required for experimental testing of the members with large diameter and thickness (eg 3.5m diameter and 125mm thickness) this research work does not involve physical testing of joints.

3.8. CONFIGURATIONS

In general terms, codes and recommended practices provided by authorities consider only geometric SCFs at the hot spots for design and effects of notches and welded fabrication are considered and allowed for in the design S-N curves, using physical tests.

This research is only focusing on the joint configuration profiles for outside matching tubes with internal transitions without any fabrication fit-

up misalignments or welding defects due to workmanship and SCFs obtained are at the geometrically critical point with high SCF as shown in Figure 3-1. The aim is to obtain a trend in variation of underlying SCFs due to different configurations rather than the actual best estimate of SCF for design, which may require assessing the effect of including other misalignments and welding defects.

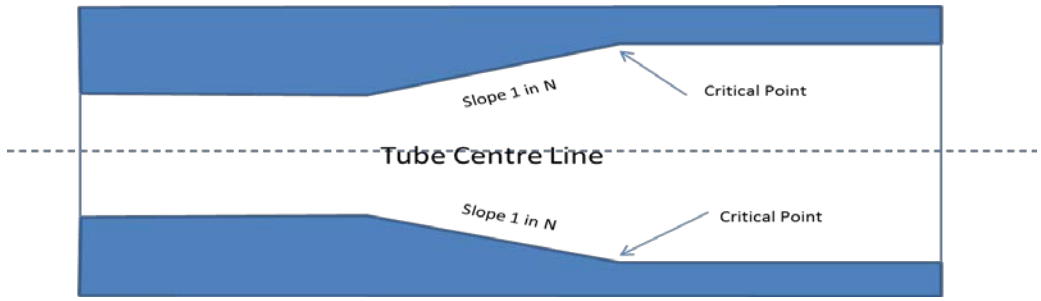

Figure 3-1 Tube Cross Section and Critical Points

Chapter 4
Analysis Methodology

4. ANALYSIS METHODOLOGY

4.1. BACKGROUND

During the years many methodologies have been developed for assessment of fatigue performance of welded structures. According to Ye, et al, (2014), classic fatigue analysis approaches can be divided into three; and then the first approach can be subdivided further:

a. Stress-life (S-N) methods:

    1. Nominal stress,
    2. Structural hot spot stress,
    3. Effective notch stress

b. Fracture mechanics approach,
c. Strain-life (ϵ-N) method

These Methods can generally be divided into global and local approaches and assessments can be based on strains, stresses, or stress intensity factors and are explained further in the following paragraphs.

Ye, Su and Han (2014), explain that :

a. Stress-Life Approach is suitable for high cycle fatigue for structures that operate within the elastic range. The method is based on determination of stresses and use of S-N curves and the Palmgren-Miner's rule to predict fatigue life. Further subdivisions of the approach are based on the method of obtaining the stresses.

According to Marquis and Samuelsson (2005)

1. The nominal stress method is a global approach based on general stress due to applied loads at the local section with local cross sectional properties taking into account gross changes in geometry. Stress can also be determined using Finite Element Method at the location. In this method local geometry and properties of the weld are not specifically evaluated but are included in the corresponding detail class and S-N curve.

2. The structural hot spot stress method is a local approach; the approach accounts for all stresses created at the structural detail, but exclude the stress concentration due to the local weld profile itself. Local weld effects are included in the S-N curve, but exclude details of notch effect caused by the weld. However, the effect of local weld toe geometry can be included in the analyses using notch stress or strain methods as explained by Radaj and Sonsino (1998).

   The structural hot spot stress approach is more commonly used to assess spot welded joints in thin sheet metal structures of the type used in automotive engineering, Radaj (1996).

3. There are a number of different notch stress approaches and more relevant information and references are given in Radaj (1996). These methods basically use maximum

stress at the root/toe of a weld or notch taking into account stress concentrations due to the effects of structural geometry as well as the presence of the weld,

b. Fracture Mechanics Approach is concerned with determination of life based on initiation and propagation of a fatigue crack to failure. In Linear Elastic Fracture Mechanics (LEFM) the initiation and growth of a crack is related to number of cycles to failure, (Ye, et al , 2014).

c. Strain- Life Approach
   This method was developed in 1960's (Ye et al, 2014) and is generally used for Low Cycle Fatigue and is concerned with crack initiation when the strain is no longer elastic.

Details of these approaches are given in Maddox (1991), Hobbacher (2003), Eurocode EN 1993-1-9 (2005), Niemi (2000) and Radaj & Sonsino (1998).

All these methods are also included in the IIW (International Institute of Welding) recommendations.

Marquis and Samuelsson (2005) graphically present the accuracy and complexity of these approaches as reproduced in Figure 4-1.

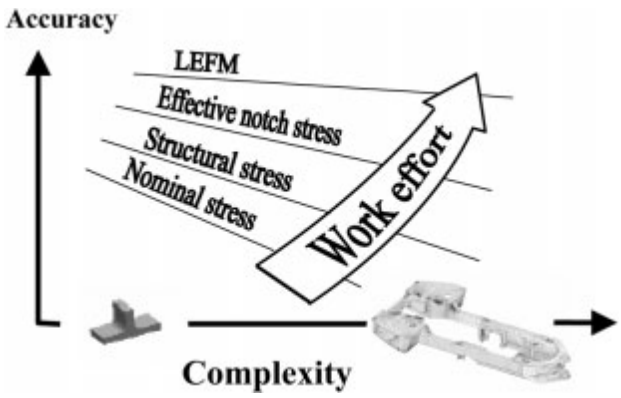

Figure 4-1 Fatigue assessment approaches: Accuracy vs Complexity

The simplest, Nominal Stress, approaches are generally utilized by the codes and standards but for complex details and structures other methods are generally employed, especially LEFM.

With increasing computer power Finite Element Analysis Methodology can be utilized to obtain stresses or geometric stress concentrations that can be used in fatigue analysis procedures.

However, accuracy of Finite Elements Analysis (FEA) Models depends on the element type, mesh sizes, meshing topology, type of numerical solution etc and a balance between the size of the model and the cost and accuracy suitable for the purpose of the analysis, hence, FEA is not exact but a good approximation method.

In the offshore industry the most common fatigue analysis procedure is based on Stress-Life Approach and the methodology where nominal stresses are augmented by the Stress Concentration Factor taking into account the stress raising effects due to geometry and using an appropriate S-N curve for which the weld effect is included in the S-N curves using fatigue testing of specimen with the specific weld geometry. This method is generally utilized for assessment of girth weld fatigue performance with SCFs obtained based on either equations or FEA.

4.2. STRUCTURAL MODEL

A philosophy has been adopted to use actual jacket leg dimensions from a number of jacket design projects to allow realistic assessment to be made and more useful and practical answers obtained.

The models use configurations, typical of jacket leg construction arrangement with large diameters and thicknesses. Jacket legs, directly support the topside structures and equipment and support the jacket structure space frame exposed to environmental wave and current loading which are constantly under varying and cyclic fatigue loading.

Jacket legs with large diameters of 2-3.5m are typical. The leg nodes with typical thicknesses of 80 to 125 mm are connected to jacket leg members with similar diameter and much thinner thickness of typically 30 to 45mm. Hence, creating thickness ratios in excess of 2 with large eccentricities and causing stress concentration points at the joints.

These types of joints are susceptible to large misalignments even with tight fabrication tolerances as a result of having centreline eccentricities due to large thickness differences.

Varying fatigue loads, combined with large static axial loads create critical locations with high stresses.

In order to assess the effects of higher thickness ratios and various thickness transitions, a number of Finite Element Models (FEM) within typical practical range of actual jacket fabrication cases have been considered.

4.3. SELECTION CRITERIA

4.3.1 Diameter to Thickness Ratios

In order to select realistic parameters, data from four UK North Sea jacket structures were obtained to determine the representative range of Diameter/Thickness (D/t) ratios on the leg sections and nodes.

Although many combinations are possible, the D/t ratio in real practice generally varies between values of 20 to 120 for typical jacket designs as shown in Table 4-1.

Similar D/t ratios for smaller brace members are possible and common.

Platform No 1 North Sea 1983		
Diameter	Thickness	
mm	mm	D/t
1800	75	24
1800	63	29
1800	50	36
1800	45	40
1800	35	51
2250	35	64
2250	75	30
2250	40	56
3250	40	81
3250	50	65
3250	90	36

Platform No 2 - North Sea 1995		
Diameter	Thickness	
mm	mm	D/t
2000	80	25
2000	65	31
2000	90	22
2000	50	40
2000	35	57
2000	55	36
1940	40	49
1800	80	23
3435	35	98
3435	100	34
5000	50	100
5000	45	111
5000	90	56

Platform No 3 - North Sea 2012		
Diameter	Thickness	
mm	mm	D/t
1500	75	20
1500	80	19
1700	85	20
1700	95	18
2000	60	33
2000	75	27
2000	80	25
2000	85	24
2000	90	22
2500	60	42
2500	65	38
2500	70	36
2500	75	33
2500	80	31

Platform No 4 - North Sea 2012		
Diameter	Thickness	
mm	mm	D/t
1500	45	33
1500	50	30
1500	75	20
1500	80	19
2000	45	44
2000	55	36
2000	60	33
2000	80	25
2500	55	45
2500	60	42
2500	90	28
2500	100	25

Table 4-1 D/t Ratios

The lower limit for D/t is approximately 20; however a value approaching 15 can sometimes be achieved for special cases based on rolling equipment available in the pipe mills at the request of designers and asset owners.

Also, in common design practice an upper limit of 80 for legs and 120 for braces are generally desired design limits.

Hence the values to cover the typical range of D/t are selected to be 40, 60, 80 and 120 which covers the most common range found in practice.

The limit of D/t equal to 120 is based on recommended practices such as NORSOK-N-004 "*Design of Steel Structures*" (2013) which states that there are two possibilities of failure for short tubular members under axial compression, such as those on jacket legs, either by Material Yielding or Buckling which depend on the D/t ratio of the member. Short members with low D/t are not usually subject to buckling and as the length increases possibility of local buckling increases.

The elastic local buckling stress formula and other nominal strength equations recommended in this code limits the dimensions to members with D/t less than 120 and t greater than 6mm.

API RP 2A allows different equations to be used with D/t less than 60 and D/t greater than 300 and in between. However, in commentary to the code clause C3.2, API states that the recommendation in the code are based on D/t less than 120 although equations are given up to 300. It also states that above D/t greater than 300 and high strength steels the equations may give conservative results.

API RP 2A also similar to NORSOK-N-004 (2013) states that with low values of D/t local buckling will be unlikely and limits the members with D/t less than 60 to be only checked for Material Yielding.

4.3.2 Diameter & Thickness Values

Four diameter/thickness (D/t) combinations have been selected to represent the variation of real jacket member sections with D/t of 40, 60, 80, and 120.

The sketch in Figure 4-2 shows a schematic jacket node/leg section. The thickness of the chord at the node (T) is assumed to vary between 50 to 125mm in steps of 25mm and the leg thickness (t) is set to be constant for each set of cases at either 25 or 50mm.

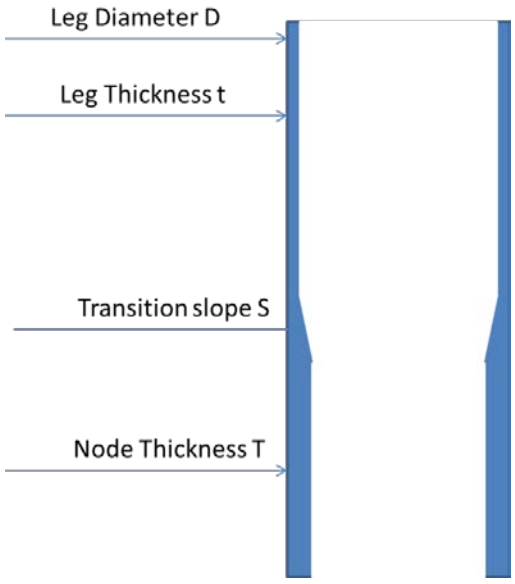

Figure 4-2 Schematic Jacket Node/Leg Section

The models considered for this study and selected cases for analysis are given in Table 4-2, which have been derived from an overall consideration of actual design values from Table 4-1.

Model	Case	Leg Diameter (D) mm	Leg Thickness (t) mm	Node Thickness (T) mm	D/t	T/t
1	1	3000	25	50	120	2
	2	3000	25	75	120	3
	3	3000	25	100	120	4
	4	3000	25	125	120	5
2	1	3000	50	75	60	1.5
	2	3000	50	100	60	2
	3	3000	50	125	60	2.5
3	1	2000	25	50	80	2
	2	2000	25	75	80	3
	3	2000	25	100	80	4
	4	2000	25	125	80	5
4	1	2000	50	75	40	1.5
	2	2000	50	100	40	2
	3	2000	50	125	40	2.5

Table 4-2 Selected Diameter and Thickness Combinations

Chapter 5
Finite Element Models

5. FINITE ELEMENT MODELS

ABAQUS Standard version 6.10, (2011), computer software has been used for all analyses. Full 3D models of joints without weld profile have been used in the analyses.

In general all model parameters have been standardized as much as possible as explained below.

The applied axial load is a pressure load of 1 unit so that the maximum Von Mises stress output represents the SCF directly. No weight has been generated for the model. Von Mises stress has been selected for the ductile steel under complex stress condition, and the thick sections under investigation.

5.1. COMMON ASSUMPTIONS

In all analyses some common constants have been used. The Elastic Modulus of Steel is assumed to be E=205GPa, Poisson ratio ν= 0.3 and density of steel, 7850 Kg/m$^{3.}$

5.2. SENSITIVITY STUDIES

Prior to modelling the study cases, a number of sensitivity studies were performed to assess the adjustments required for modelling purposes. These studies have been performed in such a way as to prevent excessively large models and limit the cost and time of analyses. Model length variations to assess boundary effects and model mesh variation sensitivities have been evaluated.

5.3. MODEL LENGTH SENSITIVITY

In order to assess and reduce the effect of boundary conditions and required distance away from the point of stress concentration, three models were analysed to study the length effect.

The models consists of 2m and 3m diameter tubes with varying thicknesses and slopes which give results as shown in Table 5-1. Results show that reducing the model length on either side of the transition from 1m to 0.5m would only affect the accuracy by less than 2%. Hence a 500mm length on either side of the transition has been used to limit the model size.

In addition, as in this study we are concerned with "trends of SCF variation" rather than focus on very high accuracy of the SCF values, the accuracy of results using shorter length model would be acceptable.

Diameter (mm)	T (mm)	t (mm)	Length (mm)	Slope 1 in	SCF Value
3000	50	25	1000	2	1.541
3000	50	25	500	2	1.577
2000	125	50	1000	2	1.747
2000	125	50	500	2	1.744
2000	125	50	1000	10	1.302
2000	125	50	500	10	1.302

Table 5-1 Length Sensitivity

A typical model cross section is shown in the Figure 5-1.

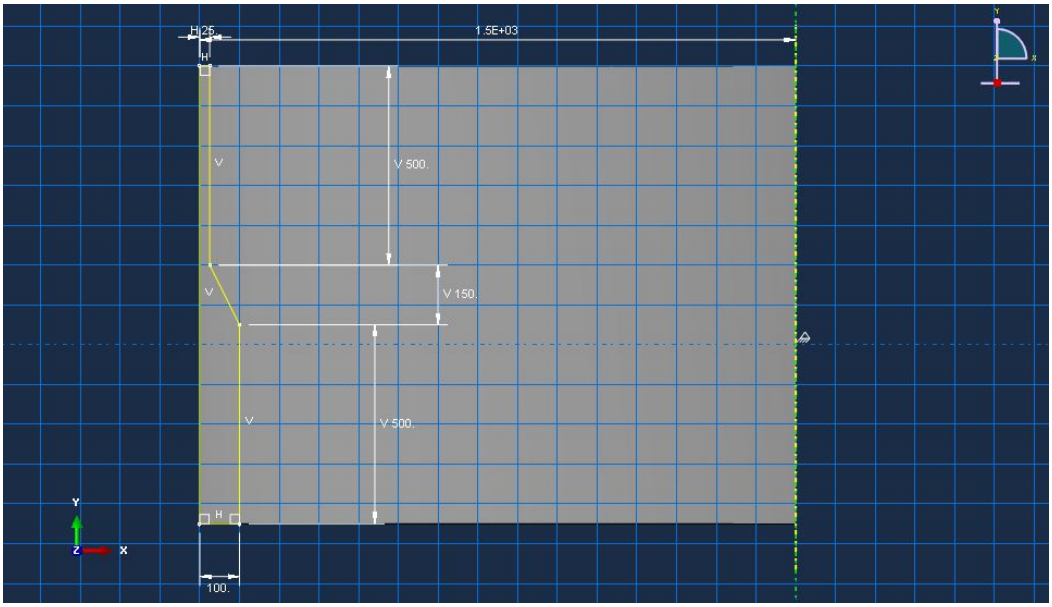

Figure 5-1 Typical Model Cross Section

5.4. MODEL MESH SIZE SENSITIVITY

The number of elements in the mesh across the thickness of the tube model affects the accuracy of the results. In order to obtain a reasonable element number with good accuracy a model with three different numbers of elements, 1, 2 or 3 elements across the thickness of the thinner member were studied. The results for the model with 3000mm diameter and T=50mm, t= 25mm and slope of 1 in 2 are given in Table 5.2:

No of Elements	Length of element (mm)	SCF Value
1	25	1.613
2	12.5	1.632
3	8.33	1.636

Table 5-2 Mesh Size Sensitivity for 3000 mm Diameter Model

As the results in Table 5.2 shows between 2 and 3 elements across the thickness the improvement in accuracy is marginal 0.2%, it was decided that 2 elements across the thickness would give enough accuracy for the purpose of the study.

The results for the model with 2000mm diameter, T=125mm, t= 50 mm and slope of 1 in 4 with various numbers of elements across the thickness is given in Table 5-3:

No of Elements	Length of element (mm)	SCF Value
1	50	1.204
2	25	1.282
3	12.5	1.356
4	6.25	1.424

Table 5-3 Mesh Size Sensitivity for 2000 mm Diameter Model

However, the results in Tables 5-3 show that models with two elements across the thickness for 50mm models are not accurate enough, for this case, and more refinement is necessary. Considering substantial increase in model size and element numbers with increasing refinement, the modelling criteria are based on the following selections:

- For models with the thinner thickness of 25 mm, each elements size is 12.5mm, with 2 elements across the thinner thickness.
- For models with thinner thickness of 50mm, again element size is 12.5mm, with 4 elements across the thinner thickness.
- For all model cases the element thickness is 12.5mm. Hence for the thicker section, model thickness is also a multiple of 12.5mm.

This practical standardization has been performed across all models, to provide high accuracy as well as keeping the models to a manageable number of total model elements less than 1 million elements.

A typical 3D Model is shown in Figures 5-3 and 5-4.

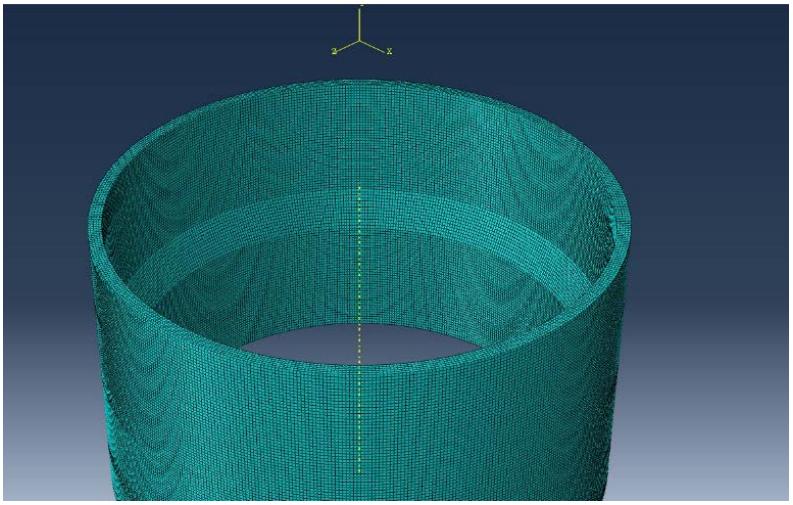

Figure 5-2 Typical 3D Model Mesh –General View

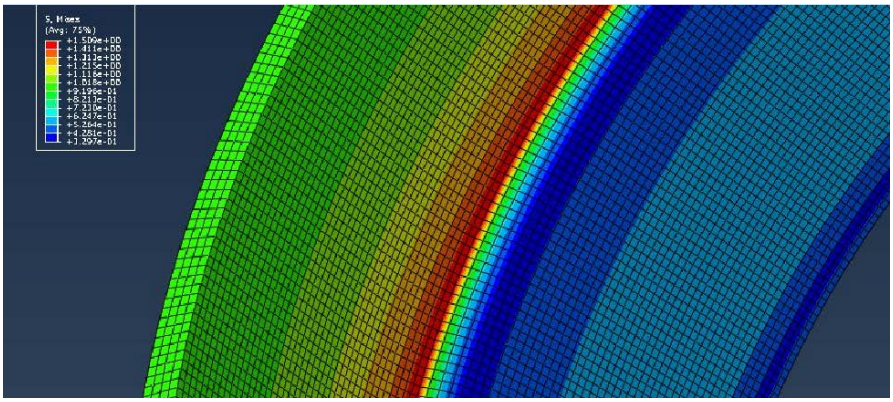

Figure 5-3 Typical 3D Model Mesh – Detailed View

5.5. MODEL ELEMENT CHOICE

The ELEMENT used for the finite element model from ABAQUS element library is C3D8, an 8 noded linear solid brick element.

The mesh and element size is based on the smallest practical size possible. The element size has been selected to have at least 2 elements across the thinner section of the model as explained in section 5.4.

In most previous studies using FEA for Stress Concentration Factor (SCF) estimation, axisymmetric thin shell elements have been used (Lotsberg, 2005) for many thin member sections up to 35-40mm.

However, in this work, use of solid element has been chosen throughout the model as the members are much thicker, up to 125 mm, than previously analysed and in the stress analysis stresses are better estimated using solid elements with more integration points. This is despite the fact that according to thin shell theory, Timoshenko & Woinowsky-Krieger (1959), the D/t ranges under study, are within applicability of the thin shell theory, and thin shell elements are still valid.

This type of solid element, Figure 5-4 and 5-5, suffers from the fact that integration points (stress calculation points) are within the element and do not represent the stress at the surface of the element, hence for more accurate absolute SCF estimation some extrapolation is required.

However, by using small elements and averaging of the stress values at all integration points a good approximation is obtained.

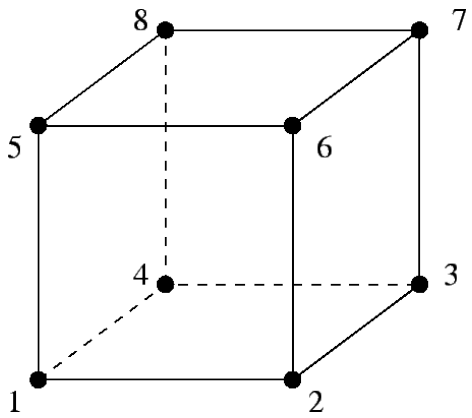

Figure 5-4 ABAQUS - C3D8 Element Node Numbers

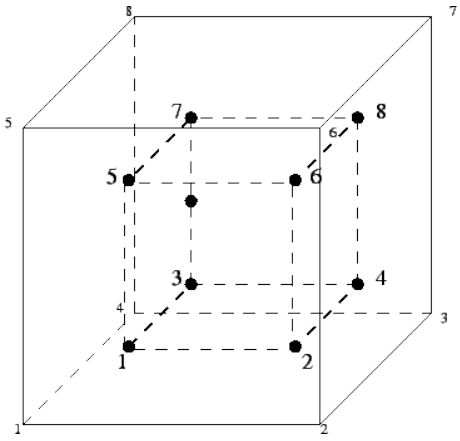

Figure 5-5 ABAQUS - C3D8 Element Integration Points

In addition, in this work, focus is on the trend and not the best estimate of SCF at the critical location. Therefore, the issue of internal integration points is considered not to be critical for this study.

5.6. THICKNESS TRANSITION SLOPES

A number of different thickness transitions slopes have been selected to be used for all cases as given in Table 5-4, which includes the current industry norm of 1 in 4. Slope of 1 in 2 is prohibited by all codes and standards as it is too close to a sharp notch but has only been added for theoretical comparisons in this study.

Thickness Transition Slope
1:2
1:4
1:6
1:8
1:10

Table 5-4 Thickness Transition Models

5.7. JOINT CONFIGURATION

The following joint size combinations, as described in section 4.3.2 and Table 4-2, have been analysed which cover typical design combination in mid leg sections of actual platform leg structures between the nodes:

Model	Node Diameter D mm	Leg Thickness t mm	D/t	Leg Diameter D mm	Node Thickness T mm
1	3000	25	120	3000	50,75,100,125
2	3000	50	60	3000	75,100,125
3	2000	25	80	2000	50,75,100,125
4	2000	50	40	2000	75,100,125

Table 5-5 Joint Configuration Models

5.8. INPUT SUMMARY

The input parameters that have been used in the assessment and analyses are summarized below:

For all models the steel properties as described in section 5.1 have been used for all analyses.

For each model, a constant diameter (D), and a constant thickness (t) representing thinner member have been selected, refer to Table 5-5, and Figure 5-6

- Models 1 & 2 Diameter D=3000, t= 25mm or t=50mm
- Models 3 & 4 Diameter D=2000, t= 25mm or t=50mm

Then for each model a number of variations of T/t have been used as follows with the upper limit of T being 125 mm

- Model 1 & 3 T/t varies as 2, 3, 4 and 5
- Model 2 & 4 T/t varies as 1.5, 2, and 2.5

For each Model and T/t, transition slopes (S) vary between, 1 in 2, 4, 6, 8 and 10, refer to Table 5-4 and Figure 5-6.

For each Model the loading is applied at the top of the model with unit pressure load on the thinner section. No structural weight has been included. The boundary condition at the bottom is fully fixed, Figure 5-6.

For each model the total length of the model varies with the length of the transition slope; however, after length sensitivity assessment a length of 500mm has been used on either side of the transition length, (refer to section 5.3).

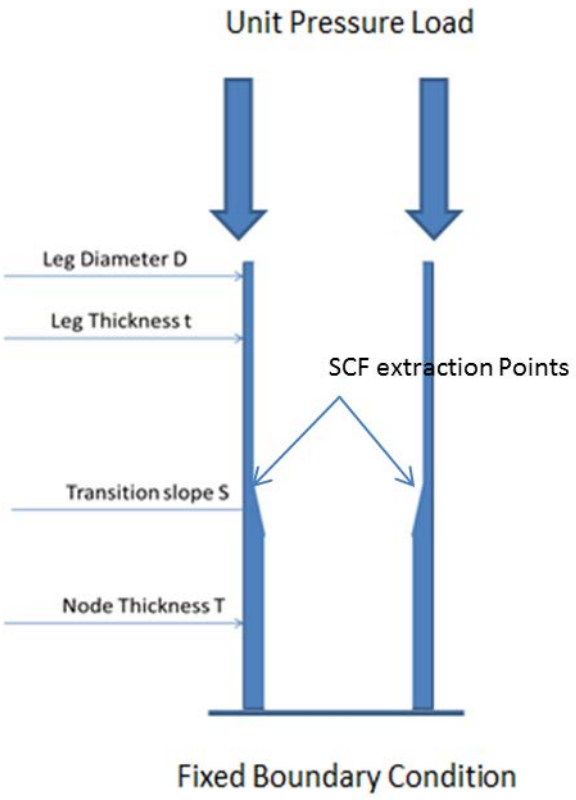

Figure 5-6 Loading, Boundary Condition, and Extraction Point

The application of unit axial pressure load to the thinner member, provides a unit nominal stress in the thinner member and simplifies the output to be read as SCF directly at the critical hot spot point (slope transition point at the thinner member) shown on the sketch in Figure 5-6 :

$$\frac{Maximum\ Output\ Stress}{Unit\ input\ Load} = \frac{Maximum\ Elevated\ Stress\ at\ the\ Hotspot}{Nominal\ Stress} = SCF$$

Chapter 6
Analysis Results

6. ANALYSIS RESULTS

6.1. FEA COMPARISON WITH DNVGL-RP-0005

Initially a model was created to assess FEA results against DNVGL recommended practice DNVGL-RP-0005 (2014) for a standard case within the limits.

The basic case chosen is a tube of 1000mm in diameter and thicknesses to be within the current T/t limits, hence T has been chosen to be 100mm and t to be 50mm with T/t =2 and D/t=20 and various transition slopes.

The results are given in Table 6-1. Strictly speaking only the case with transition slope of 1 in 4 is as per DNVGL recommended practice, all other slope cases are not within the limits.

However, from the results shown in Table 6-1 and Figure 6-1, it can be seen that DNVGL equation compared with FEA results provides a conservative values for all cases of alternative slope transitions

Slope	FEA	DNVGL
2	1.427	1.447
4	**1.324**	**1.395**
6	1.254	1.350
8	1.210	1.310
10	1.172	1.274

Table 6-1 Comparison of FEA and DNVGL Results

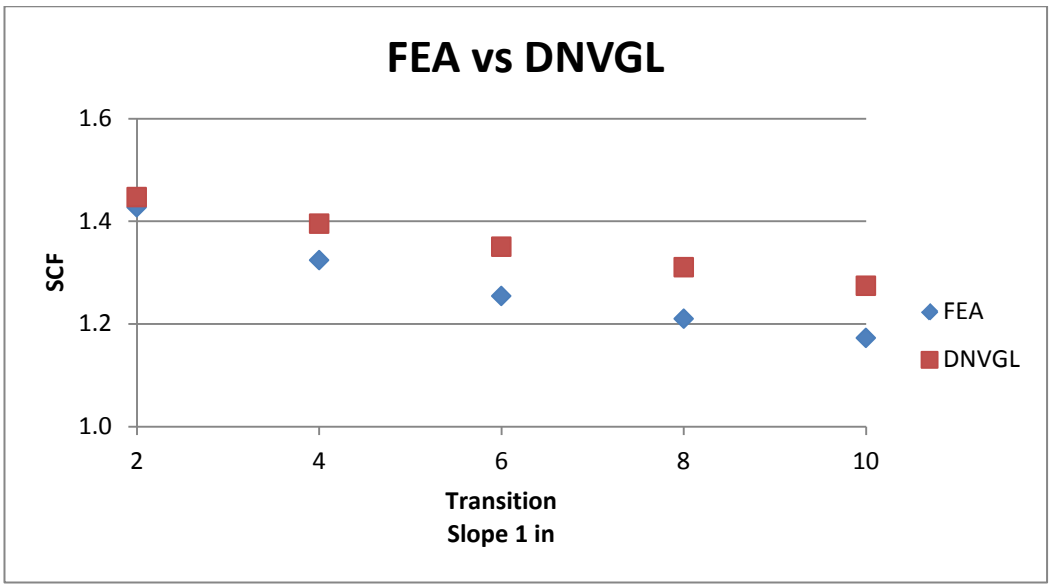

Figure 6-1 Comparison: FEA vs DNVGL

This analysis was performed to compare the results against theoretically derived and empirically adjusted equations. The graph shows that the results are close to the theoretical equations (to within 1% to 8%), and as FEA results depend on the mesh size and number of elements of the model this exercise shows that our modelling approach is suitable with a good practical accuracy for our purpose of assessing trends in variation of SCFs, and as previously stated, the focus of this research is on trends and not the evaluation of actual SCF values.

Therefore, basically four models have been studied covering wide range combinations of large diameter and thicknesses for jacket platforms, as outlined in section 4.3.2

6.2. MODEL 1

Model 1, consists of a 3000mm diameter tube with thickness of 25mm representing the thinner section and upper limit of D/t equal to 120 connected to a thick walled nodal joint. This D/t represents the upper bound used in practical design of members.

Four cases of thick walled node with various thicknesses of 50, 75, 100 and 125mm, have been analysed representing thickness ratios (T/t) of 2, 3, 4, and 5.

The SCF results obtained from FEA are summarized in Table 6.2

Diameter (D)	3000mm	D/t= 120		
Thickness (t)	25mm			
	Case 1	Case 2	Case 3	Case 4
	50:25	75:25	100:25	125:25
T/t	2	3	4	5
Slope				
1:2	1.577	1.636	1.649	1.640
1:4	1.534	1.637	1.650	1.663
1:6	1.49	1.559	1.572	1.599
1:8	1.446	1.481	1.478	1.474
1:10	1.404	1.408	1.401	1.398

Table 6-2 Model 1 Results

It can be deduced from the result in Table 6-2 that, for the same T/t (column wise), the calculated SCF diminish for all cases, as the slope becomes shallower, as shown in Figure 6-2.

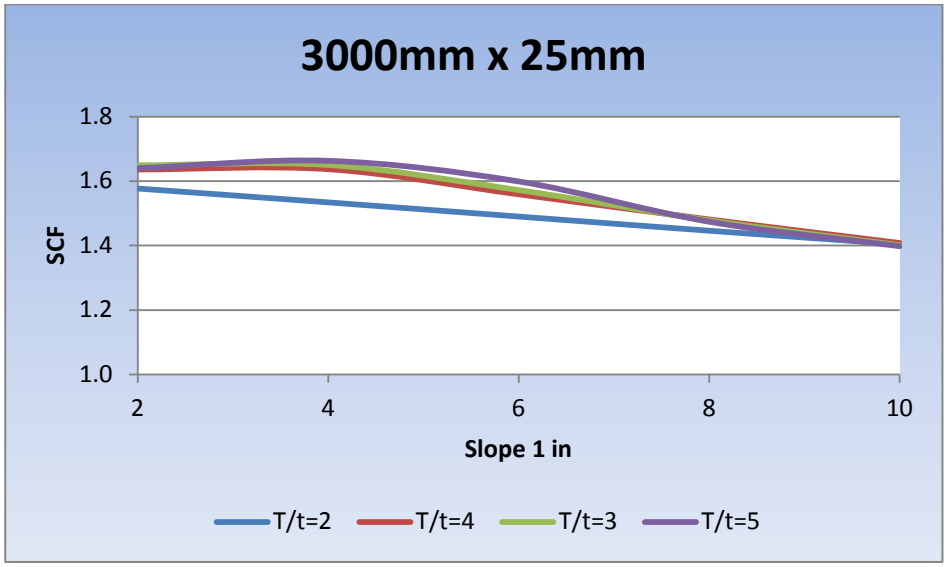

Figure 6-2 SCF vs Transition Slopes (3000 mm ϕ x 25 mm t with various T/t)

The reduction in SCF for each T/t can be better visualized as normalized variation of SCF for each case is compared with the standard 1 in 4 slope and tabulated (column wise) as a fraction in Table 6-3 for all T/t cases. This finding is significant in terms of reducing SCF for thick sections. The reduction for T/t of 2 is approximately 8% and for T/t of 5 about 16%.

Diameter (D)	3000mm	D/t=120		
Thickness (t)	25mm			
	Case 1	Case 2	Case3	Case 4
	50:25	75:25	100:25	125:25
T/t	2	3	4	5
Slope				
1:2	1.03	1.00	1.00	0.99
1:4	1	1	1	1
1:6	0.97	0.95	0.95	0.96
1:8	0.94	0.90	0.90	0.89
1:10	0.92	0.86	0.85	0.84

Table 6-3 Model 1 Normalized Variation

The standard thickness ratio of T/t = 2 with slope of 1:4 has an SCF of 1.534 (Table 6-2). However, if T/t increases to 4, SCF increases to 1.650. But if the slope is reduced to 1:8 the SCF is reduced by 3.7% (1.478/1.534) compared with T/t=2 and slope of 1:4. The decrease in SCF would be 15% (1.401/1.650) for slope of 1:10 for the same T/t=4. Indicating increase in SCF for higher T/t can be compensated and reduced by shallower slopes.

It can be seen from the graphs presented in Figures 6-3 to 6-5 that for steep slopes the SCF tend to increase as the T/t increases. However, for shallower slopes the trend of SCF increase is insignificant in practical design terms, Figures 6-6 and 6-7. In addition, the lower thickness ratio of T/t equal to 2 has in general the lowest SCF. However, if used in practice, it severely restricts design options, and increases the potential for use of pup-pieces, with additional extra costs in steel, welding material, and fabrication cost and time.

From Table 6-2, Figure 6-8 combines trends for all cases, it can be concluded that for higher thickness ratios (T/t), SCF can be reduced if the slope of transition is reduced. The trend of increase in SCF decreases as the slope becomes shallower, Figure 6-9. The rate may become very flat or even negative (decrease in SCF) for very shallow slopes.

The indication from results of this case is of practical significance for the design of members, especially on jacket legs, as it indicates that if nodal thickness is large, with a shallow slope, it can be welded directly to thinner members of leg sections without the use of pup-pieces, hence substantial savings in costs. Further evaluation of this indication is followed in the other models.

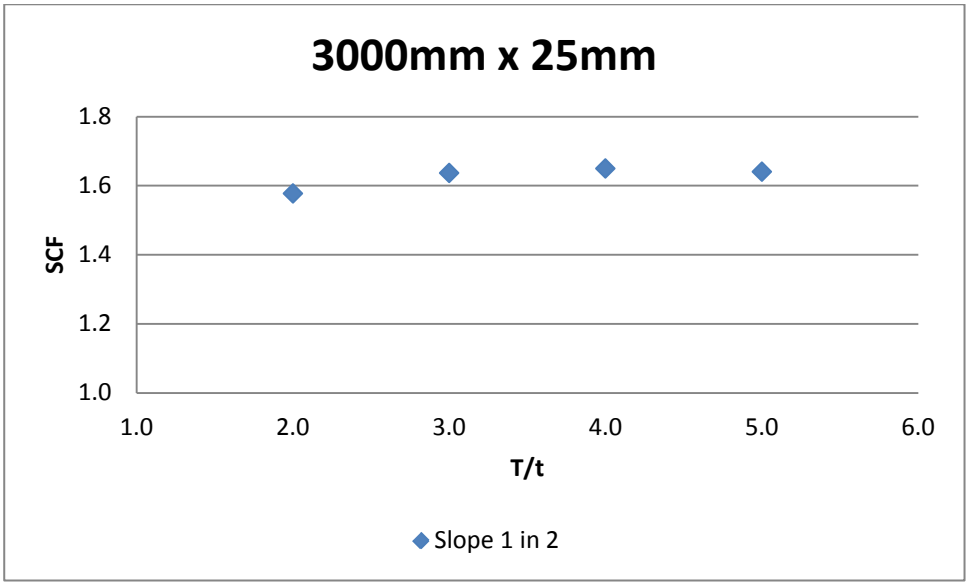

Figure 6-3 SCF vs T/t for slope 1 in 2

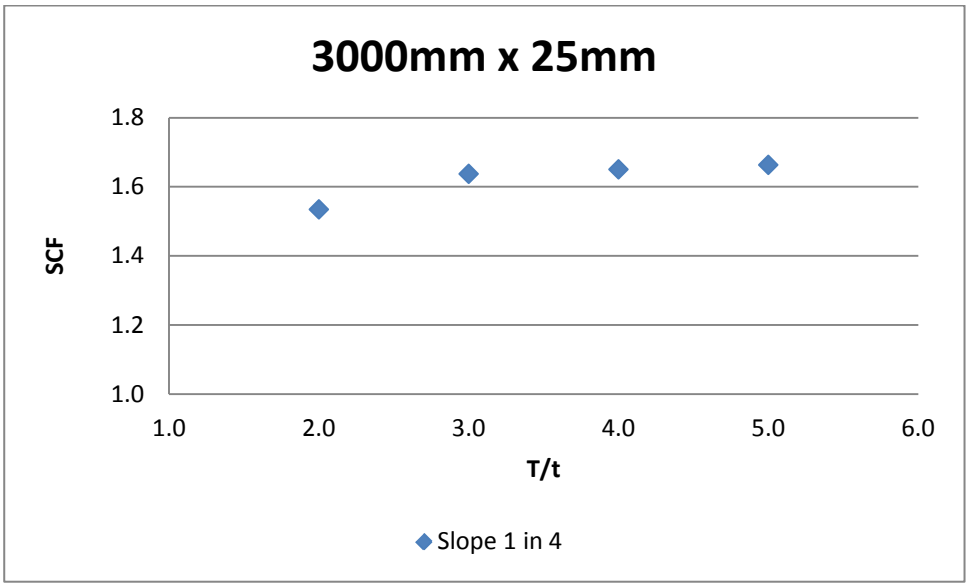

Figure 6-4 SCF vs T/t for slope 1 in 4

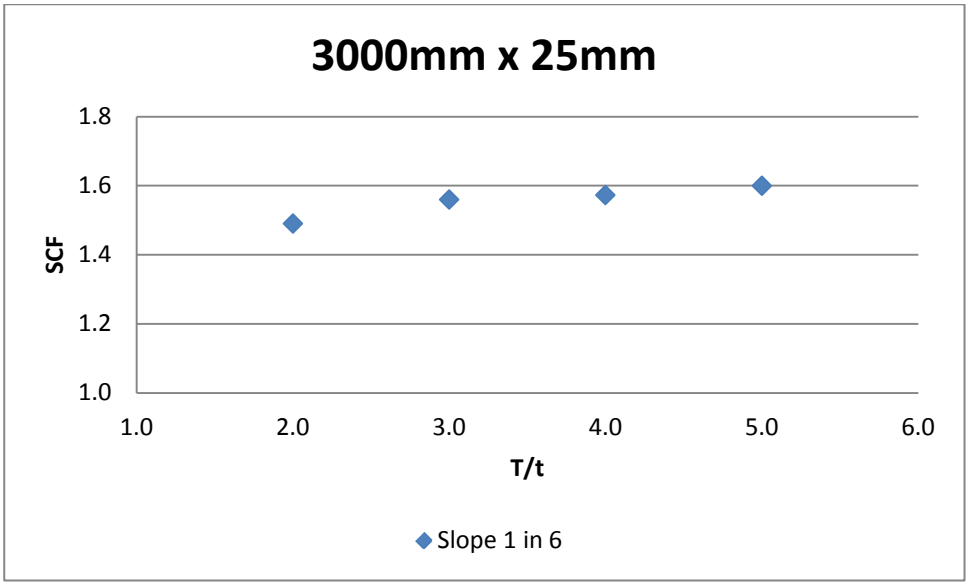

Figure 6-5 SCF vs T/t for slope 1 in 6

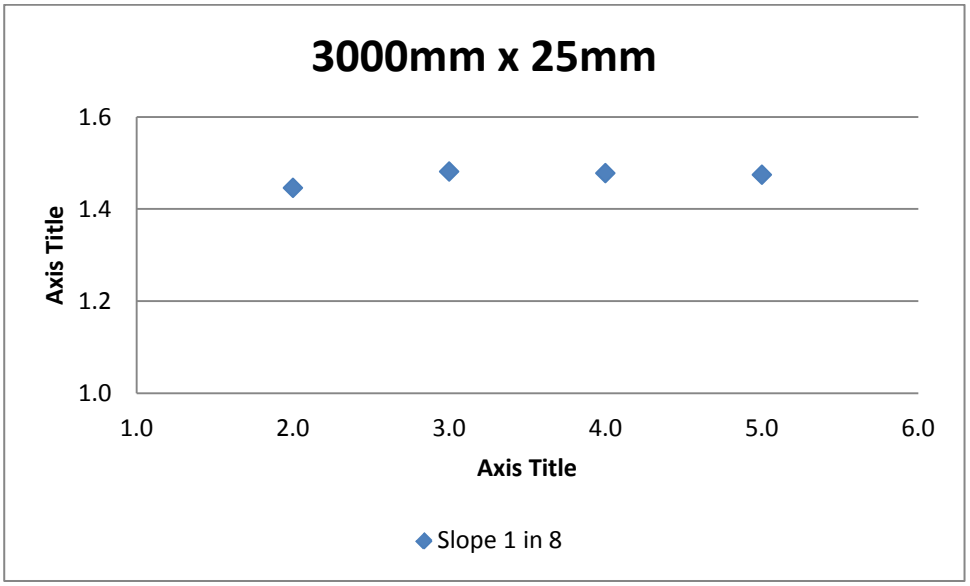

Figure 6-6 SCF vs T/t for slope 1 in 8

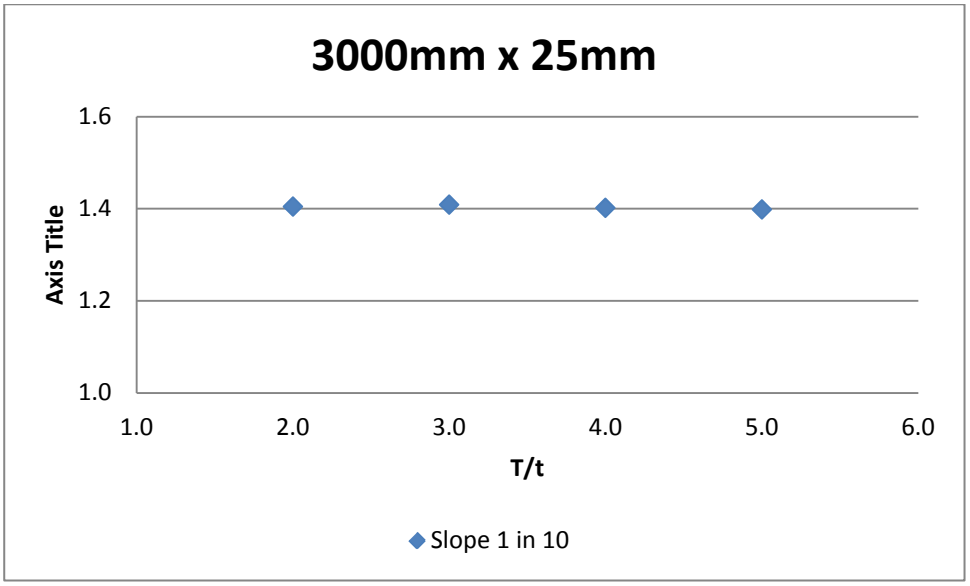

Figure 6-7 SCF vs T/t for slope 1 in 10

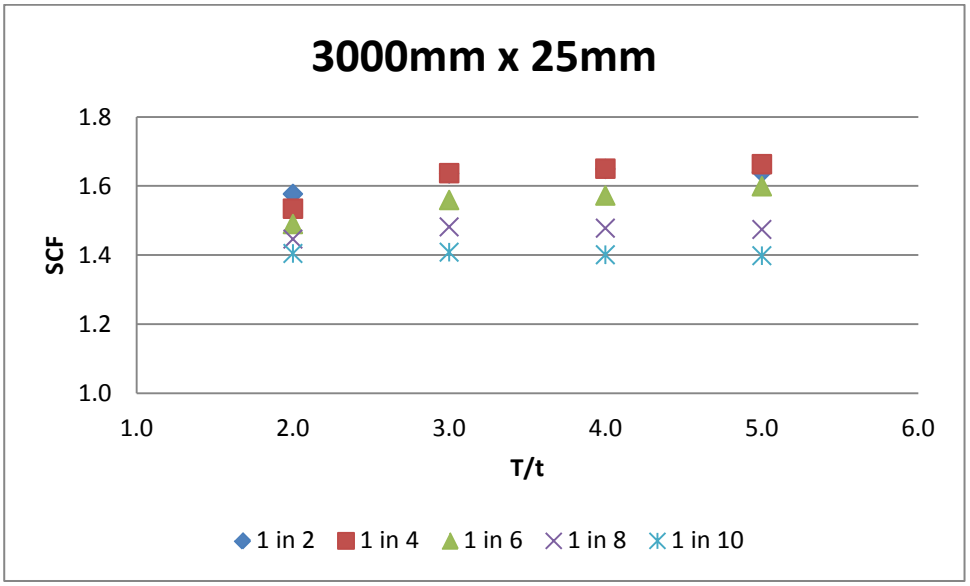

Figure 6-8 SCF vs T/t for all slopes combined – Model 1

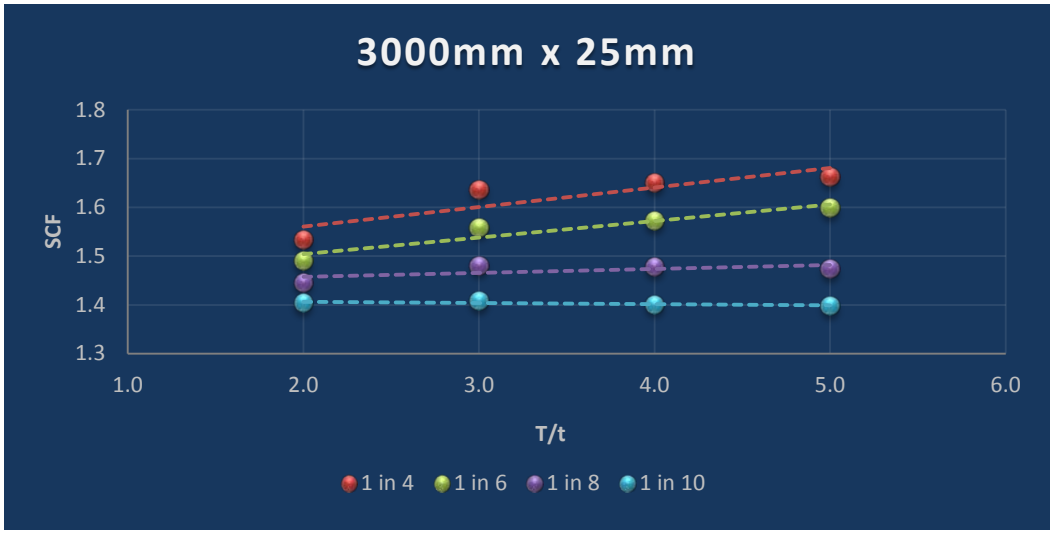

Figure 6-9 SCF Trend Variation - Model 1

It is noted that in some instances the SCF values obtained for a constant slope deviate from the continuous linear trend line, Figure 6-9. Also in some instances the SCF for a higher T/t is slightly lower than a lower T/t, e.g. for slopes of 1:8 and 1:10 in Table 6-2.

As all the parameters for all models are standardized, this effect can only be attributed to the effect of model size and the number of elements and topology in the model which affect the numerical accuracies of the results. Because as T/t increases and/or length increases, due to longer slope of transition, the model becomes larger and requires more elements. The model with more elements generally provides a better numerical estimation.

In these analyses the model size variation from one T/t to the next or from one slope to the next will generally create a difference of approximately 250,000 to 500,000 addition elements depending on thickness, resulting in this type of variation, which is within practical engineering accuracies and normal to any numerical analyses and FEA. This effect does not affect the results and the suggested trend behaviour and conclusion obtained from the analyses.

6.3. MODEL 2

Model 2, consists of a 3000mm diameter tube with thickness of 50mm (D/t=60) connected to a thick walled nodal tube. Three cases of thick walled node with various thicknesses of 75, 100 and 125mm, have been analysed representing thickness ratios (T/t) of 1.5, 2 and 2.5.

The Table 6-4 summarizes the results for this model.

Diameter (D)	3000mm	D/t=60	
Thickness (t)	50mm		
	Case 1	Case 2	Case3
	75:50	100:50	125:50
T/t	1.5	2	2.5
Slope			
1:2	1.532	1.709	1.763
1:4	1.469	1.605	1.674
1:6	1.423	1.521	1.549
1:8	1.384	1.444	1.447
1:10	1.346	1.374	1.366

Table 6-4 Model 2 Results

In this model, again, the result indicate that, with shallower transition slopes the calculated SCF diminish for all three cases of constant T/t, as shown in Table 6-4 and Figure 6-10. The reduction is 8% for T/t=1.5 to as much as 18% for T/t=2.5 compared with values for slope of 1:4. This shows there is a considerable gain in using a shallower slope.

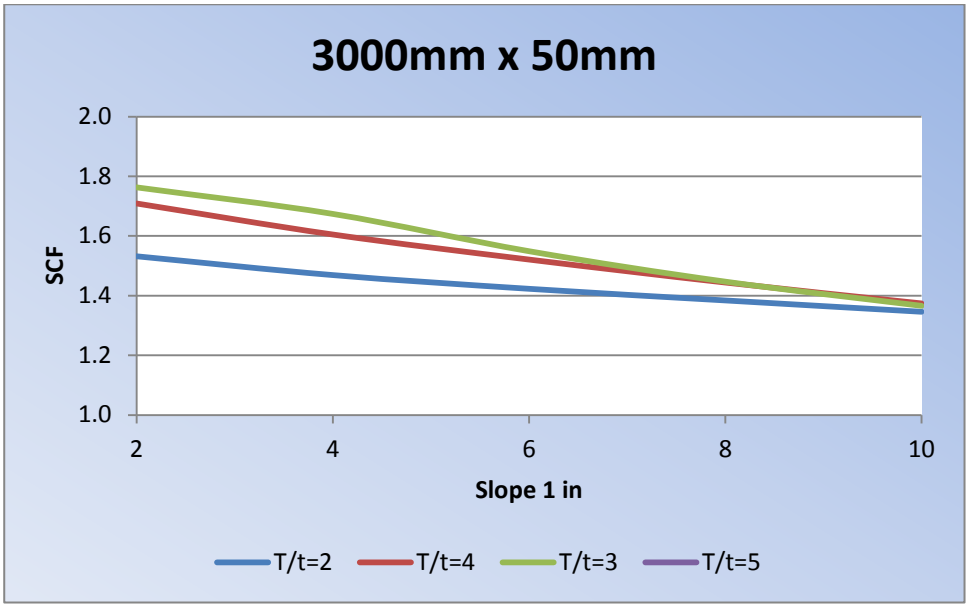

Figure 6-10 SCF vs Transition Slopes (3000 mm ϕ x 50 mm t with various T/t)

The standard T/t=2 with slope of 1:4 has an SCF of 1.605, Table 6-4

However, from the other results in Table 6-4, if thickness ratio increases to 2.5, SCF increases to 1.674 an increase of 4.3% and if slope becomes shallower to 1:6 the SCF is reduced by 3.5% (1.549/1.605) when compared with T/t=2 and slope 1:4 and 7.4% (1.549/1.674) when compared with T/t=2.5 and slope of 1:4.

Further reductions can be obtained for even shallower slope of 1:8 reducing the SCF by 13.5%. (1.447/1.674) and for the slope of 1:10 the SCF is reduced by a substantial amount of 18.4% (1.366/1.674).

But, the lower thickness ratio of T/t= 1.5, in Table 6-4, has the lowest SCF. However, this would limit the options available for design in practice, which would require pup-pieces with substantial cost penalties as described before for model 1.

Variation of SCF for each (T/t) case is compared with the standard 1:4 slope as a fraction and is tabulated below in Table 6-5 for all three cases.

Diameter (D)	3000mm	D/t=60	
Thickness (t)	50mm		
	Case 1	Case 2	Case3
	75:50	100:50	125:50
T/t	1.5	2	2.5
Slope			
1:2	1.04	1.06	1.05
1:4	1	1	1
1:6	0.97	0.95	0.93
1:8	0.94	0.90	0.86
1:10	0.92	0.86	0.82

Table 6-5 Model 2 Normalized Variation

Again, for this model as well, from Figures 6-11 to 6-15, it can be concluded that for higher thickness ratios (T/t), SCF can be reduced if the slope of transition is reduced.

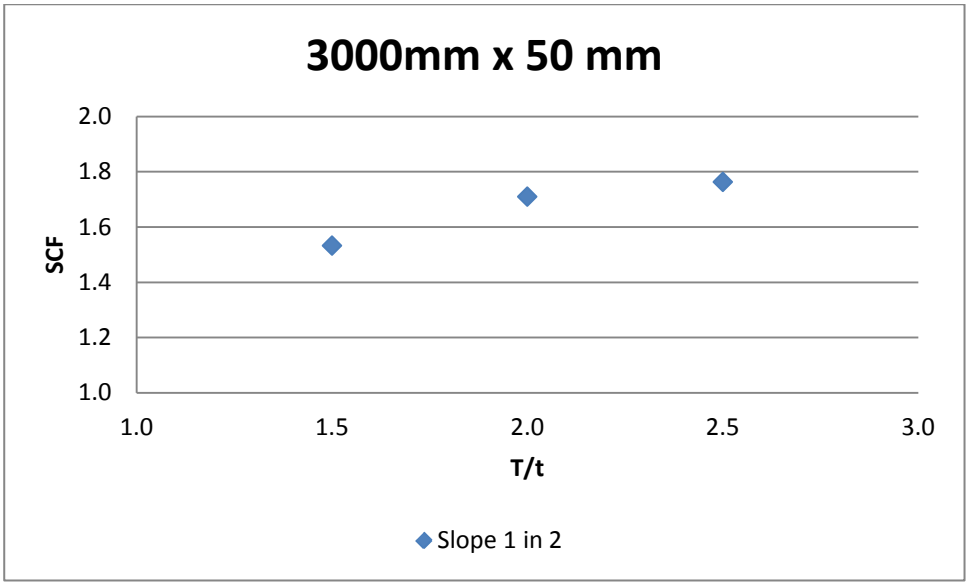

Figure 6-11 SCF vs T/t for slope 1 in 2

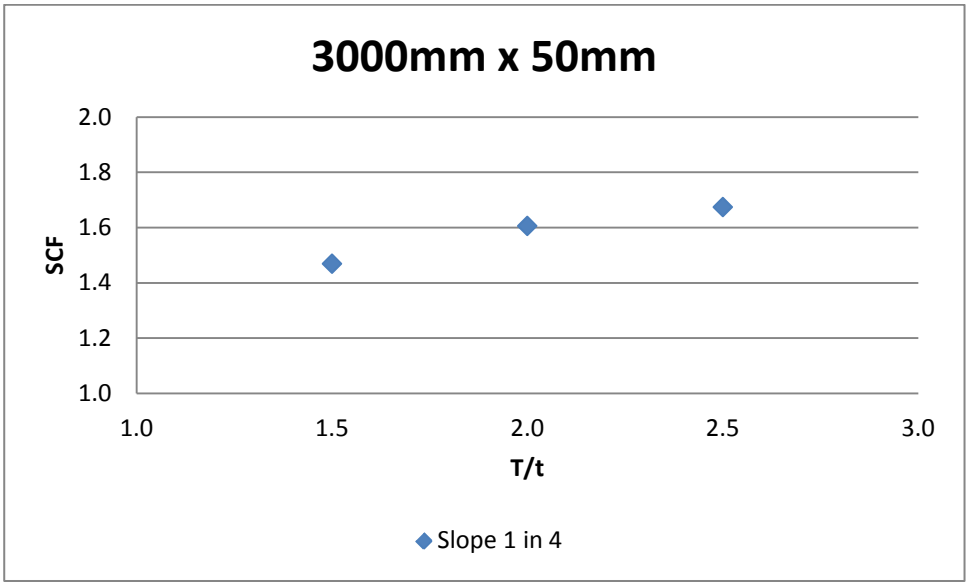

Figure 6-12 SCF vs T/t for slope 1 in 4

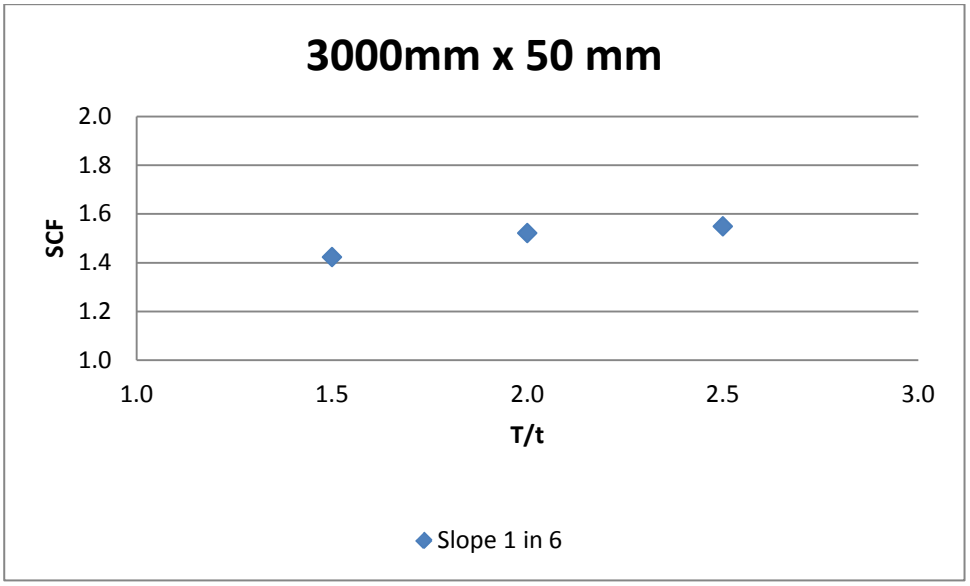

Figure 6-13 SCF vs T/t for slope 1 in 6

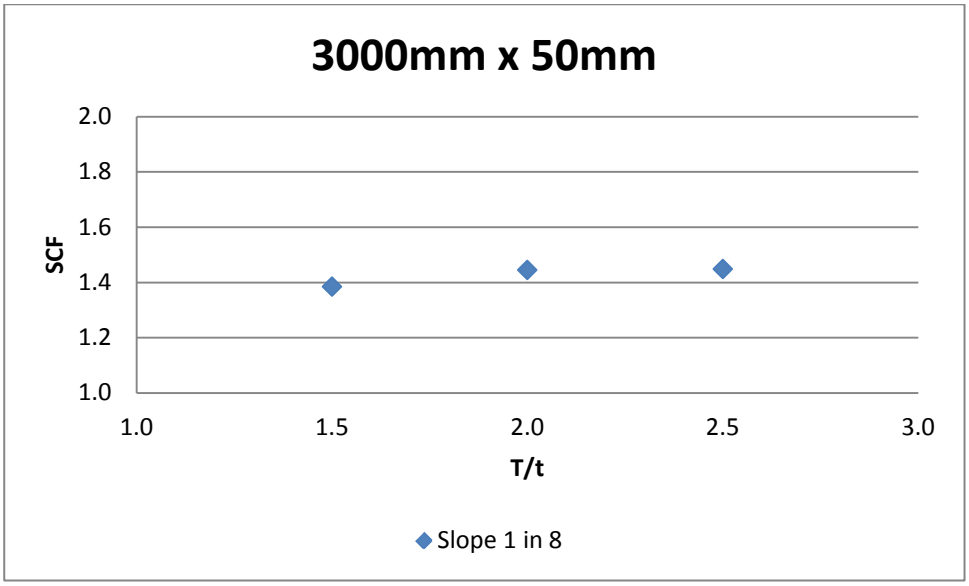

Figure 6-14 SCF vs T/t for slope 1 in 8

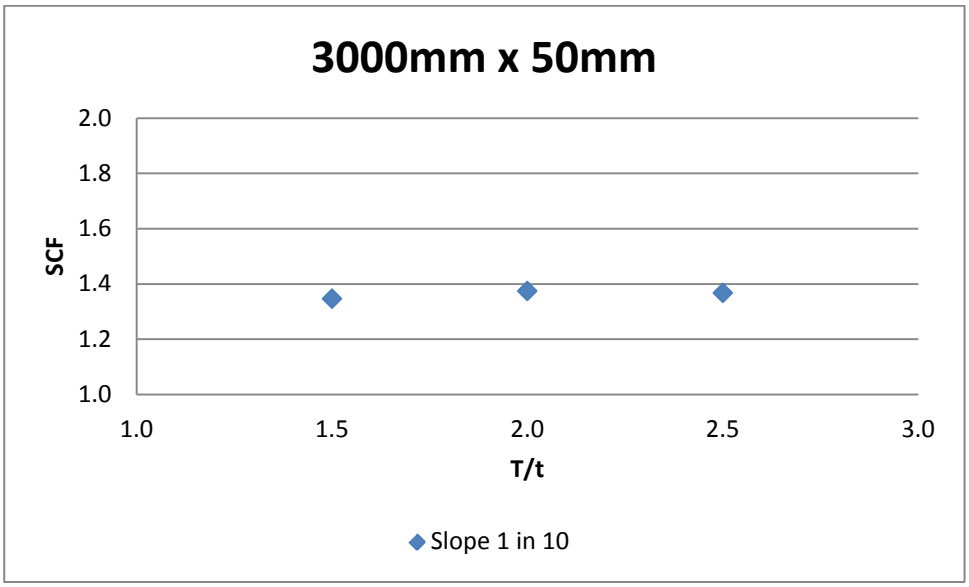

Figure 6-15 SCF vs T/t for slope 1 in 10

Variation of SCF for each (T/t) for all slopes are shown in Figures 6-11 to 6-15. It can be seen that for all slopes the SCF tend to increase as the T/t increase, however, as the slope becomes shallower the increase in SCF is reduced, and in practical design terms increase becomes minimal as shown in Figures 6-16.

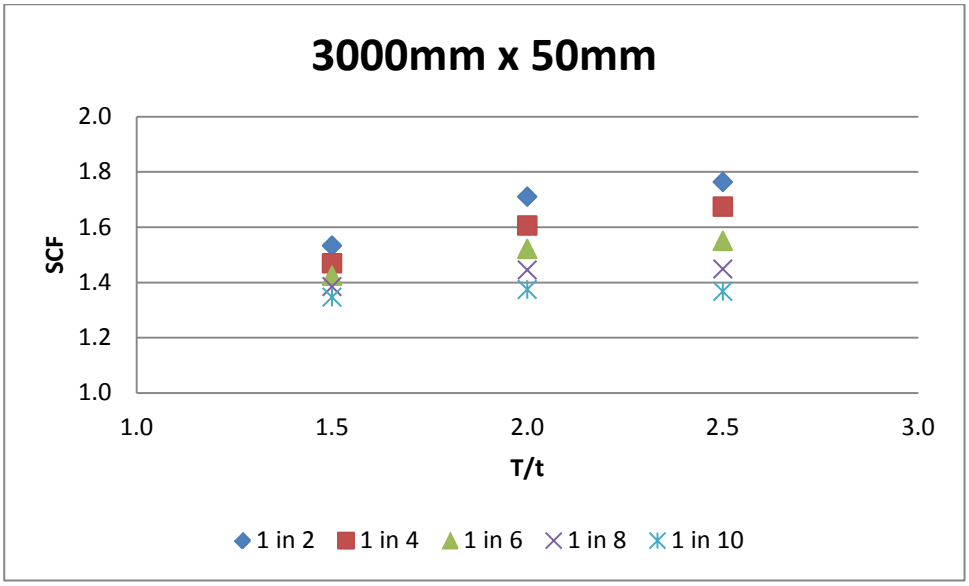

Figure 6-16 SCF vs T/t for all slopes combined – Model 2

Figure 6-16 shows that for higher T/t ratios steeper slopes have higher SCFs and they can are reduced by reduction in slope. These results indicate that there is a similar trend for all cases so far considered as in the Model 1. Figure 6-17 shows the SCF increase "trend lines" as the T/t increases for all transition slopes. However, the rate of increase diminish as the slope is reduced.

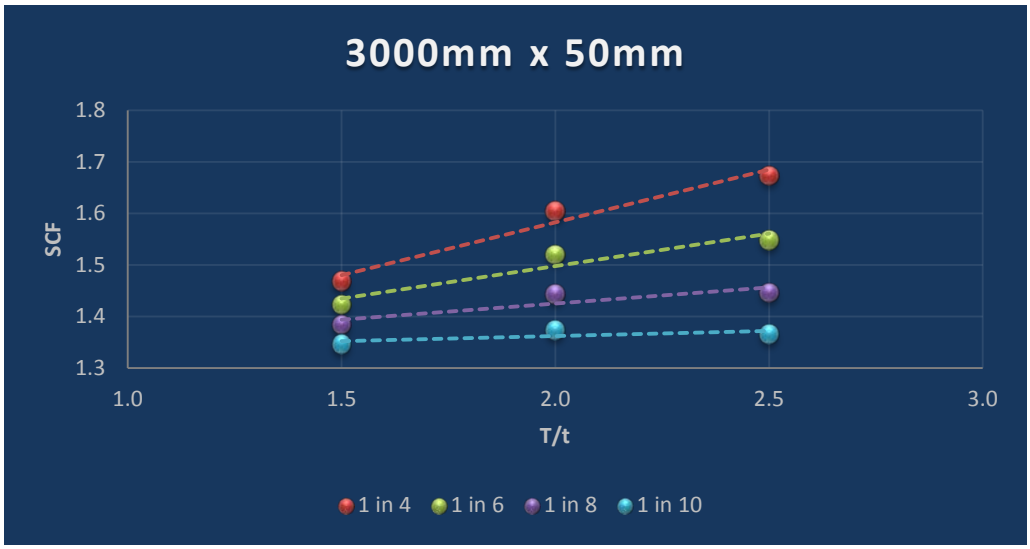

Figure 6-17 SCF Trend Variation - Model 2

6.4. MODEL 3

Model 3, consists of a 2000mm diameter tube with thickness of 25mm (D/t= 80) connected to a thick walled nodal tube. Four cases of thick walled node with various thicknesses of 50, 75, 100 and 125mm, have been analysed representing transition slopes of 2, 3, 4, and 5.

Diameter (D)	2000mm	D/t=80		
Thickness (t)	25mm			
	Case 1	Case 2	Case 3	Case 4
T/t	50:25	75:25	100:25	125:25
Slope	2	3	4	5
1:2	1.546	1.586	1.643	1.656
1:4	1.494	1.618	1.605	1.612
1:6	1.441	1.516	1.496	1.516
1:8	1.394	1.406	1.400	1.397
1:10	1.348	1.338	1.333	1.332

Table 6-6 Model 3 Results

Similar to Models 1 and 2, it can be deduced from the result that, with shallower transition slopes the calculated SCFs diminish for all four cases of T/t, as shown in Table 6-6.

The change in SCF between thickness ratios (T/t) of 2 and 5 for a standard slope transition of 1:4 is an increase of 7.9% (1.612/1.494), and for a slope of 1 in 10 there is reduction of 1.1%

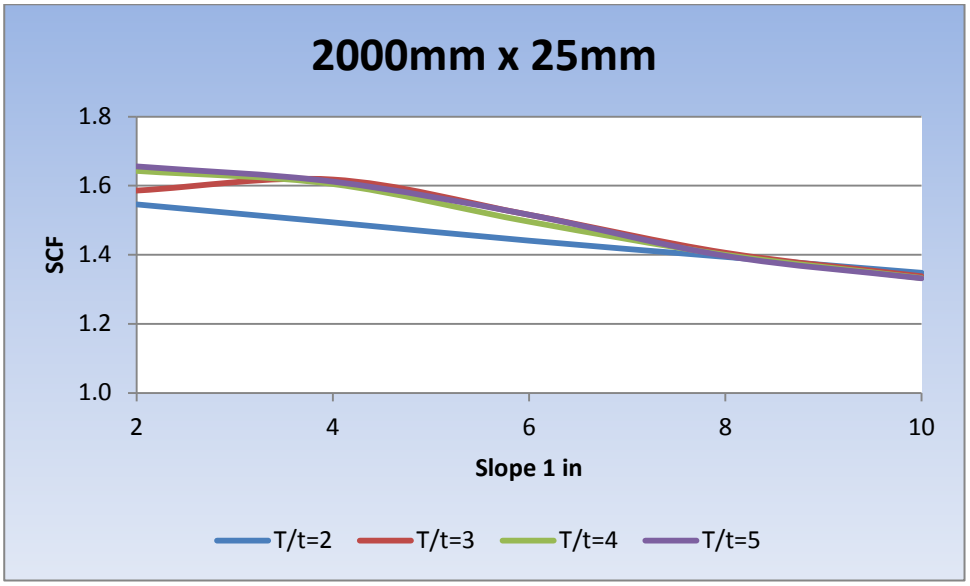

Figure 6-18 SCF vs Transition Slopes (2000 mm ϕ x 25 mm t with various T/t)

The standard thickness ratio of 2 with slope of 1:4 has an SCF of 1.494 as shown in Table 6-6.

However, if thickness ratio increases to 4, the SCF increases to 1.605.

However, if the slope becomes shallower to 1:6 the SCF remains almost the same, an increase of 0.1% (ie 1.496/1.494) compared with T/t of 2 and slope of 1:4 and a reduction of 6.7% (1.496/1.605) compared with T/t= 4 and slope of 1:4.

Further reduction in SCF can be obtained for even shallower slope of 1:8 reducing the SCF by 12.3%. (ie 1.400/1.605) for the same T/t=4.

Again a conclusion could be drawn that for higher thickness ratios (T/t), SCF can be reduced if the slope of transition is reduced. This is the same conclusion as for other models.

Normalized variation of SCF for each T/t with respect to the standard T/t=2 and slope of 1:4 is given in Table 6-7.

Diameter (D)	2000mm	D/t=80		
Thickness (t)	25mm			
	Case 1	Case 2	Case 3	Case 4
	50:25	75:25	100:25	125/25
T/t	2	3	4	5
Slope				
1:2	1.03	0.98	1.02	1.03
1:4	1	1	1	1
1:6	0.96	0.94	0.93	0.94
1:8	0.93	0.87	0.87	0.87
1:10	0.90	0.83	0.83	0.83

Table 6-7 Model 3 Normalized Variation

Similarly, as for previous models, for each transition slope, the SCFs are plotted in Figures 6-19 to 6-23.

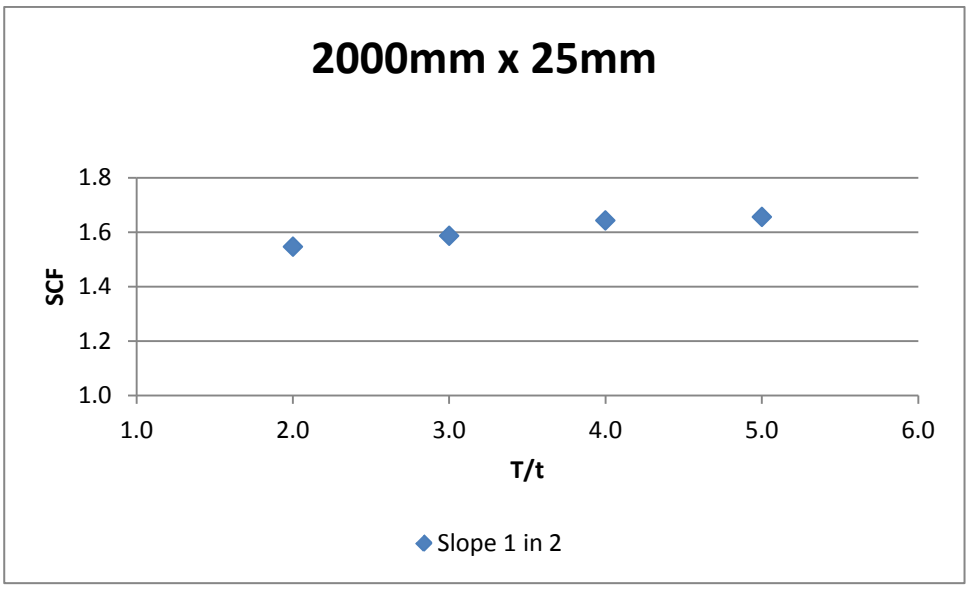

Figure 6-19 SCF vs T/t for slope 1 in 2

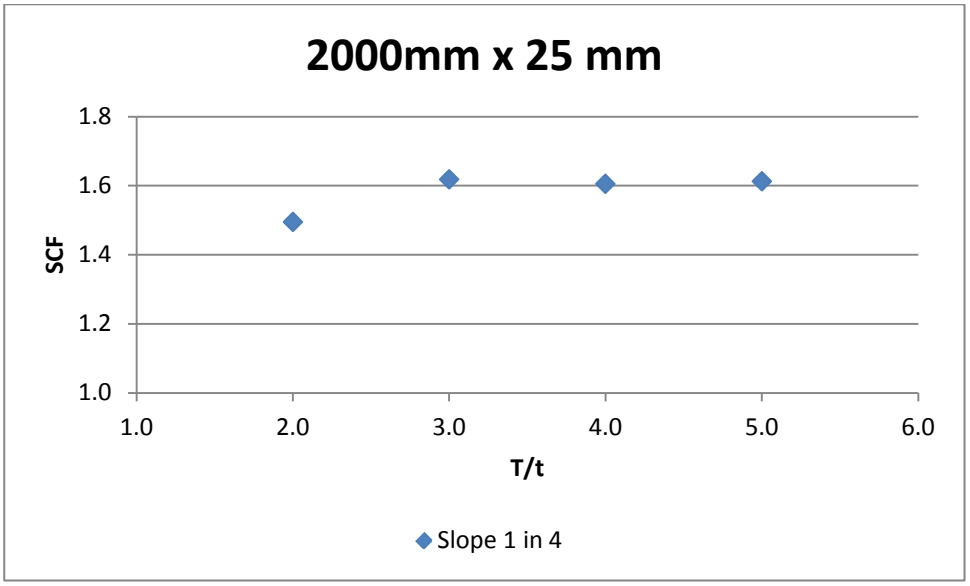

Figure 6-20 SCF vs T/t for slope 1 in 4

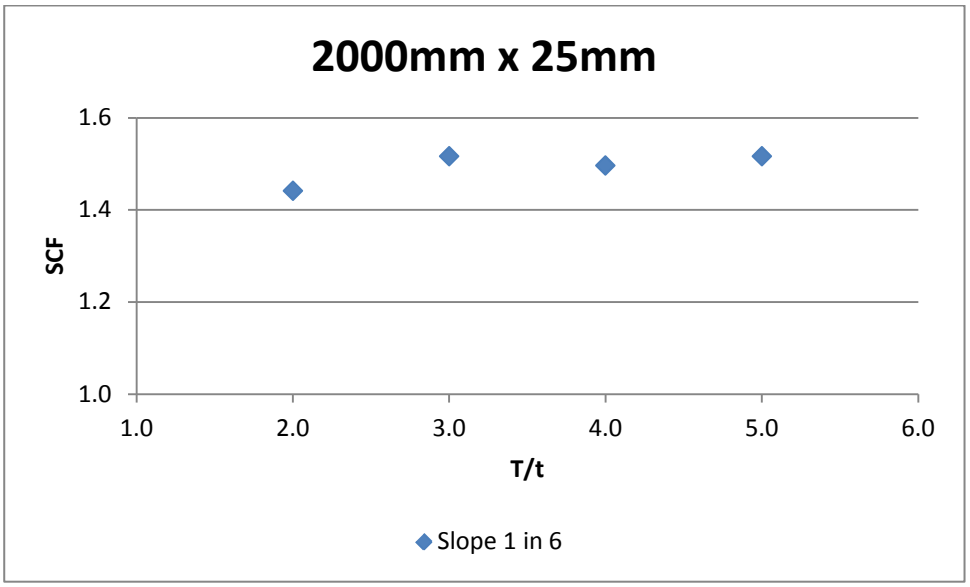

Figure 6-21 SCF vs T/t for slope 1 in 6

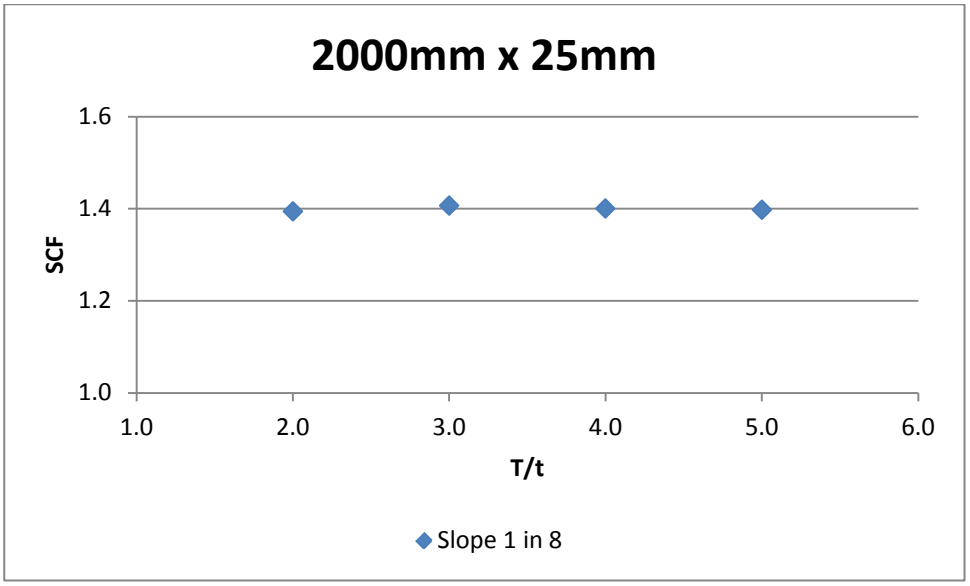

Figure 6-22 SCF vs T/t for slope 1 in 8

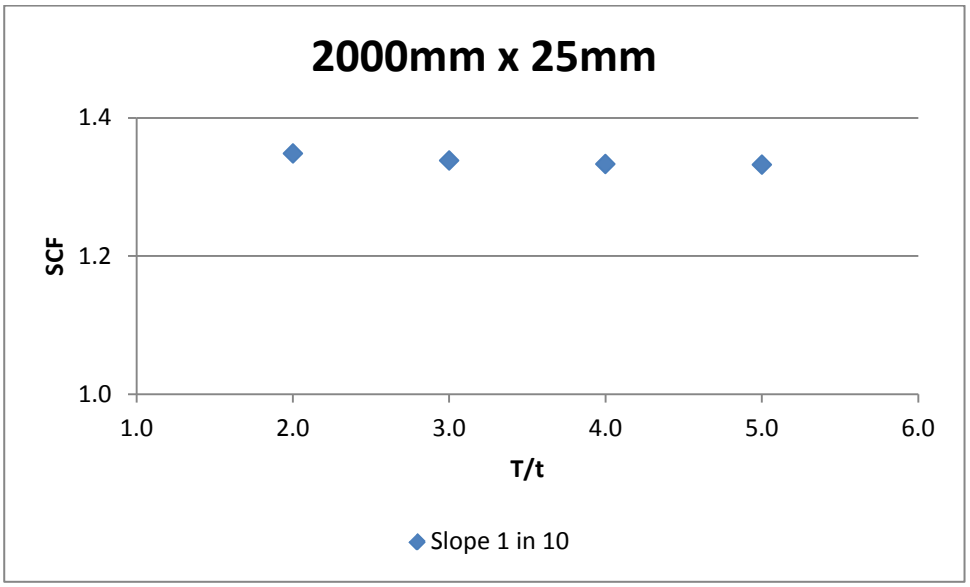

Figure 6-23 SCF vs T/t for slope 1 in 20

The trends for the SCF values resulted from analysis of this model are shown in Figures 6-24 and 6-25. It can be seen that the rate of increase of SCF decreases as the slope becomes shallower and even for the 1:10 the trend reverses to a slight decrease.

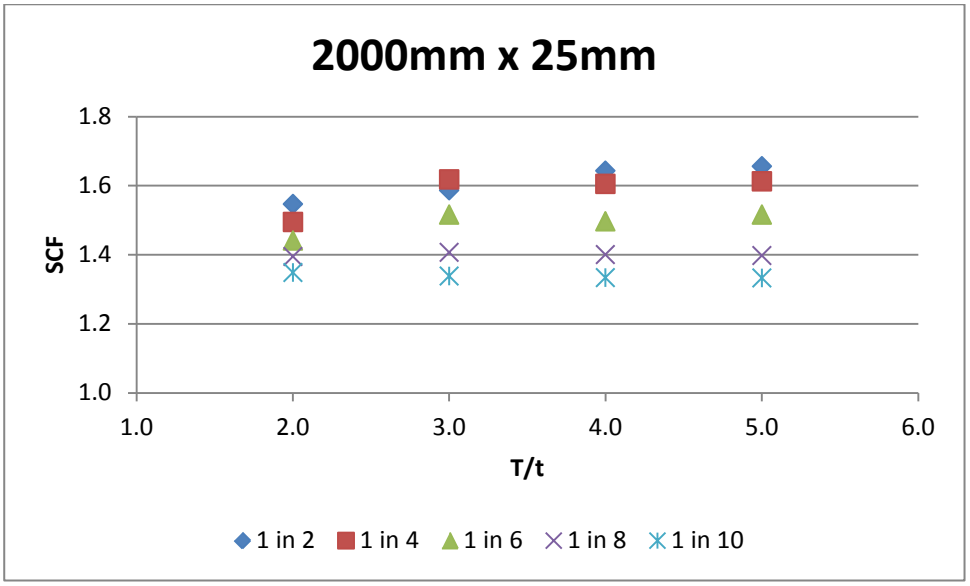

Figure 6-24 SCF vs T/t for all slopes combined – Model 3

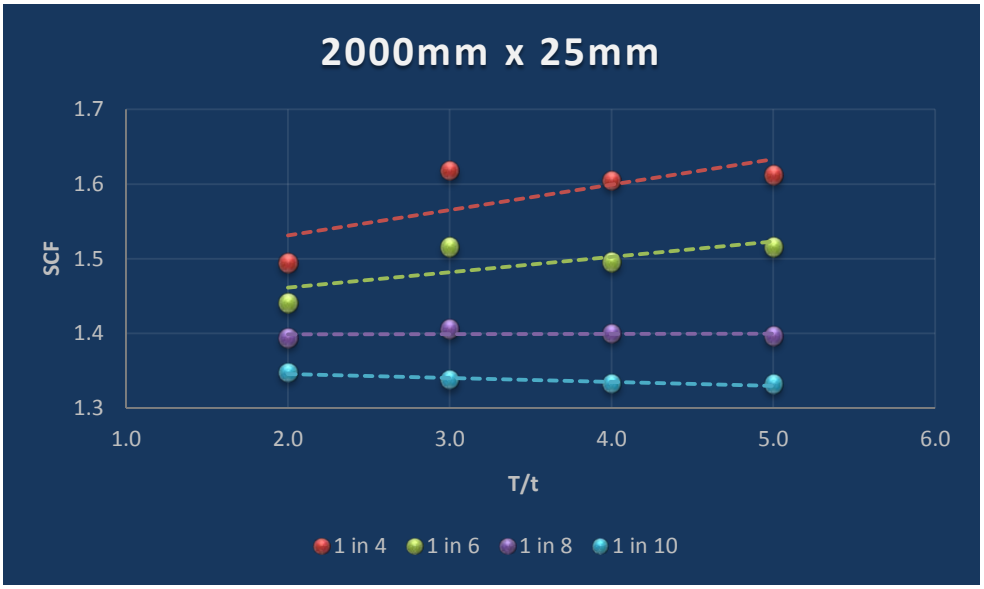

Figure 6-25 SCF Trend Variation - Model 3

This potential behaviour of reversed slope could be significant for reduction of SCF but may not be practically possible and further investigation beyond slope of 1:10 is needed, both theoretically and physically, to evaluate if it is possible to produce such a shallow slope during fabrication.

6.5. MODEL 4

Model 4, consists of a 2000mm diameter tube with thickness of 50mm (D/t=40) connected to a thick walled nodal tube. Three cases of thick walled node with various thicknesses of 75, 100 and 125mm, have been analysed representing transition slopes of 1.5, 2 and 2.5.

Diameter (D)	2000mm	D/t=40	
Thickness (t)	50mm		
	Case 1	Case 2	Case 3
	75:50	100:50	125:50
T/t	1.5	2.0	2.5
Slope			
1:2	1.509	1.705	1.744
1:4	1.437	1.563	1.621
1:6	1.384	1.461	1.475
1:8	1.339	1.377	1.372
1:10	1.297	1.309	1.302

Table 6-8 Model 4 Results

It can be seen from the result shown in Table 6-8, that with shallower transition slopes the calculated SCF diminish for all four cases of T/t. This is similar to all other cases.

The reduction in SCF in this model is more pronounced than the other models, by as much as 20% for T/t=2.5, (1.302/1.621).

Similar to other models, for a constant T/t, as the transition slope becomes shallower, the SCF rapidly reduce for all cases, as indicated in Figure 6-26

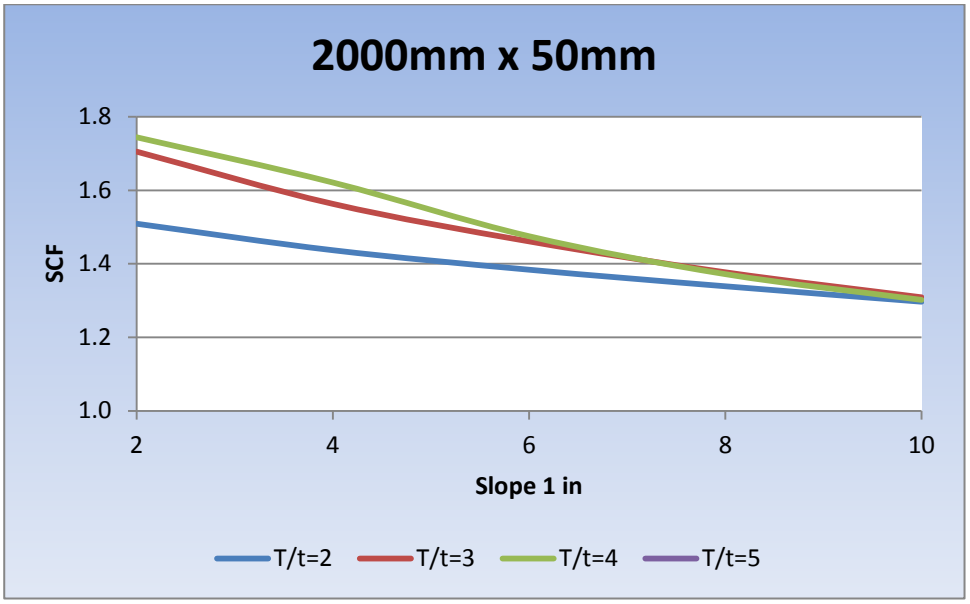

Figure 6-26 SCF vs Transition Slopes (2000 mm ϕ x 25 mm t with various T/t)

Table 6-8 shows the normalized variation of SCF with respect to the standard 1:4 slope for all T/t, which again highlights the rapid reduction in SCF as the slope becomes sallower.

Diameter (D)	2000mm	D/t= 40	
Thickness (t)	50mm		
	Case 1	Case 2	Case 3
	75:50	100:50	125:50
T/t	1.5	2.0	2.5
Slope			
1:2	1.05	1.09	1.08
1:4	1	1	1
1:6	0.96	0.93	0.91
1:8	0.93	0.88	0.85
1:10	0.90	0.84	0.80

Table 6-9 Model 4 Normalized Variation

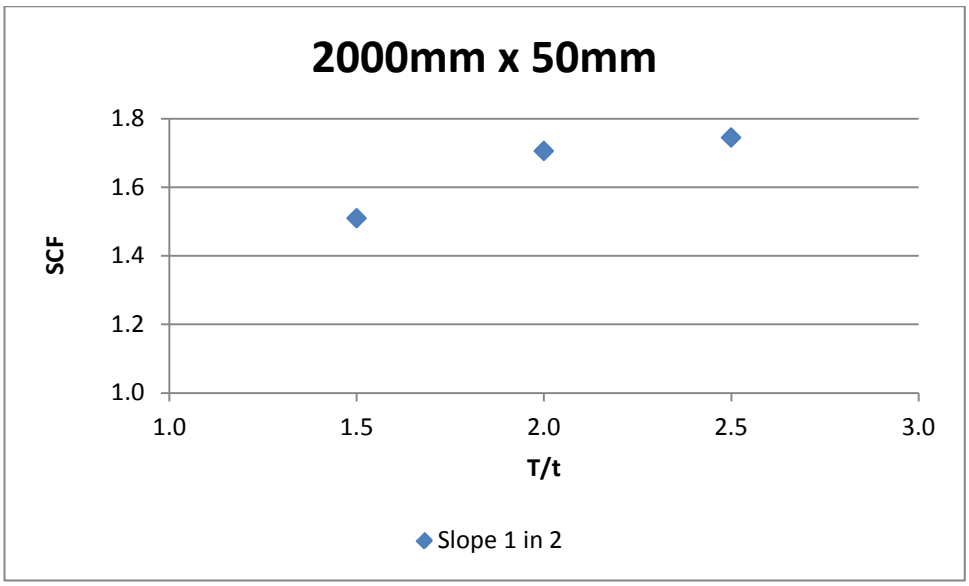

Figure 6-27 SCF vs T/t for slope 1 in 2

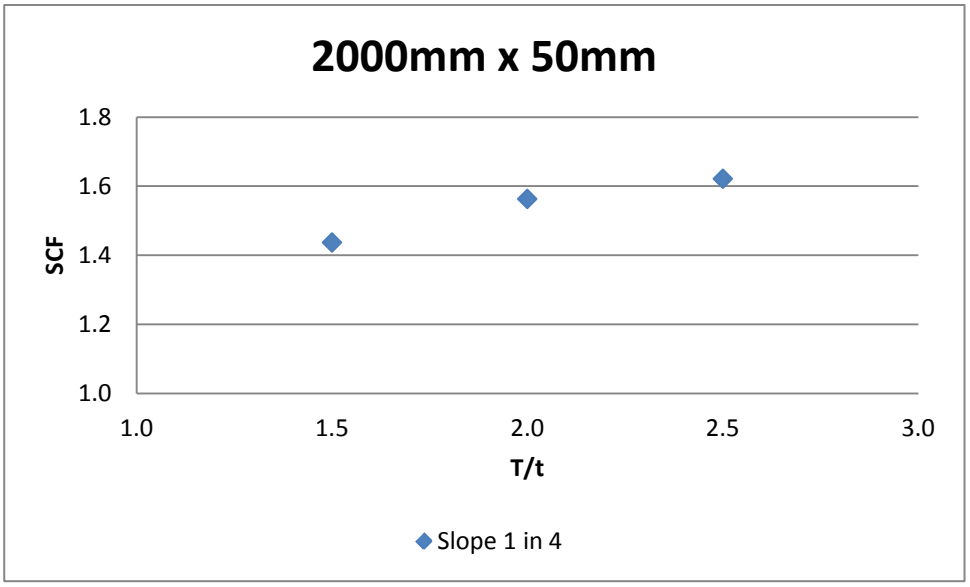

Figure 6-28 SCF vs T/t for slope 1 in 4

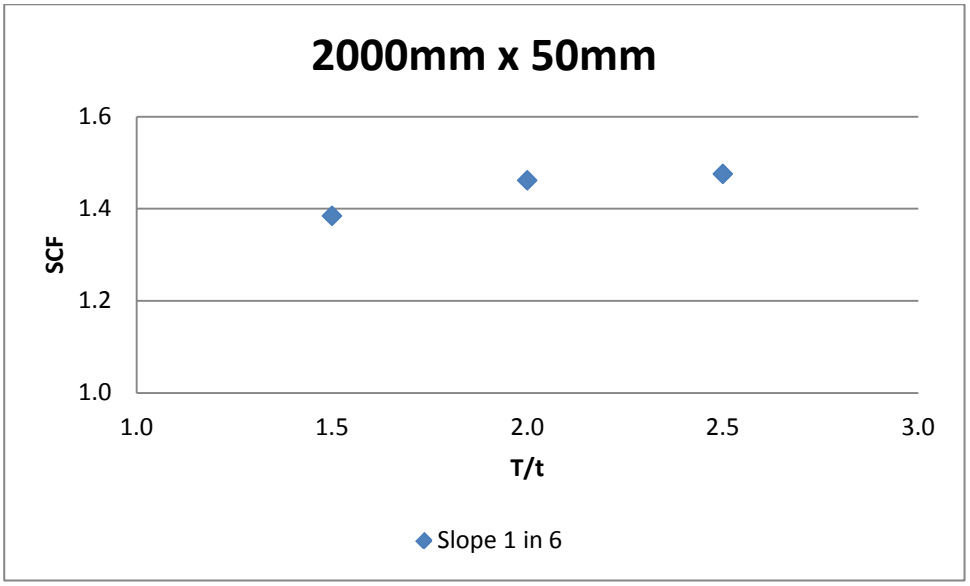

Figure 6-29 SCF vs T/t for slope 1 in 6

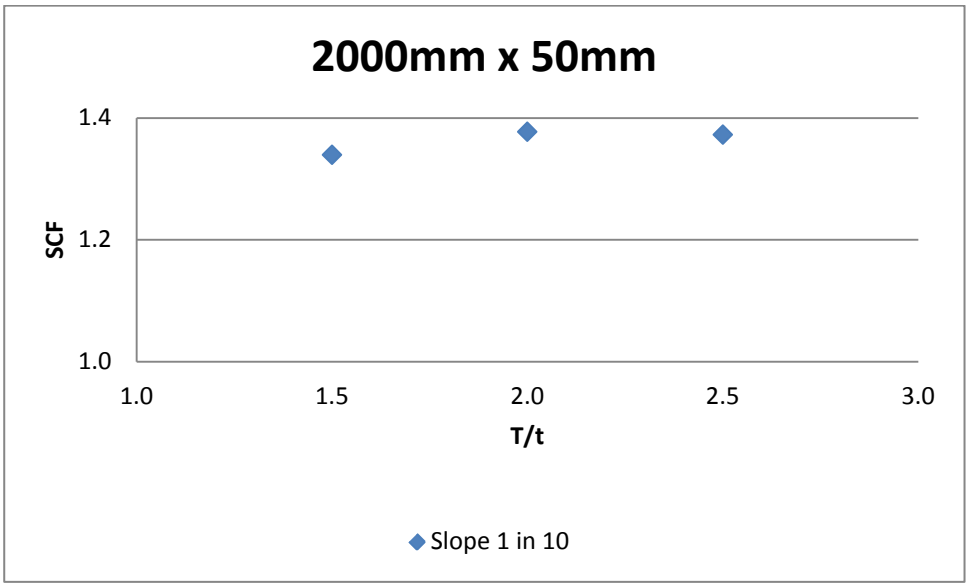

Figure 6-30 SCF vs T/t for slope 1 in 8

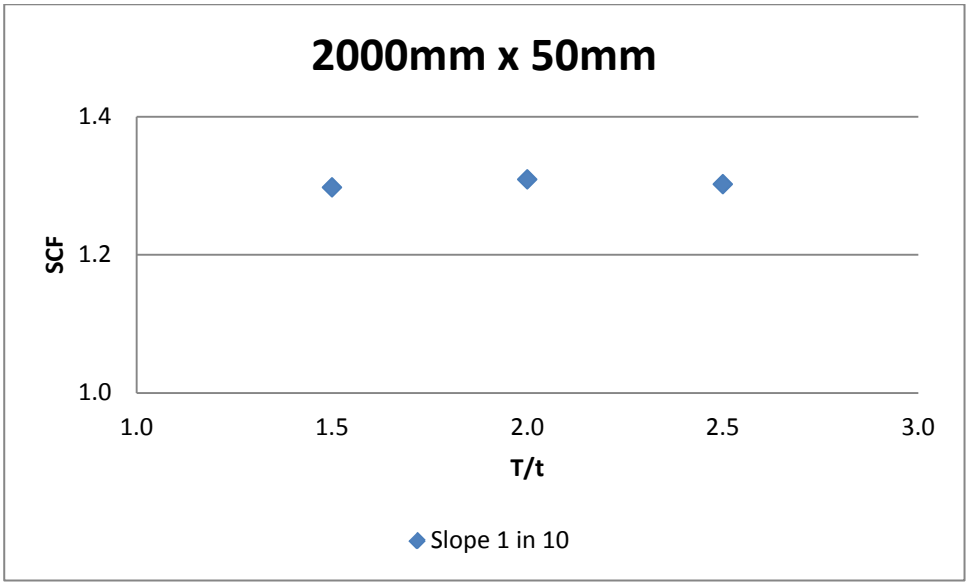

Figure 6-31 SCF vs T/t for slope 1 in 10

The trends for the SCF values resulted from analysis of this model are shown in Figures 6-32 and 6-33. It can be seen that the rate of increase of SCF decreases as the slope becomes shallower and for the 1:10 the increase is very slight, almost flat as shown in Figure 6-33.

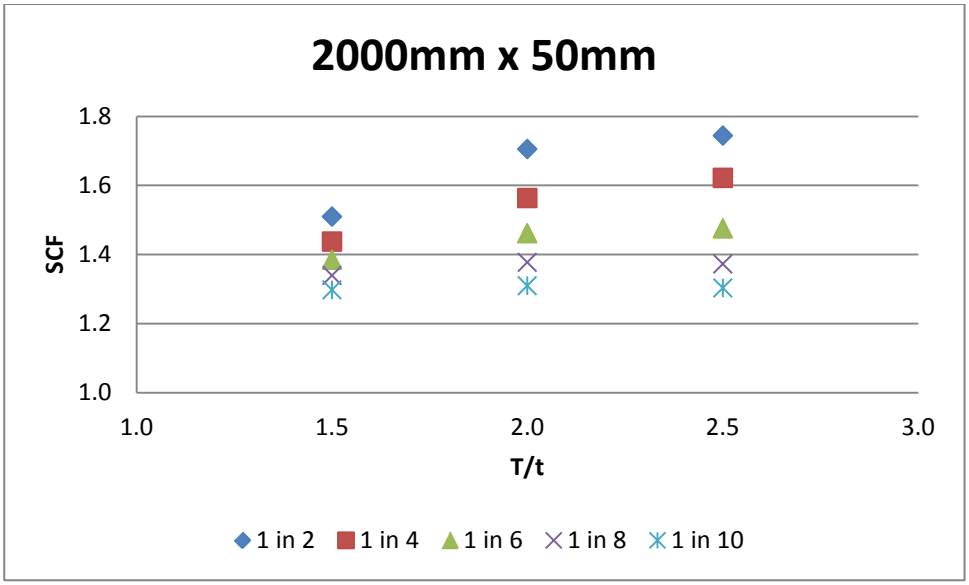

Figure 6-32 SCF vs T/t for all slopes combined – Model 4

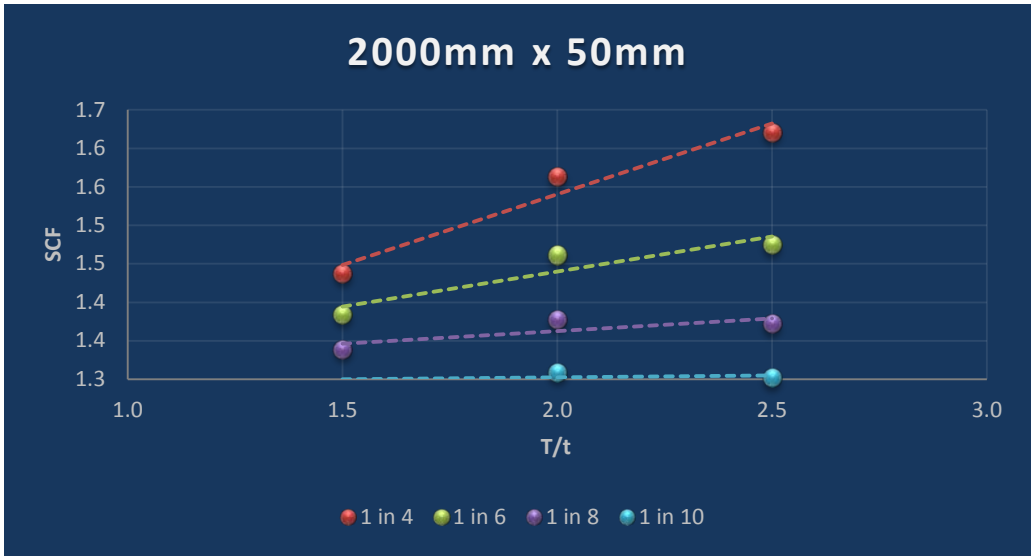

Figure 6-33 SCF Trend Variation - Model 4

Figure 6-33 also shows that for higher T/t, the decrease in SCF is much higher by changing the slope from 1:4 to 1:10, than for smaller T/t.

Chapter 7
Transition Zone Stress Distribution

7. VARIATION OF STRESS ALONG THE TRANSITION

In order to assess variation of stress along the transition zone, two models were created and compared. The models are identical in all parameters except the lower length of the model representing a longer section.

The parameters used are as follows:

Diameter =3000mm

T = 50mm

t =25mm

Upper Section length = 500mm

Lower Section length = short model 500mm and long model 3000mm.

The stress distribution along the whole cross section was examined using a "PATH" feature in ABAQUS extending from the thinner section to the thicker section. The model with shorter lower section (500mm) is shown in Figure 7-1

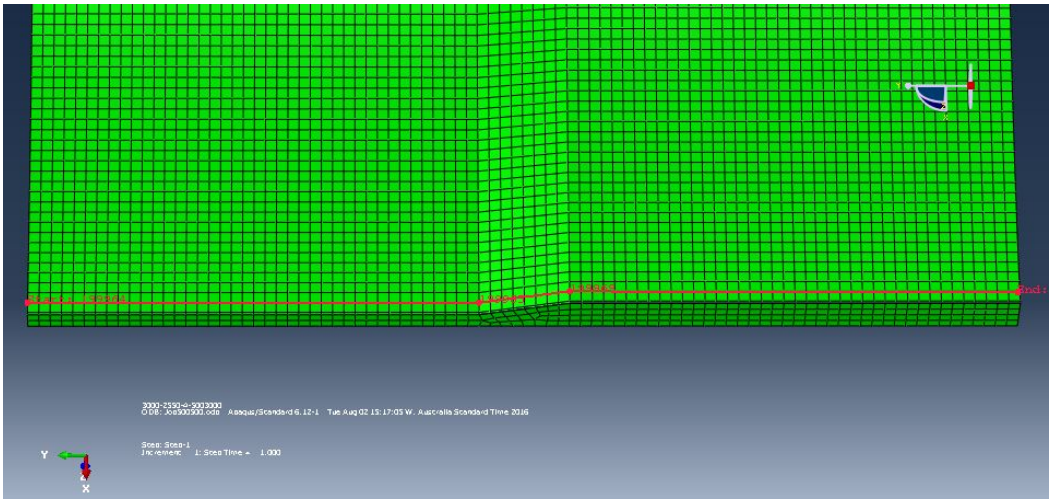

Figure 7-1 Typical Path

The stress distribution for the shorter model with slope of 1:4 is presented in Figure 7-2

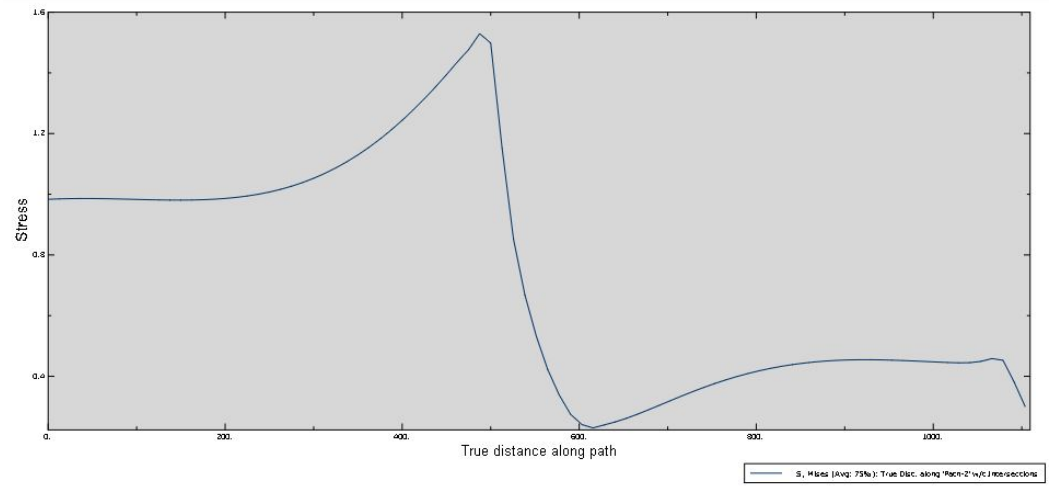

Figure 7-2 SCF Variation along the Short Model

From Figure 7-2 it can be seen that the stress variation curve indicates distinct zones along the model from top to bottom of the model (left to right in the Figure):

1 – Unit stress at the start of the thinner section

2 – Unit stress moves along the thinner member

3 – Increase in stress with approach towards the transition

4 – Maximum stress at the thinner end of the transition section

5 – Rapid stress reduction along the transition as cross section increases

6 – Minimum stress at the thicker end of the transition section

7 – Increase in stress, at a much lower value, passed the end of the transition and into the thicker section

8 – Stabilization of the stress through the thicker section

9 – Drop off of the stress due to model end boundary condition

The stress distribution curve for the longer model with slope of 1:4 is presented in Figure 7-3

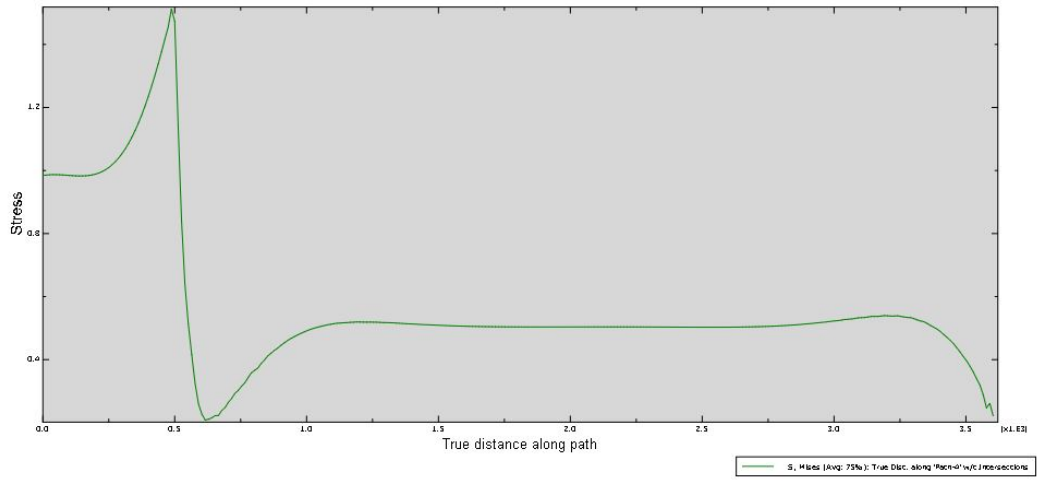

Figure 7-3 SCF Variation along the Long Model

It can be seen that the same pattern is repeated for the longer model, with a longer section of stress stabilization zone along the thicker member.

Chapter 8
Effect of Fabrication Misalignment

8. EFFECT OF MISALIGNMENT

Comprehensive study of the fabrication issues are not part of this research work. However, a critical issue during fabrication has been assessed. During fabrication there is a possibility of misalignment at the joints due to non-aligned fit-up or due to thickness tolerances or variation and non-circularity of the diameter around the tubes. The maximum allowable misalignment at a joint as specified by EEMUA 158 (2014) should not be greater than 10% of the thickness of the thinnest member or 3mm for a single sided weld or 6mm for a double sided weld whichever is less.

For joints with varying thicknesses, there is always an eccentricity due to no aligned centre lines of the two sections. Misalignment due to fabrication can increase or decrease the eccentricity and affect and increase the SCF, (Figure 2-12, 2-13).

The variation of SCF increase, due to misalignment, is assessed for different transition slopes of 1:4, 6 and 8 for the models under study.

8.1. MODEL A

Model A is subset of model 1, case 1 (ref section 6.1) that is, a 3000mm diameter member with T=50 and t=25 and transition slopes of 1 in 4, 6 and 8. The maximum misalignment of 10% (2.5mm) has been used.

The summary of results for this model is shown in Figure 8-1

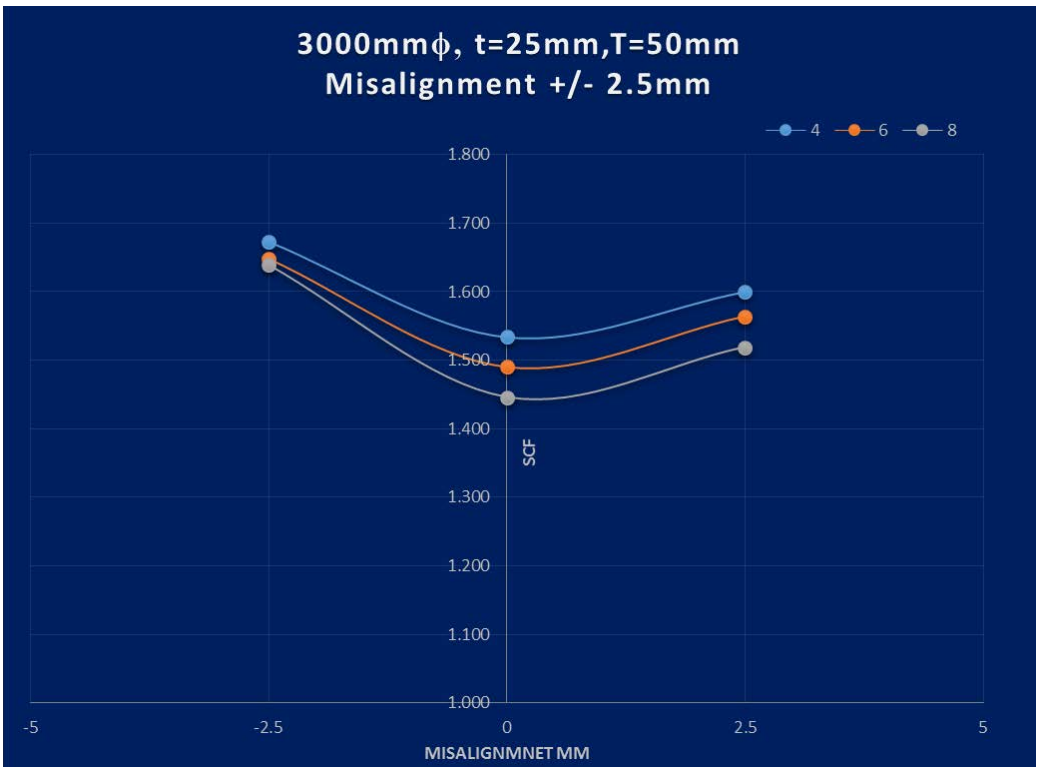

Figure 8-1 SCF Variation with Slope and Misalignment - Model A

8.2. MODEL B

Model B is subset of model 2, case 3 (ref section 6.2) that is, a 3000mm diameter member with T=125 and t=50 and transition slopes of 1 in 4, 6 and 8. The maximum allowable misalignment according to EEMUA 158 (2014) is 10% of t, 3mm, or 6mm depending on welding procedure, however, a value of 10% (5mm) has been used.

The summary of results for this model is shown in Figure 8-2

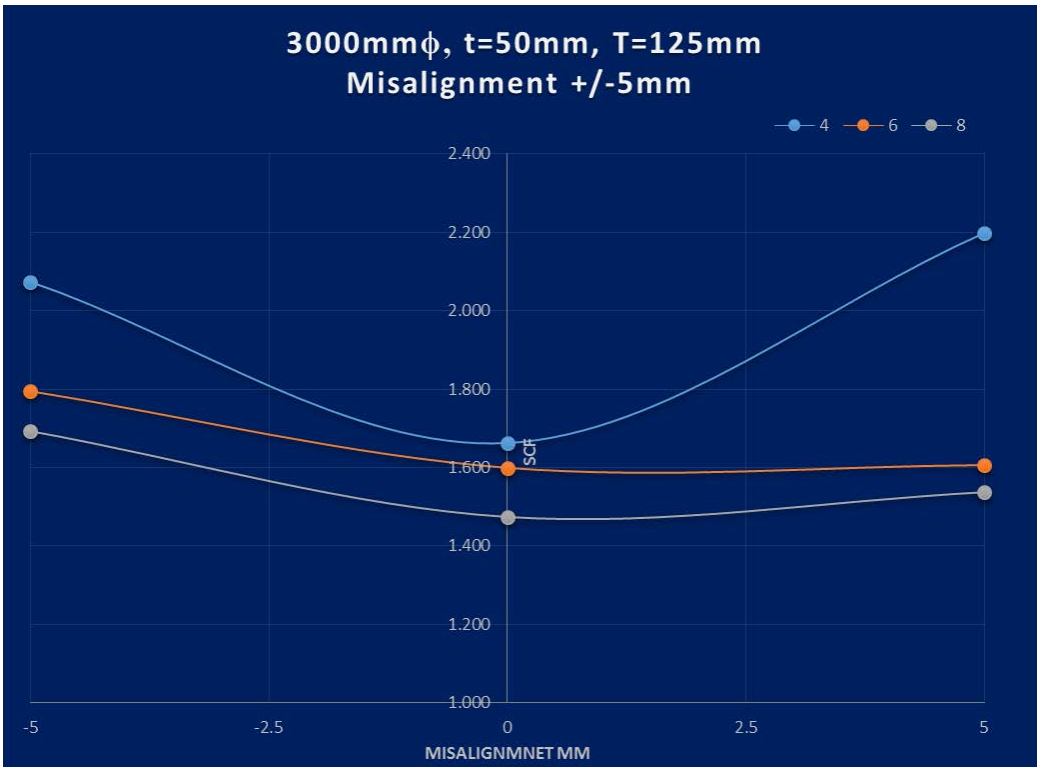

Figure 8-2 SCF Variation with Slope and Misalignment - Model B

8.3. MODEL C

Model C is subset of model 3, case 1 (ref section 6.3) that is, a 2000mm diameter member with T=50 and t=25 and transition slopes of 1 in 4, 6 and 8. The maximum allowable misalignment of 10% (2.5mm) has been used.

The summary of results for this model is shown in Figure 8-3

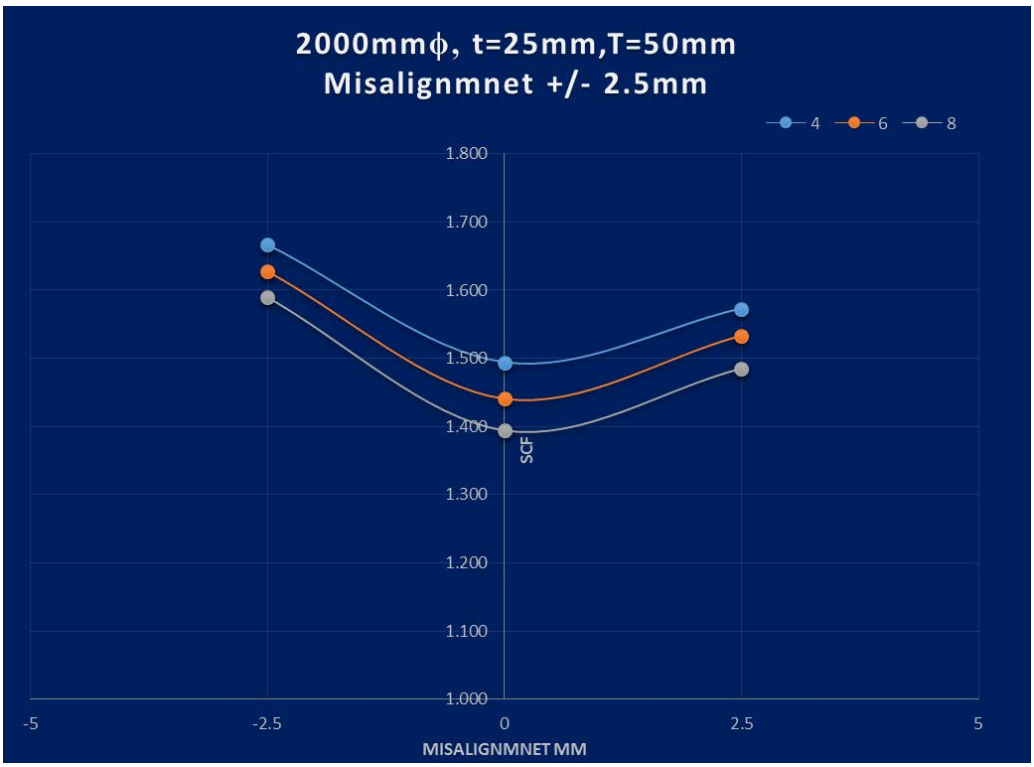

Figure 8-3 SCF Variation with Slope and Misalignment - Model C

8.4. MODEL D

Model D is subset of model 4, case 3 (ref section 6.4) that is, a 2000mm diameter member with T=125 and t=50 and transition slopes of 1 in 4, 6 and 8. Similar to Model B, a maximum misalignment of 10% (5mm) has been used.

The summary of results for this model is shown in Figure 8-4

It can be concluded that both positive and negative misalignments increase the SCFs for all cases, to a varying degree.

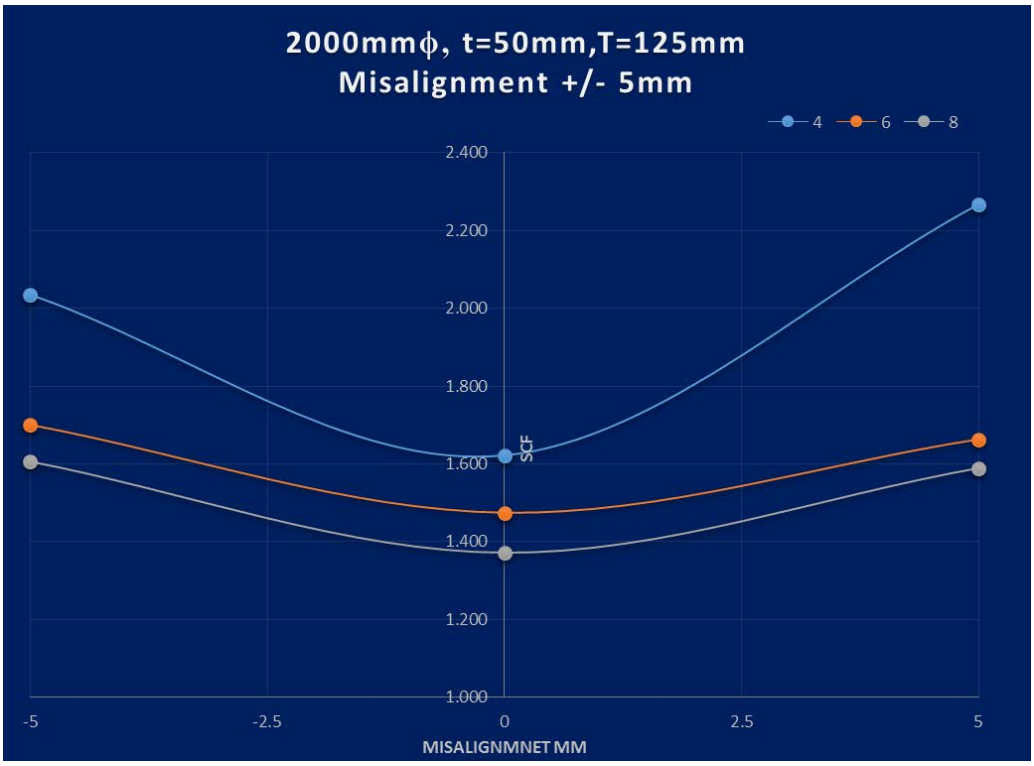

Figure 8-4 SCF Variation with Slope and Misalignment - Model D

Chapter 9
Conclusions
and
Recommendations

9. CONCLUSIONS AND RECOMMENDATIONS

Research was performed to summarize previous historic information regarding theoretical, experimental and numerical studies conducted on typical circumferential tubular joint configurations and weld preparations to be used for offshore structural thick nodes and members.

A number of models were analysed to assess cases outside current code limitation and provide some insight into the findings, and viability of relaxation of these limitations, the conclusions and recommendations for future work are summarized in the following sections.

9.1. CONCLUSIONS

It was found that for a number of decades the practical norms from 1970's have been carried through without further investigation to assess the situations designers are confronted with in day to day design.

Codes and standards have kept all the norms the same for the past 40 years.

This research has shown that there are potential alternatives that could:

- Reduce time and cost of analysis and design
- Reduce and save steel and welding material
- Reduce fabrication time and cut costs
- Reduce jacket weight

The current norms based on historic practices since early 70s for design of offshore jacket structures, which are the basis for this research, are:

1. Thickness ratio (T/t) limit of two abutting joints for cylindrical members to be less than 2
2. Pup-Pieces to be used, if thickness ratios are higher than 2:1
3. The slope of transition at the joint to be fabricated at 1 in 4

The results of this research have shown in all cases considered, for higher thickness ratios (T/t) up to 5, SCFs increase or remain within close proximity of values when compared to the values with the standard limit of T/t = 2, depending on the slope of transition.

However, SCF for T/t greater than 2 can be reduced by as much as 10-15% if the slope of transition is reduced to a much shallower slope, as much as 1 in 8 or 1 in 10.

The conclusions from the work in this thesis are of major practical significance in design of thick members, especially on jacket legs, as the results indicate that if leg nodal tube thickness is large with a shallow slope it can be welded directly to thinner members of the leg tubes without the use of pup-pieces, hence substantial savings in costs

These identified alternatives are currently not considered in any recommended codes of practice. Practical design situations require substantial analyses to find a suitable low cost solution by repetitive selection of pup piece sizes with different thicknesses to be able to minimize the cost of steel and welding while complying with the code and remaining within the limit of T/t less than or equal to 2.

DNVGL-RP-0005 (2014) *"Fatigue Design of Offshore Steel Structures"* Recommended Practice clause 3.3.7.3 clearly states that:

a) Thickness transitions are normally to be fabricated with slope 1:4
b) The effect of diameter in relation to thickness may be included by the use of equations given, provided that the thickness ration T/t is less than or equal to 2.

However, DNVGL-OS-C401 (2015) "*Fabrication and Testing of Offshore Structures*" states that the slope of transition should not be steeper than 1 in 4, but restricts the T/t to maximum of 2.

The above recommended practices can easily be adhered to and incorporated in the design for small diameter and thickness members, such as pipelines and risers which are usually less than approximately 1.2m in diameter (48" diameter pipes) with thickness less than approximately 40mm and some of the smaller bracing members in jacket structures of similar sizes.

However, for the larger diameter members especially jacket legs with 2m, 3, 5 or even 10m in diameter with thicknesses up to 125mm fabricated or with higher thicknesses of 200 or 250mm in some cast nodes, these rules are prohibitively restrictive.

The research has shown that these norms may need to be revised as alternatives prove to be more cost efficient in terms of material and fabrication. The advantages obtained and highlighted in this research project should be taken into account in the future for design of large diameter jacket legs.

The research has concluded that thickness ratios of up to 5 can be used if the shallower slopes are considered. The effect on SCF at the joint in all cases studied is that shallower slopes provide lower SCFs. Nowadays; the machining technology is commonly available to be able to provide a perfect shallow slope.

In design of jackets weight minimization is crucial if the jacket is to be lift installed, especially when the lift weight is close to the limit of lifting of the designated vessels.

Relaxation or revisions of the current limits in the design and fabrication codes would allow removal of unnecessary pup-pieces, reduction of welding requirements on thick sections, and reduction of overall jacket design weight, as well as substantial reduction in material and fabrication costs.

9.2. RECOMMENDATIONS

The industry norms and practices may need revisions to be incorporated into the future codes and standards.

Two pathways are recommended as potential future work to be able to justify revisions in the codes of practice:

1- Conduct further large number of finite element analyses for many other possible joint combinations to re-confirm the findings of this thesis.

2- Conduct a number of large scale tests on thin tubes with D/t in the range of 80 - 120 connected to thicker tubes with T/t up to 5, with

various slopes as shallow as 1:6 to 1:10, to re-affirm findings and compare with numerical simulations.

Subject to these confirmations, authorities may then consider revising the recommendation to assist designers in providing better designs and asset operators in saving substantial costs.

Chapter 10

References

10. REFERENCES

1. ABAQUS (2011)

   ABAQUS Version 6.10, Dassault Systèmes Simulia Corp. Providence, Rhode Island, USA

2. Alivev, H. Foundation (2016)

   History of Development of Oil Industry, Accessed 27th Jan http://www.azerbaijan.az/portal/index_e.html?lang=en

3. Almar Naess A (1999)

   Fatigue Handbook: Offshore Steel Structures 3rd edition. Tapir

4. Anderson, T.L., (2005)

   Fracture Mechanics - Fundamentals and Applications, 3rd Edition, CRC Press

5. Akita, Y, Maeda, T, Yada, T and Sakai, K. (1971)

   Effect of welding distortion on brittle fracture initiation in pressure vessels, Institution of Mechanical Engineering, Conference on Practical Applications of Fracture Mechanics to Pressure Vessel Technology, Paper C3

6. American Bureau of Shipping, (2014)

   ABS *Guide for Fatigue Assessment of offshore Structures*

7. American Petroleum Institute,
API "*Recommended practice for Planning, Designing and Constructing fixed offshore platforms*", API RP2A, various Editions, American Petroleum Institute, Washington, DC.

8. American Welding Society, ANSI/AWS D3.5 1993 (R2000)
Guide for Steel Hull Welding

9. British Standard Institute, BS 7910 (2015),
Guide to Methods for assessing acceptability of flaws in metallic structures

10. British Standard Institute BS 7608 (2014),
Guide to Fatigue Design and Assessment of Steel Products

11. Burdekin, F. M. (1979)
The effect of deviation from intended shape on fracture and failure.
Paper C12/79, Institution of Mechanical Engineer

12. Callan, M. D., Wordsworth, A.C., Livett, I.G., Boudreaux R.H., Huebsch, F.J. BP (1981), Magnus Platform Internally Stiffened Bracing Node Studies, OTC 4109 Offshore Technology Conference, Houston, USA

13. Confidential Oil Company (2011)
Production Utility and Quarters Jacket fatigue Analysis
02-Dec, Confidential Report

14. Confidential Oil Company (2011)
Well Head Jacket fatigue Analysis
02-Dec, Confidential Report

15. Connelly, L.M and Zettlemoyer, N., (1993)
Stress Concentration at Girth Welds of Tubulars with Axial Wall Misalignment, Proceedings of Fifth International Symposium, on Tubular Structures Nottingham, UK.

16. Department of Energy (1984)
Background to new fatigue design guidance for steel welded joints in offshore structures, Report of the Department of Energy Guidance Notes, Revision Drafting Panel, HSMO, London, 1984.

17. Det Norske Veritas (2011)
Fatigue Design of Offshore Steel Structures, DNV RP-C203

18. Det Norske Veritas (2010)
Fabrication and Testing of Offshore Structures, DNV RP-C401

19. DNV-GL (2014)
Fatigue Design of Offshore Steel Structures, DNVGL RP-0005,

20. Engineering Equipment and Materials Users Association, (1994)
Construction Specifications for Fixed Offshore Structures in the North Sea, EEMUA 158

21. Engineering Equipment and Materials Users Association, (1998) *Construction Specifications for Fixed Offshore Structures in the North Sea*, EEMUA 158, Amendment No1 & 2,

22. Engineering Equipment and Materials Users Association, (2000) *Construction Specifications for Fixed Offshore Structures in the North Sea*, EEMUA 158 , Amendment No3, September

23. Engineering Equipment and Materials Users Association, (2014) *Construction Specifications for Fixed Offshore Structures in the North Sea*, EEMUA 158, 3rd Edition, January 1

24. Efthymiou, M. and Durkin, S. (1985)

'Stress Concentrations in T/Y and gap/overlap K-joints.'

Proceedings Conference On the Behaviour of Offshore structure, Delft, Elsevier Science Publishers, Amsterdam, , pp429-40

25. Furnes Olav and L¢set Oystein (1981)

Shell structures in offshore platforms: design and application

Engineering. Structures. Vol. 3, July

26. Eurocode EN 1993-1-9 (2005),

Design of Steel Structures,

27. Gunn, K .W., Mclester, R., (1960)

Effect of mean stress on fatigue properties of aluminium alloy butt welded joints. British Welding Journal, 7, (3), pp 201-208

28. Gurney, T. R., (1968)
Fatigue of Welded Structures, Cambridge University Press

29. Gurney, T. R., (1979)
Fatigue of Welded Structures, Cambridge University Press, 2nd Edition

30. Heshmati, E (1990)
Practical Aspects of Design of Thick-Walled Nodes for Offshore Structures, Offshore technology Conference , OTC 6485, Houston, Texas, USA

31. Heshmati, E. Guy,R. Livett, I, Lewis, G. (1986)
Analysis methods and Inspection Procedures for Single sided closure Welds in Offshore Structures, Offshore Technology Conference, OTC5315, Houston, Texas, USA

32. Harrison, J. D. Burdekin, F. M. and Young, J. A. (1968)
A Proposed acceptance standard for weld defects based upon suitability for service, Welding Institute, 2nd Conference on the significance of defects in welds, 1968

33. Health and Safety Executive, UK (2001)
Offshore Technology Report OTO 2001 015, Steel

34. Health and Safety Executive, UK (1999)
Offshore Technology Report OTO 1999 022
Fatigue Life Implications for Design and Inspection for Single Sided Welds at Tubular Joints

35. Health and Safety Executive, UK (2001)
Offshore Technology Report OTO 2001 083
Comparison of fatigue provisions in codes and standards

36. Hobbacher, A, (2003)
Recommendations on Fatigue of Welded Joints and Components, International Institute of Welding, Paris, IIW-XIII-1965 – 03 / XV-1127 – 03

37. Hobbacher, A, (2008)
Recommendations on Fatigue of Welded Joints and Components, International Institute of Welding, Cambridge, England, IIW-1823-07 ex XIII-2151r4-07/XV-1254r4-07

38. Irick J. T., Birdwell J. R., Henkhaus E. J., Hayes D. A., Mania G. A., (1980)
Design and installation of the main pass 72 Mud slide resistant platform, Offshore Technology Conference, OTC 3878, Houston, Texas, USA

39. International Organization for Standardization ISO 6520 (2007)
Welding and Allied Processes, Classification of geometric imperfections in metallic materials Part 1, Fusion Welding,

40. James D. P. Edward D. C. and Christian J. R., (1971)
Fatigue Consideration in the design of Pipelines,
Welding Institute Conference on Improving Welded Product Design, Paper No 8

41. Kuang, J.G., Potvin, A.B. and Leick, R. D. (1975)
Stress Concentration in Tubular Joints
In " Proc.7th Annual Offshore Technology Conference", OTC2205, Houston, TX, 1975, pp. 593-612.

42. Lie S. T, Lan S. (2000)
Computer prediction of misaligned welded joints
Advances in Engineering Software 31, 65–74

43. Lloyd's Register of shipping, (1991)
Stress concentration factors for tubular complex joints

44. Lotsberg, I, (2009)
Stress Concentrations due to misalignment at butt welds in plated structures and at girth welds in tubular,
International Journal of Fatigue, Vol 31, No8-9, 1337-1345.

45. Maddox, S J, (1985)
Fitness for purpose assessment of misalignment in transverse butt welds subjected to fatigue loading, International Institute of Welding, IIW Document XIII-1180-85

46. Maddox, S. J., (1991)
Fatigue Strength of Welded Structures, Abington, Cambridge

47. Maddox, S J, (1997)
Developments in fatigue design codes and fitness for service assessment methods. International Conference on performance of dynamically loaded welded structures, Welding Research Council

48. Maddox, S. J., (2004)
Calculation of Secondary Bending Stress Due to Axial misalignment in Girth Welded Joints Document no. WEE37-0018-04

49. Maddox S J, Beck J B, G R Razmjoo, (2008)
An Investigation of the Fatigue Performance of Riser Girth Welds Journal of Offshore Mechanics and Arctic Engineering, FEBRUARY Vol. 130 (1)

50. Marquis and Samuelsson (2005)
Modelling and fatigue life assessment of complex Structures, Mat.-wiss. u. Werkstofftech. 2005, 36, No. 11

51. Miner, M. A., (1945)
Cumulative Damage in Fatigue,
J. Applied Mechanics, 12, A159-A164

52. Nishimaki K, (1969)
Fatigue strength of butt joints with misalignment.
Report on Research into the Fatigue Strength of High Tensile Steels by 95th Research Committee of the Shipbuilding Research Association of Japan

53. Niemi, E., (2000)
Structural Stress Approach to Fatigue Analysis of Welded Components: Designer's Guide, International Institute of Welding, Paris, IIW-XIII-1819 – 00.

54. Priddle, E. K., (1973)
Fatigue in Boiler tube but welds. Part 2: The effect of defect severity. IIW Doc XII-679-73

55. Palmgren, A., (1924),
Die Lebensdauer von Kugellagern, Verfahrenstechinik, Berlin, Vol.68, pp. 339-341

56. Radaj,D (1996)
Review of fatigue strength assessment of non-welded and welded structures based on local parameters, Int. J. Fatigue Vol. 18, No 3, pp. 153-170

57. Radaj,D. and Sonsino, C. M. (1998)
Fatigue assessment of welded joints by local approaches, Abington, Cambridge

58. Radaj,D. and Sonsino, C. M., Fricke, W., (2006)
Fatigue assessment of welded joints by local approaches, 2nd edition, Woodhead Publishing, Cambridge

59. Rupp, A., Grubisic, V. and Radaj, D. (1990)
MaterialpriiJung, 32, t 7534

60. Rupp, A., Grubisic, V. and Radaj, D. (1994)
Rechnergesttitzte AuslegungpunktgeschweiBter Bauteile'. DVM-Berichte, AK Betriebsfestigkeit, pp. 159-175

61. Romejin A, (1994)
The Fatigue Behaviour of multi-planar tubular Joint,
HERON, Vol 39, No 3

62. Sawada Y., Idogaki, S., Sekita K (1979)
Static and Fatigue Tests On T-Joints Stiffened By an Internal Ring
OTC 3422, Offshore Technology Conference, Houston, USA

63. Schijve J. (1994)
Fatigue predictions and scatter. Fatigue Fract Eng Mater Struct; 17:3, 81–96.

64. Schijve, J. (2005)
Statistical distribution functions and fatigue of structures
International Journal of Fatigue 27, 1031–1039

65. Schempf, F. Jay., (2007)
Pioneering Offshore: The Early Years, Pennwell Publishing, USA

66. Spangenberg, L., (1874) *Ober das Verhalten der Metalle bei wiederholten Anstrengungen.* Z. Bauw. 24, 473-495 and 25,78-98

67. Tomkin B., (1979)
Fatigue Failure criteria for thick walled cylindrical pressure vessels, International Journal of Pressure vessels and Piping, Volume 1, Issue1, P37-59

68. Timoshenko S, and Woinowsky-Krieger S. (1959)
Theory of Plates and Shells, 2nd Edition, McGraw-Hill Book Company

69. UK Department of Energy (1974)
Offshore Installations: Guidance on Design, Construction and Certification, 1st Edition 1974 to 4th Edition. HMSO, Consolidated Edition, 1993 (plus Amendment No. 3, 1995). Withdrawn 1998 by Operations Notice 27].

70. Wordsworth, A.C. and Smedley, G.P. (1978)
In "Proceeding of European Offshore Steel Research Seminar", Cambridge, UK, November, paper 31.

71. Wylde J G, Maddox S J, (1979)
Effects of misalignment on fatigue strength of transvers butt welded joint, Paper Presented at IMechE Conference 'Significant of Deviation from design Shapes', March

72. Webster, S. E., Walker, F., Wood, A., M. (1981)
Cast Steel Nodes - Their Manufacture and Advantages to Offshore Structures, Society of Petroleum Engineers of AIME, October, 1999-2005

73. Wohler, A. (1867)
Versuche uber die Festigkeit der Eisenbahnwagenachsen, Zeitschrift fur Bauwesen,10; English summary, Engineering, Vol.4, pp.160-161.

74. Xu S. H., Yang F.Y., Jian L.Q., Gu, M. W, Song Z., R., Yao, D. W., Liu, Q. C (2015) *Study of New Welding Tubular Joint Used For Jackets*
5th International Conference on Advanced Design and Manufacturing Engineering (ICADME 2015)

75. Ye, Su and Han (2014)
A State-of-the-Art Review on Fatigue Life Assessment of Steel Bridges, Mathematical Problems in Engineering, Volume 2014, Article ID 956473, Hindawi Publishing Corporation

Appendix A
Definitions

APPENDIX A - DEFINITIONS

In order to facilities readership and provide a background to the terminology used in industry and requirements in the design of offshore structures, the following definitions are made.

Definition of nodal construction is given in the Figure A.1 below (NORSOK Standard: N-004, 2013).

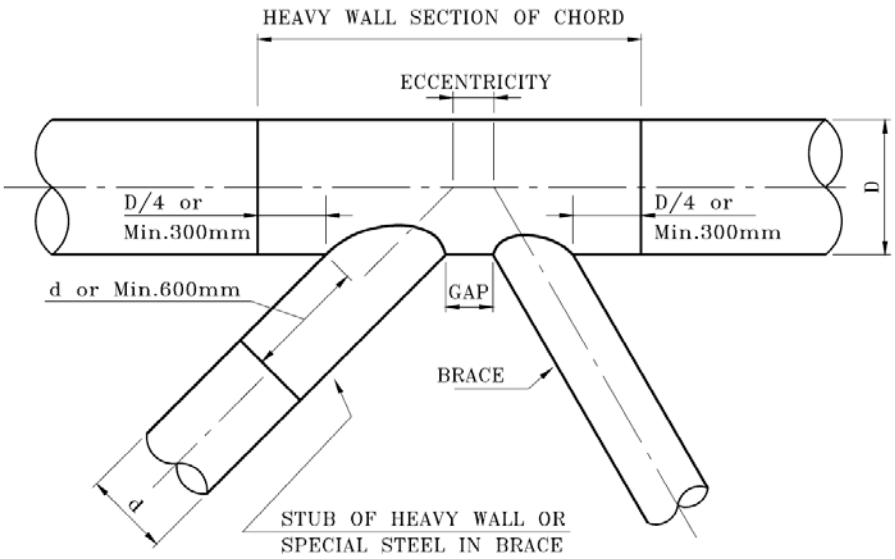

Figure A.1 Node Configuration & Definitions

Nodal construction requires thick wall ***"CHORD CAN"*** sections within thickness range of 50mm-125mm, to reduce SCFs for the connecting brace members, (Heshmati, 1990).

However, as shown in Figure A.2, connecting members, ***"nominal chord"***, on both side along the ***"chord can"*** may require smaller thicknesses for strength and buckling resistance, hence large thickness transitions may occur from the thick sections to thinner sections.

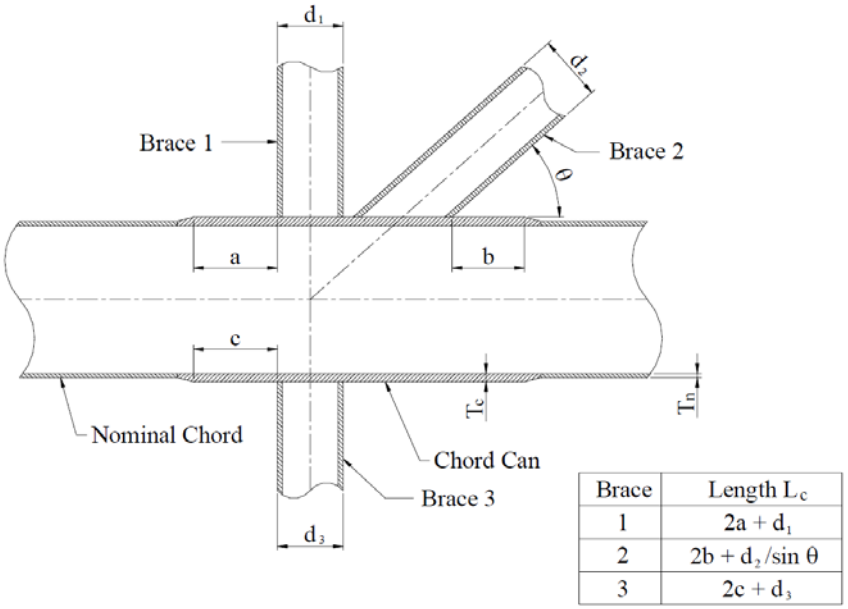

Brace	Length L_c
1	$2a + d_1$
2	$2b + d_2/\sin\theta$
3	$2c + d_3$

Figure A-2 Node Configuration & Definitions

The thickness transition could be located either externally with internal diameter matching (Figure A-3) or internally with external diameter matching (Figure A-4) or from both sides with thickness centerline matching (Figure A-5).

However, although all configurations have been used in many designs, the external diameter in many cases is usually kept constant for uniformity in design and ease of plate rolling with an identical external diameter and the transition located internally.

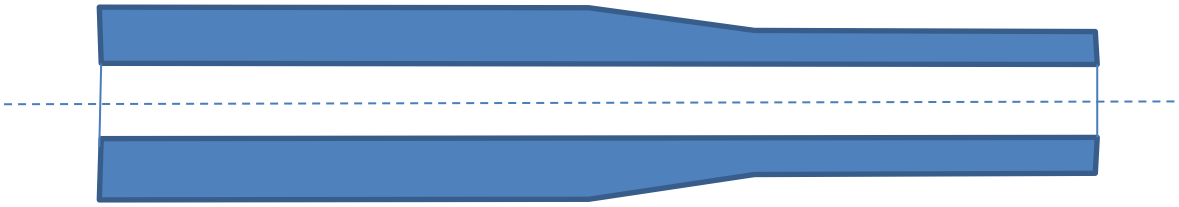

Figure A-3 Transition from Outside – Internal Diameter Matching

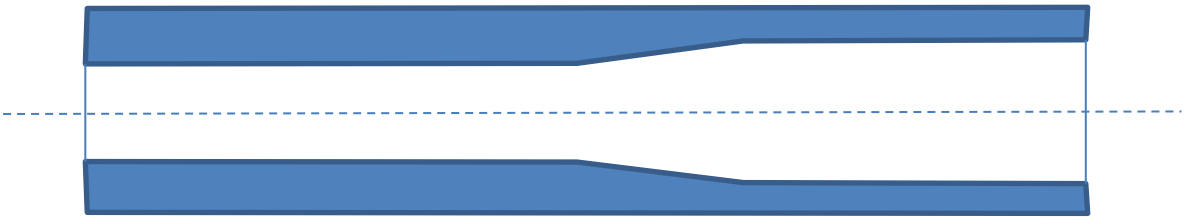

Figure A-4 Transition from Inside – External Diameter Matching

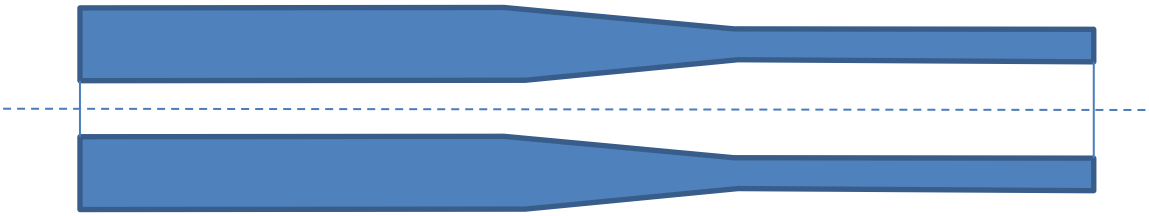

Figure A-5 Transition from Both Sides – Thickness Centerline Matching

Appendix B
Typical Model Plots

APPENDIX B – TYPICAL MODELS PLOTS

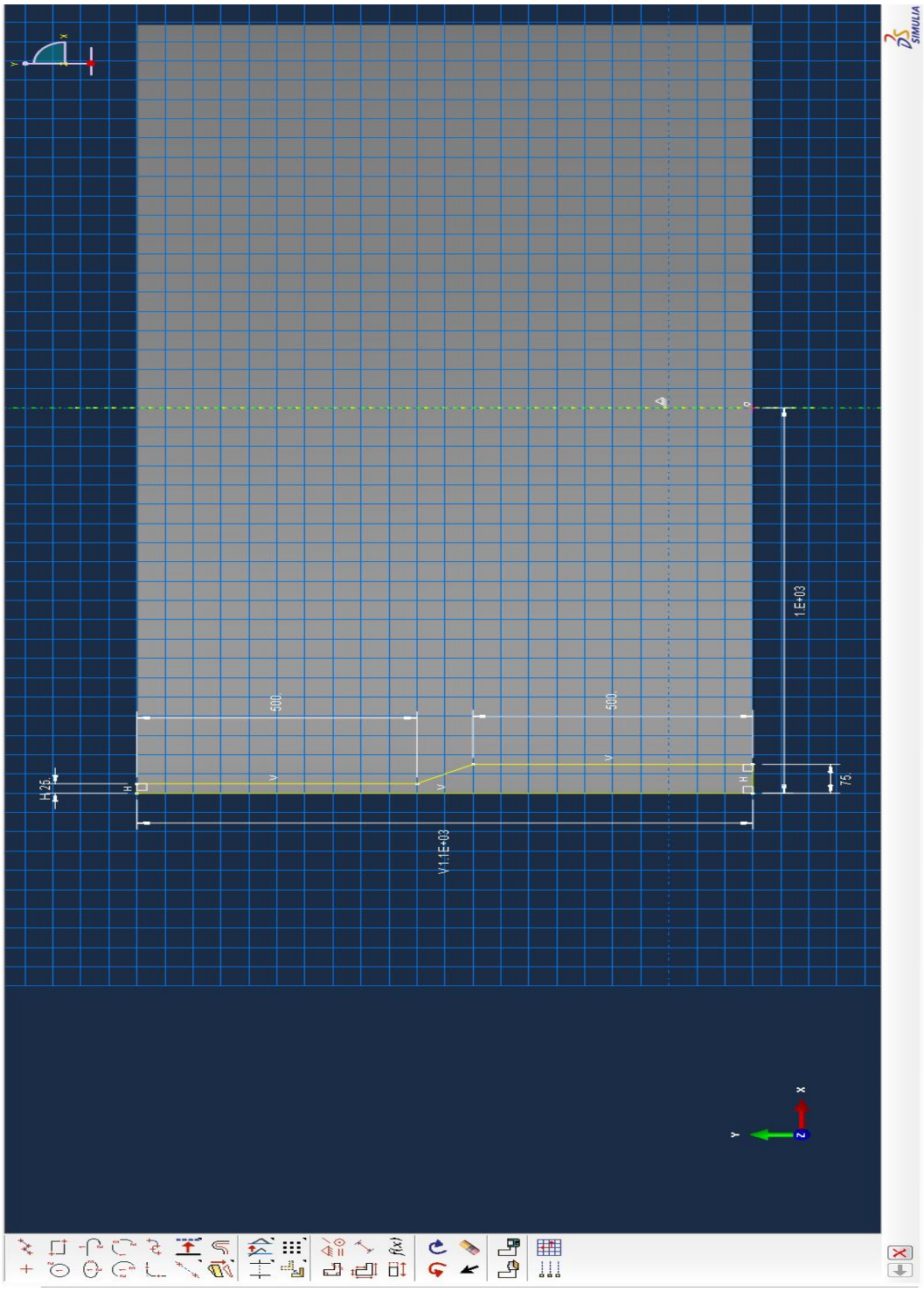

D=2000 mm, t= 25, T=75, T/t=3, Slope 1 in 2

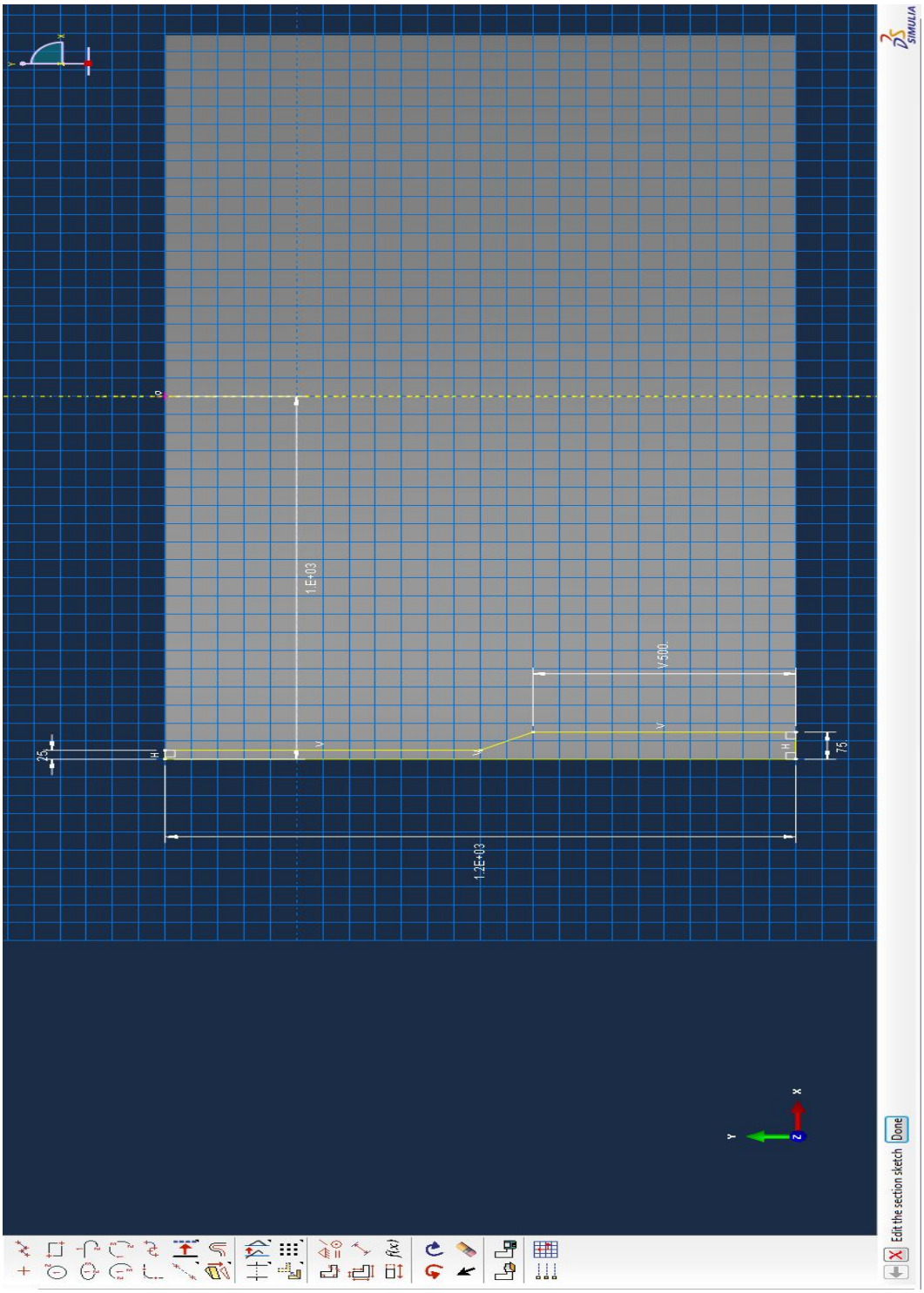

D=2000 mm, t= 25, T=75, T/t=3, Slope 1 in 4

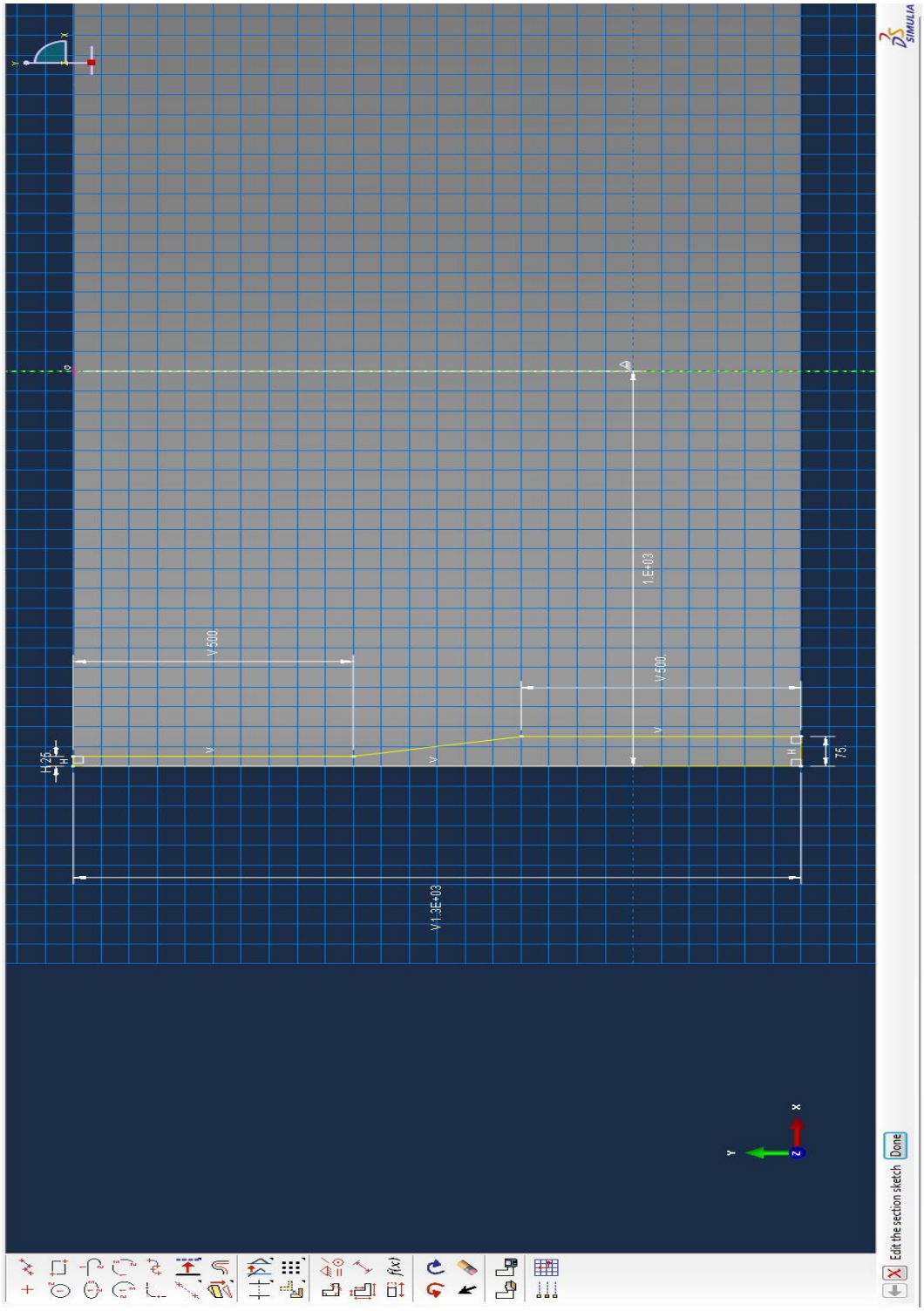

D=2000 mm, t= 25, T=75, T/t=3, Slope 1 in 6

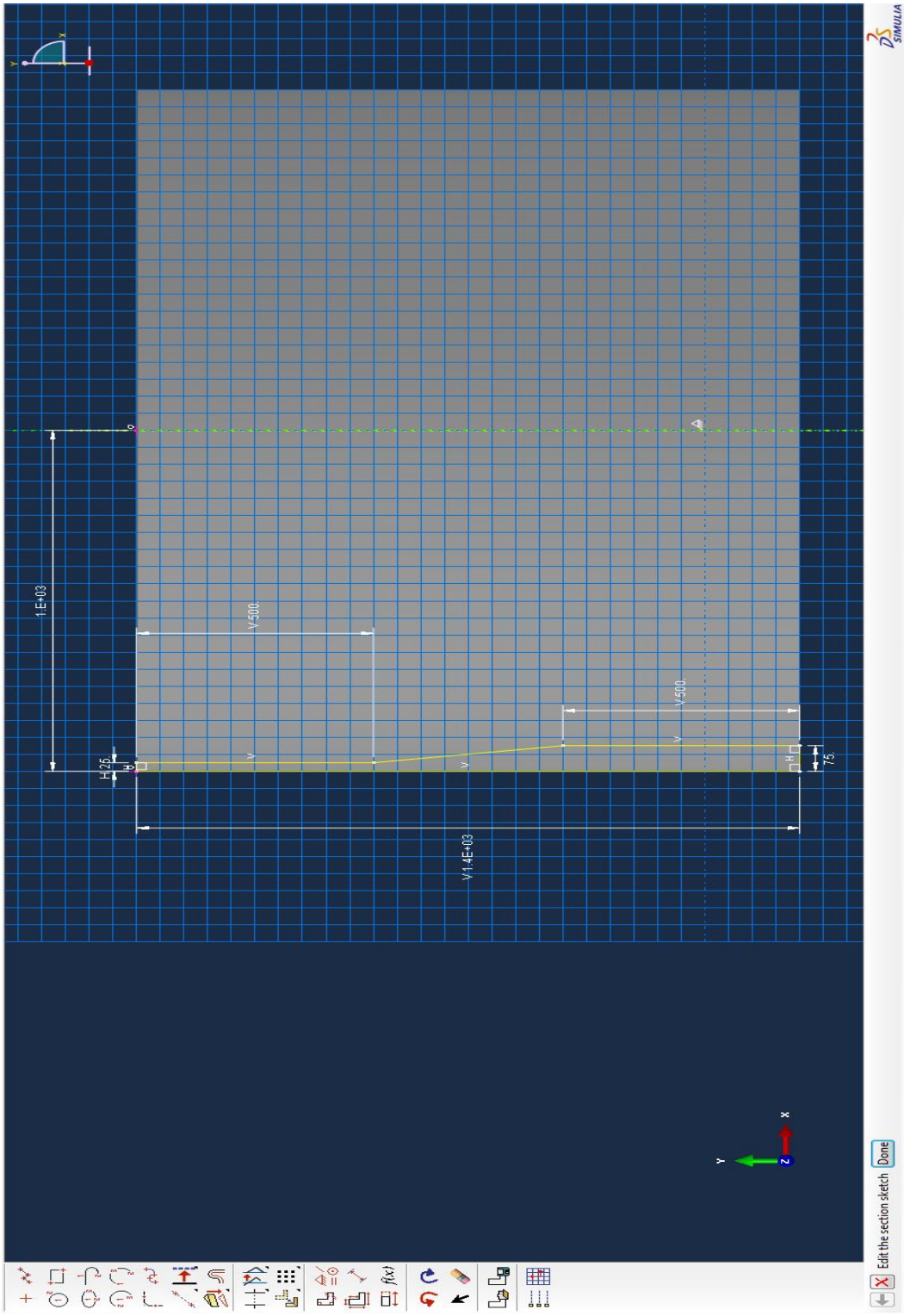

D=2000 mm, t= 25, T=75, T/t=3, Slope 1 in 8

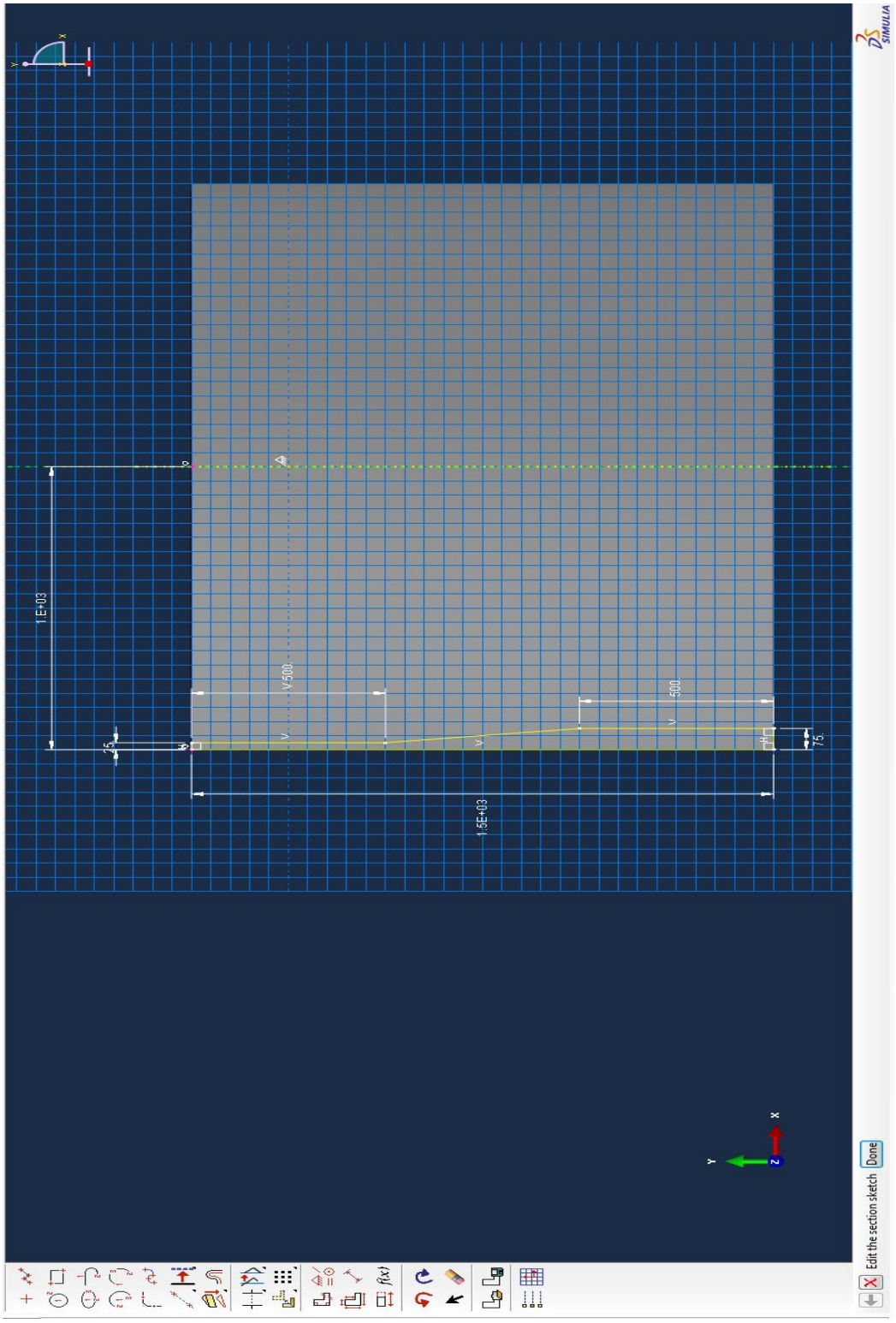

D=2000 mm, t= 25, T=75, T/t=3, Slope 1 in 10

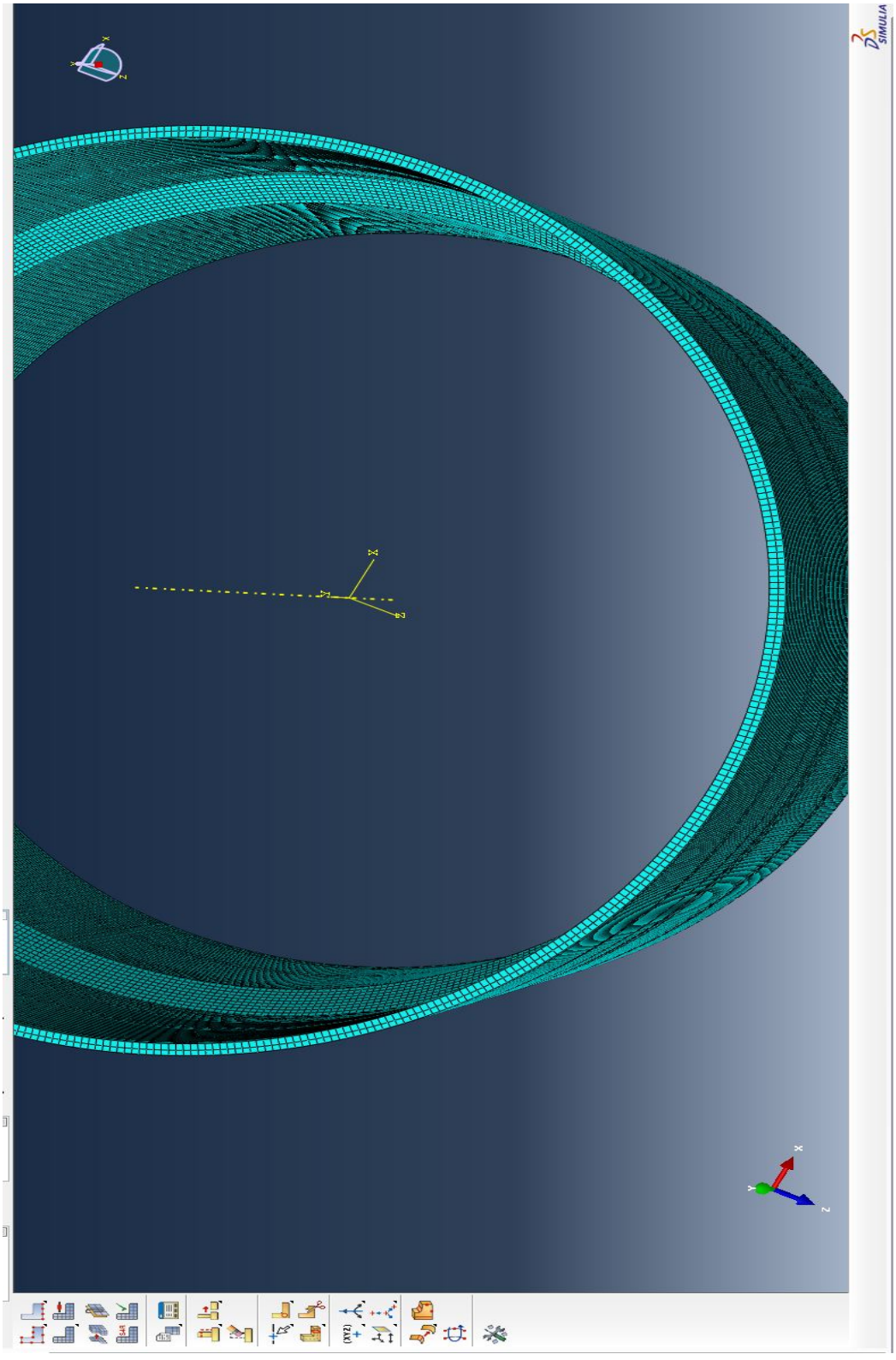

Typical Mesh

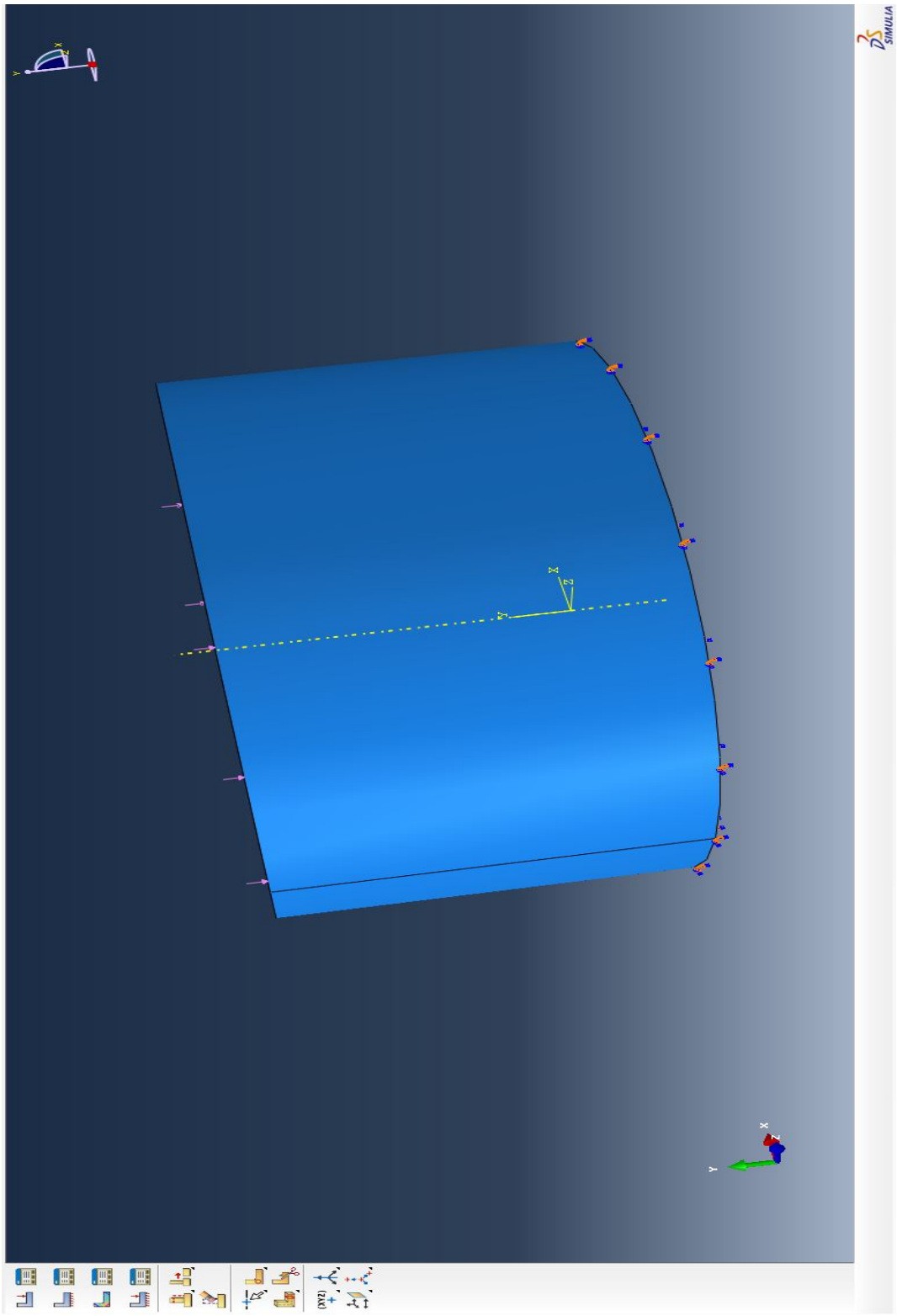

Typical Axial Load and Boundary Conditions

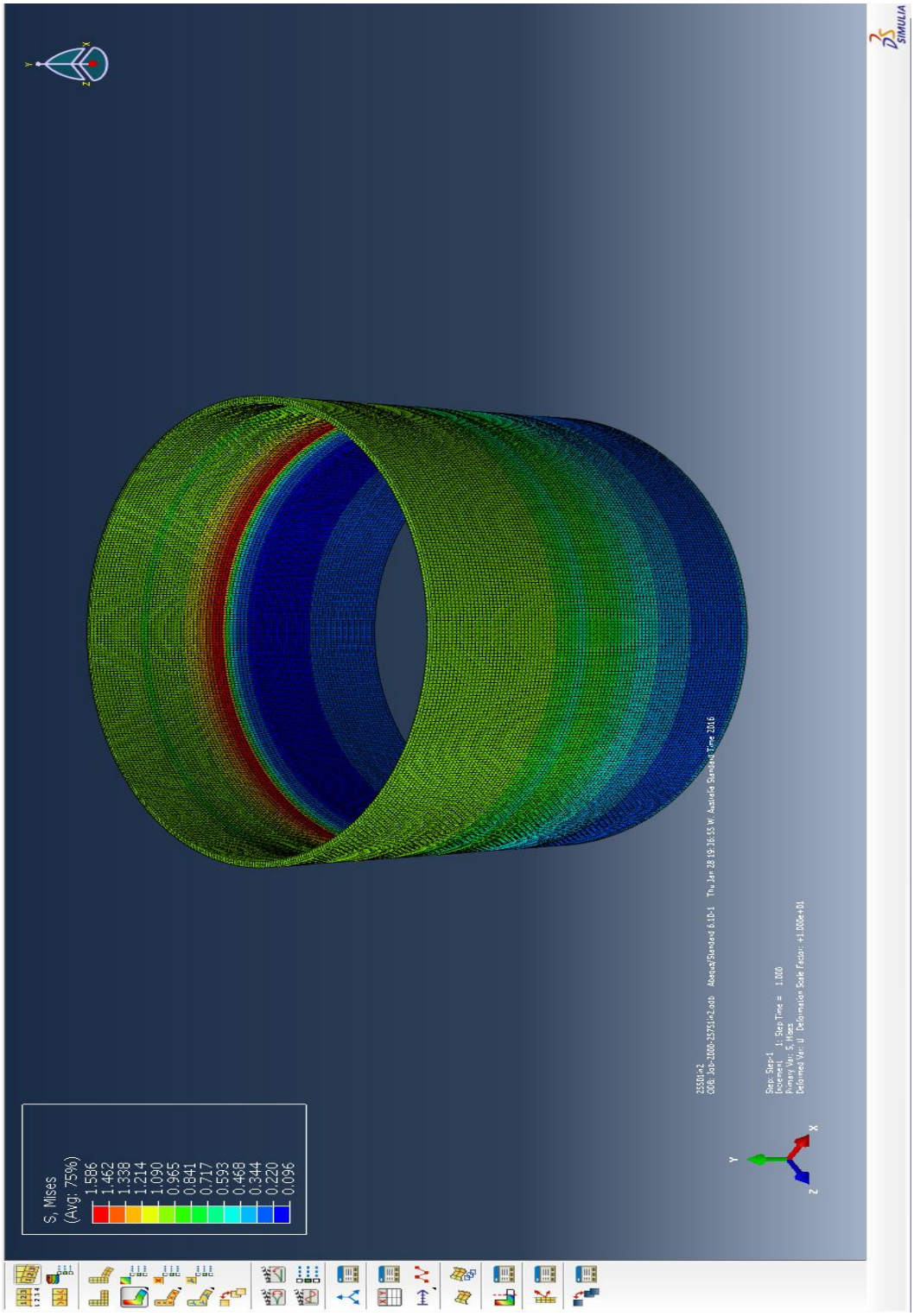

Results for D=2000 mm, t= 25, T=75, T/t=3, Slope 1 in 2

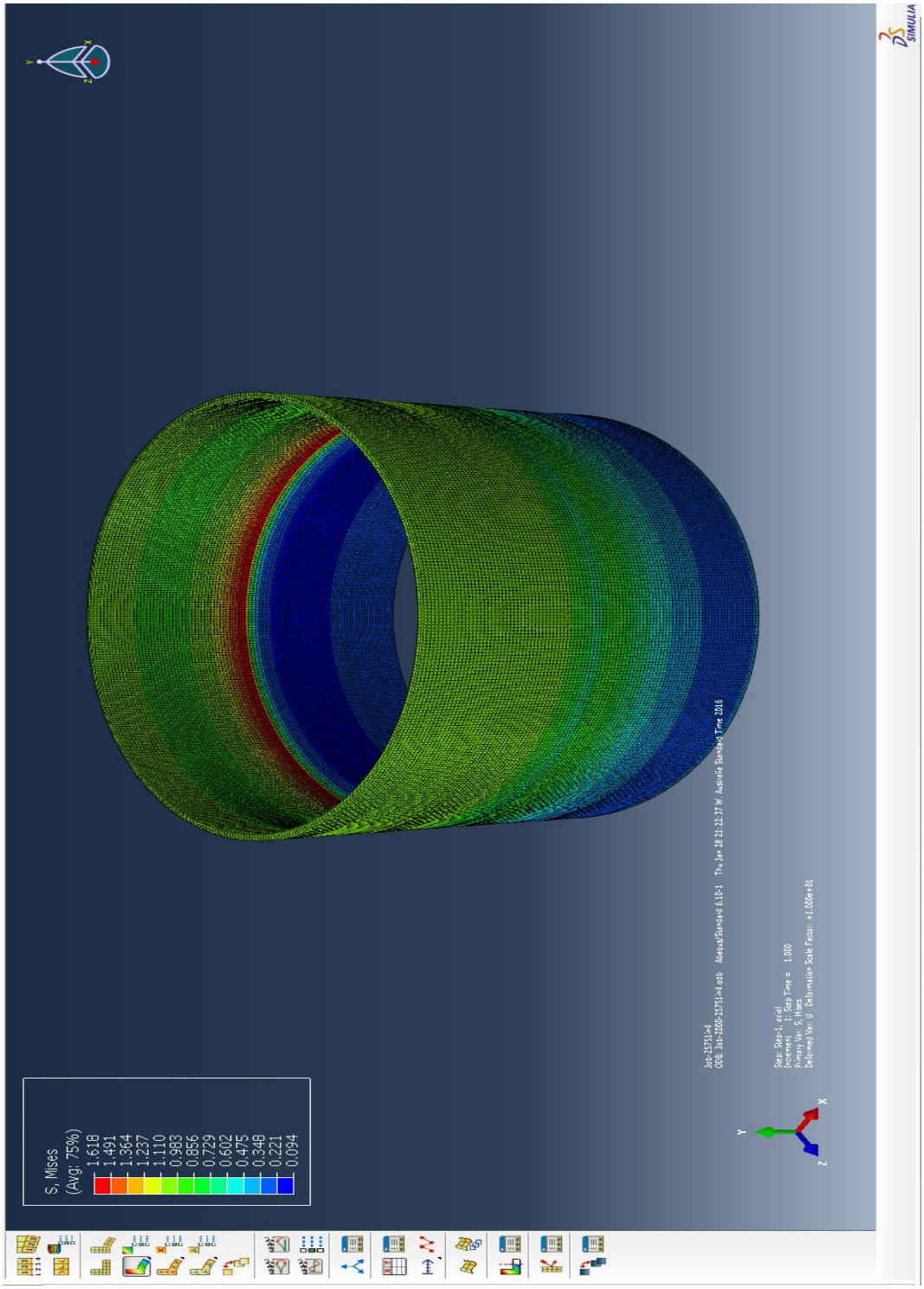

Results for D=2000 mm, t= 25, T=75, T/t=3, Slope 1 in 4

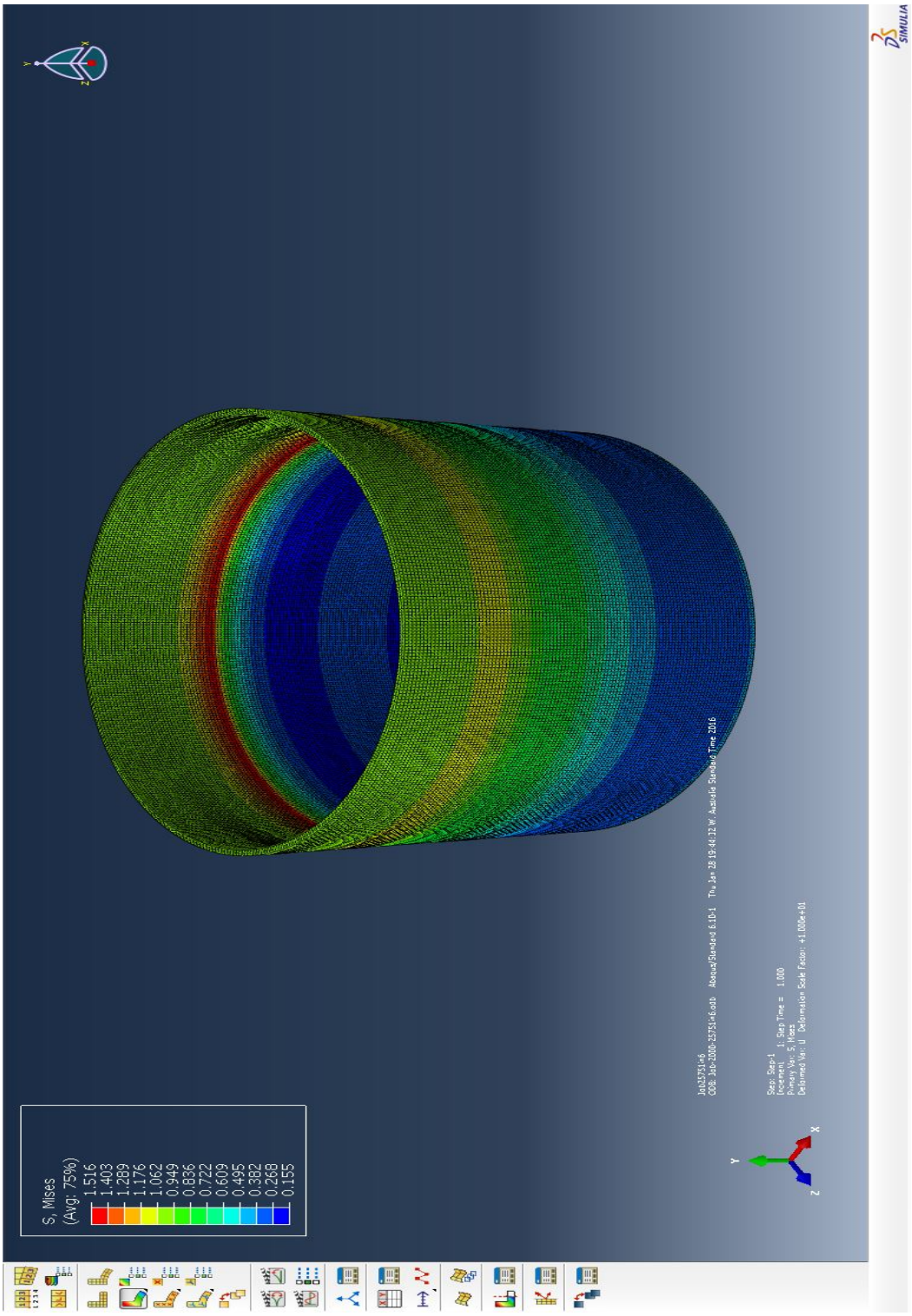

Results for D=2000 mm, t= 25, T=75, T/t=3, Slope 1 in 6

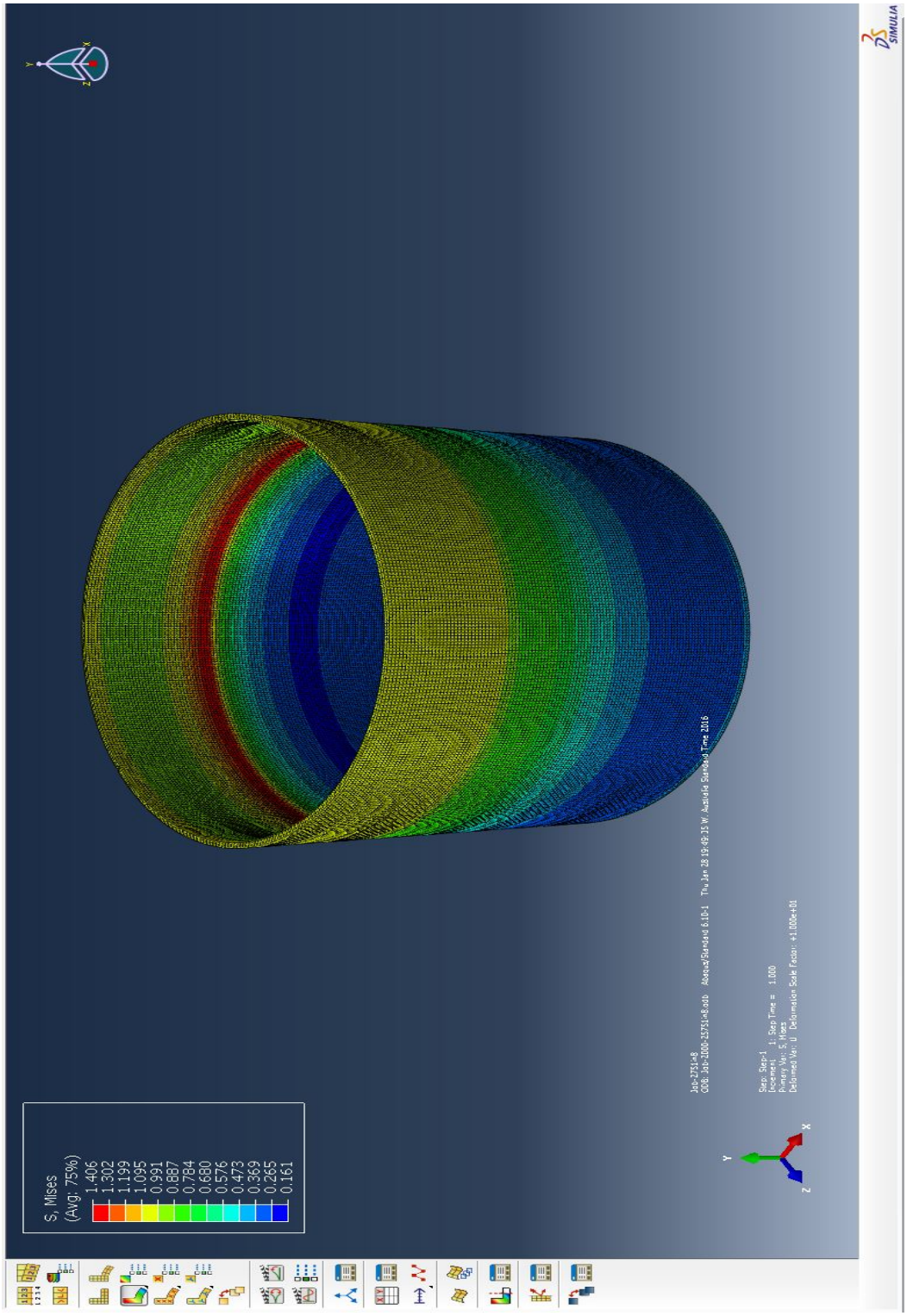

Results for D=2000 mm, t= 25, T=75, T/t=3, Slope 1 in 8

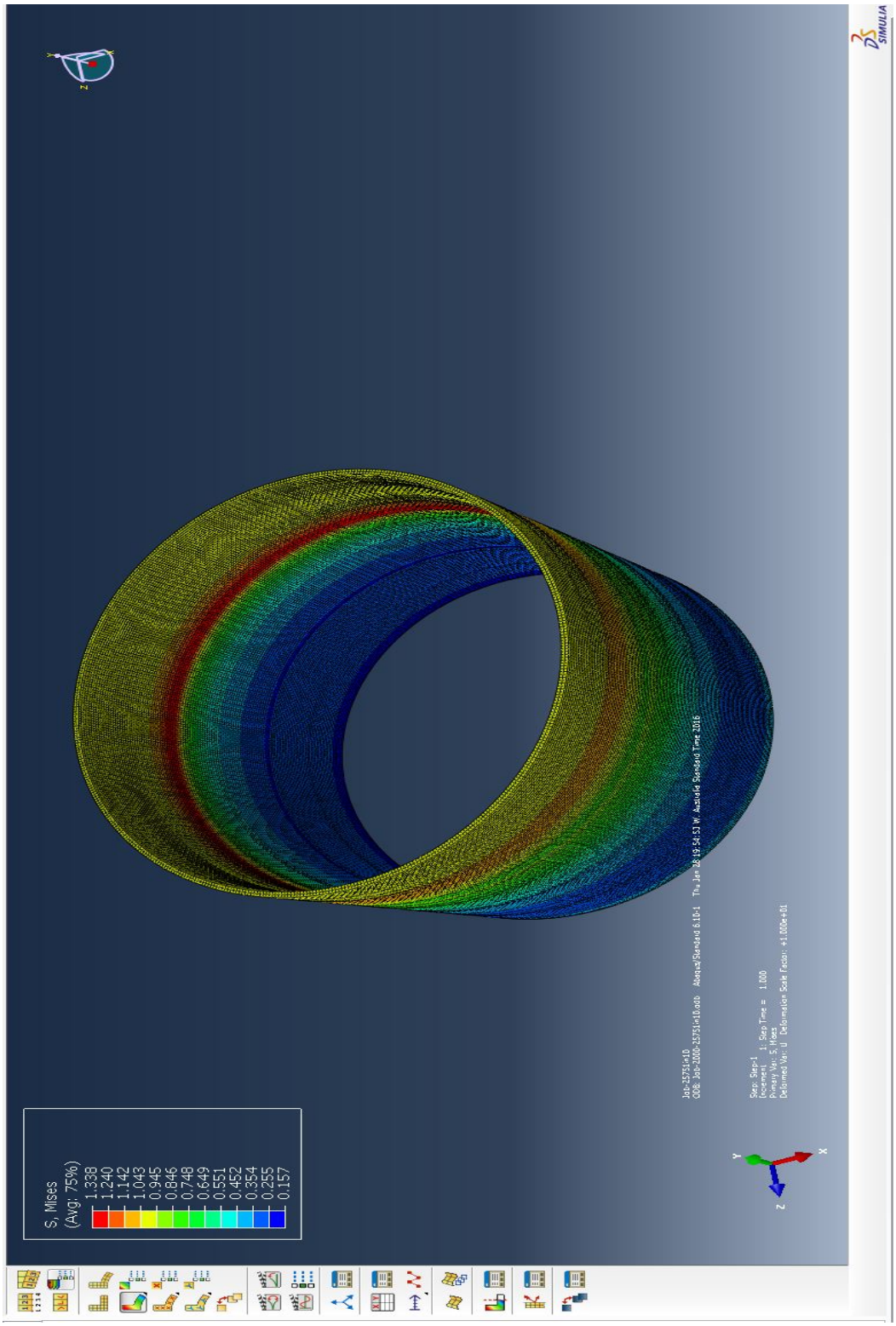

Results for D=2000 mm, t= 25, T=75, T/t=3, Slope 1 in 10

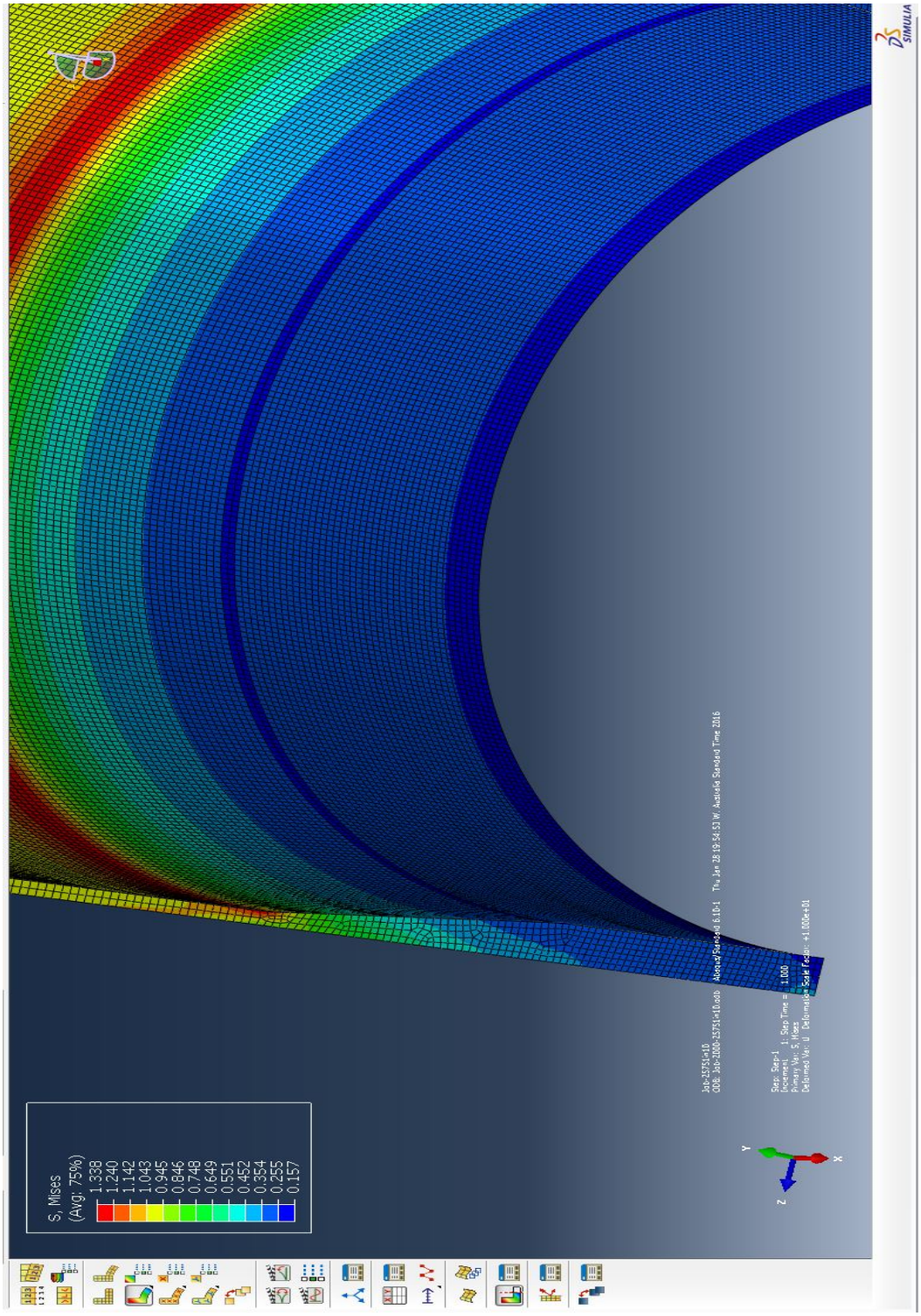

Section Results for D=2000 mm, t= 25, T=75, T/t=3, Slope 1 in 10

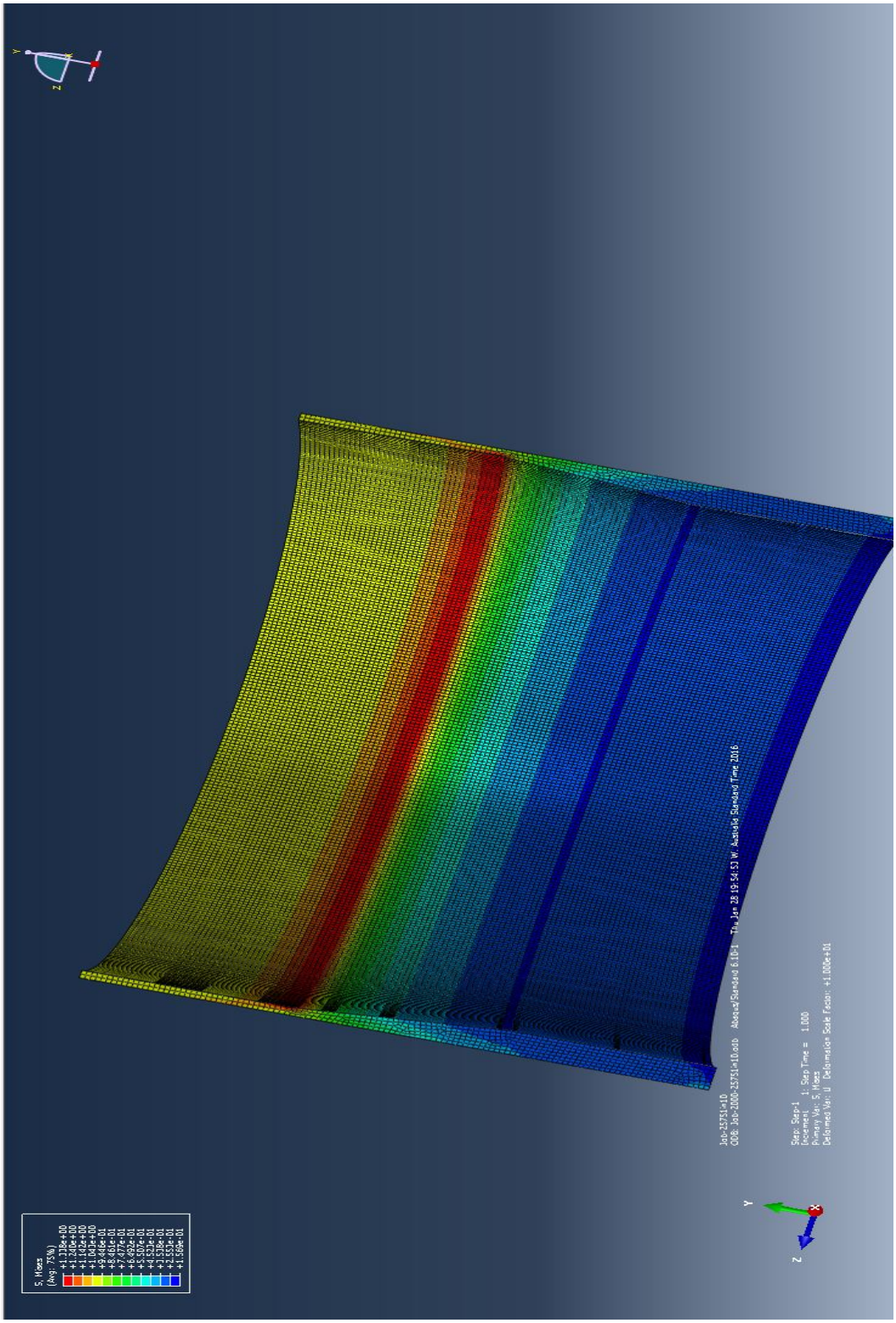

Section Results for D=2000 mm, t= 25, T=75, T/t=3, Slope 1 in 10